IST-4-027756 WINNER II

D6.13.12 v1.0

Final CG "local area" description for integration into overall System Concept and assessment of key technologies

Contractual Date of Delivery to the CEC:	*31.10.2007 (M22)*
Actual Date of Delivery to the CEC:	**31.10.2007**
Author(s):	S. Rouquette-Léveil, G. Auer, I. Cosovic, R. Fracchia, M. Haardt, E. Jorswieck, P. Karamolegkos, M. Navarro, S. Pfletschinger, A. Piątyszek, R. Pintenet, F. Römer, M. Sternad, T. Svensson, A. Tyrrell, M. Wódczak
Participant(s):	*MOT, CTH, CTTC, PUT, TUI, KTH, DOC, NTUA*
Workpackage:	*WP6, System concept*
Estimated person months:	**11**
Security:	**PU**
Nature:	**R**
Version:	1.0
Total number of pages:	86

Abstract:

This document presents the description and the assessment of the Local Area proof of concept. It also describes self-adaptation enablers for the WINNER system concept beyond the Local Area case, but with evaluation in local area scenario.

Keyword list:

Local Area concept group, self-organisation

Disclaimer:

Executive Summary

The European research project WINNER develops a new radio access system which aims at providing wireless access for a wide range of services and applications across all radio environments and deployment scenarios, with one single adaptive system concept. The design of such flexible and ubiquitous radio access system requires the joint use of most advanced techniques in the digital communication domain, including adaptive modulation, channel coding, spatial processing, interference mitigation etc. However, to ensure flexibility and efficient operation in various environments, the single WINNER system concept can be tuned to various deployment scenarios.

The goal of the Concept Groups is to coordinate the definition of a specific set of operating parameters and algorithms suited to a specific deployment. Three concept groups have been defined, respectively targeting Wide Area, Metropolitan Area and Local Area deployment. This deliverable addresses the Local Area scenario and presents the performance evaluation of the WINNER system concept derived for local area use.

In order to provide a wide range of services across a wide range of environment, the WINNER system concept must include flexibility and adaptation features. In particular, one of the WINNER key benefit is its ability to self-adapt to varying environment thanks to various self-adaptation mechanisms spread all other the radio interface stack. This report also presents these enablers of self-organisation at each layer and the related performance assessment studies.

Due to the complexity of each technique, the document does not aim at providing an exhaustive description and evaluation but rather provides an overview with links to other WINNER deliverables for further reading. The main features are listed below:

- Adaptive modulation and coding is used to adapt the physical modulation and coding schemes to a varying environment. Due to the OFDM nature of the waveform, two techniques can be defined for link adaptation: frequency-adaptive transmission and non-frequency adaptive transmission. Simulation results are provided for evaluation of modulation and coding techniques, and for evaluation of frequency-adaptive transmission. A flexible implementation of HARQ that provides a seamless transition from incremental redundancy to chase combining is also presented. The whole study addresses all types of environment.

- Two synchronisation procedures are particularly relevant to the local area scenario. A PHY layer algorithm to operate in licence-exempt case is presented. Detection and cancellation of narrowband interference allow having almost the same performance as in the no interference case. A self-organised synchronisation approach is also described, based on the analysis of pulse-coupled oscillator. Simulation results for a fully decentralised self-synchronisation of network equipment are provided, showing that the proposed method works well in a local area context.

- In local area deployment, distributed antenna techniques are used to benefit from the four remote antenna arrays. Performance evaluation results that take into account CSI imperfections are presented in uplink, based on Alamouti coding, and in downlink, with regular block diagonalisation or successive MMSE precoding to cancel user interference. These results show that high spectral efficiencies are attained in both cases.

- A specific algorithm (Static Routing information Enhanced Algorithm for Cooperative Transmission) is investigated to benefit from cooperative relaying. This algorithm allows adapting the cooperation between source and relays to the topology of the environment. Direct transmission, conventional relaying and cooperative relaying are compared.

- When discussing the multiple access schemes, the already introduced classification between frequency-adaptive and non-frequency adaptive transmission applies perfectly to the resource allocation schemes. Resource multiplexing is discussed, especially in context of TDD.

- A decentralized MAC protocol to dynamic and interference aware chunk selection is applied to the WINNER TDD mode. The ability to facilitate self-organized interference management is presented for a local area peer-to-peer network. The performance improvement compared to benchmarks systems is demonstrated through simulation results for several criteria.

- The WINNER handover algorithm consists of two independent triggers, one for maintaining the wireless connection, and another for maximizing the network performance. Simulation results for intra-mode handover between local area cells, and for inter-mode handover between local area and metropolitan area cells show the effectiveness of the proposed handover trigger.

- Spectrum resource management is presented with focus on short-term spectrum assignment. For performance evaluation, two radio access networks operating in TDD mode are considered, one with local area deployment and the other one with metropolitan area deployment. Two algorithms are compared for cell pair selection.

This deliverable focuses on performance assessment of the WINNER system concept in Local Area context. For system evaluation across all deployment scenarios, it should be taken into consideration with the deliverables [WIN2D61310] and [WIN2D61311] that present the performance assessment of the WINNER system concept in wide area and metropolitan area cases respectively.

Authors

Motorola (MOT)		
	Stéphanie Rouquette-Léveil	Phone: +33 1 69354824 Fax: +33 1 69354801 e-mail: stephanie.rouquette@motorola.com
	Roberta Fracchia	Phone: +33 1 69354846 Fax: +33 1 69354801 e-mail: roberta.fracchia@motorola.com
	Rémy Pintenet	Phone: +33 1 69354833 Fax: +33 1 69354801 e-mail: remy.pintenet@motorola.com

Chalmers University of Technology / Uppsala University (CTH/UU)		
	Tommy Svensson	Phone: +46 31 772 1823 Fax: +46 31 772 1782 email: tommy.svensson@chalmers.se
	Mikael Sternad	Phone: +46 704 250 354 Fax: +46 18 555 096 e-mail: mikael.sternad@signal.uu.se

Centre Tecnològic de Telecomunicacions de Catalunya (CTTC)		
	Stephan Pfletschinger	Phone: +34 93 645 29 15 Fax: +34 93 645 29 01 email: stephan.pfletschinger@cttc.es
	Monica Navarro	email: monica.navarro@cttc.es

Poznań University of Technology (PUT)		
	Adam Piątyszek	Phone: +48 61 665 3936 email: adam.piatyszek@et.put.poznan.pl
	Michał Wódczak	Phone: +48 61 665 3917 email: mwodczak@et.put.poznan.pl

Ilmenau University of Technology (TUI)		
	Florian Römer	Phone: +49 3677 69 1269 Fax: +49 3677 69 1195 e-mail: florian.roemer@tu-ilmenau.de
	Martin Haardt	Phone: +49 3677 69 2613 Fax: +49 3677 69 1195 e-mail: martin.haardt@tu-ilmenau.de

Royal Institute of Technology (KTH)		
	Eduard Jorswieck	Phone: +46 8 790 65 77 Fax: +46 8 790 72 60 e-mail: eduard.jorswieck@ee.kth.se

DoCoMo (DoC)		
	Gunther Auer	Phone:+49 89 5682 4219 Fax: +49 89 5682 4301 e-mail: auer@docomolab-euro.com
	Ivan Cosovic	Phone: +49 89 5682 4229 Fax: +49 89 5682 4301 e-mail: cosovic@docomolab-euro.com
	Alexander Tyrrell	Phone:+49 89 5682 4235 Fax: +49 89 5682 4301 e-mail: tyrrell@docomolab-euro.com

National Technical University of Athens (NTUA)		
	Pantelis Karamolegkos	Phone: +30 210 7721513 e-mail: karamolegos@telecom.ntua.gr

Table of Contents

List of Acronyms and Abbreviations

Δf	Subcarrier distance
f_c	carrier frequency
T_G	Guard interval/cyclic prefix duration
T_N	OFDM symbol duration (without guard)/single carrier block length
λ	wavelength
β	pulse roll-off factor
θ_{3dB}	3dB beamwidth of antenna element pattern
ARQ	Automatic Repeat Request
AWGN	Additive White Gaussian Noise
B-EFDMA	Block-Equidistant Frequency Division Multiple Access
B-IFDMA	Block-Interleaved Frequency Division Multiple Access
BCH	Broadcast (Transport) Channel
BER	Bit Error Rate
BLDPCC	Block LDPC Code
BLER	Block Error Rate
BPSK	Binary Phase Shift Keying
BS	Base Station
CC	Convolutional Code
CDF	Cumulative Density Function
CG	Concept Group
CQI	Channel Quality Indicator
CRC	Cyclic Redundancy Check
CWER	Code Word Error Rate
DAC	Direct Access Channel
DCA	Dynamic Channel Allocation
DBTC	Dual-Binary Turbo Code
FDD	Frequency Division Duplex
FEC	Forward Error Correction (Coding)
FER	Frame Error Rate
FSU	Flexible Spectrum Use
GMC	Generalised Multi-Carrier
GoB	Grid of Beams
GoS	Grade of Service
GW	GateWay
HARQ	Hybrid Automatic Repeat Request
HwC	Horizontal sharing with Coordination
HwoC	Horizontal sharing without Coordination
IFDMA	Interleaved Frequency Division Multiple Access
IP	Internet Protocol
ISD	Inter Site Distance
LA	Local Area
LDC	Linear Dispersion Codes
LDPC	Low-Density Parity-Check Code
LLR	Log-Likelihood Ratio
LOS	Line-Of-Sight

LT	Long Term
MA	Metropolitan Area
MAC	Medium Access Control
MCS	Modulation and Coding Scheme
MI	Mutual Information (link-to-system level interface, [BRUN05])
MI-ACM	Mutual Information based Adaptive Coding and Modulation
MIMO	Multiple Input Multiple Output
MMSE	Minimum Mean Square Error
MSE	Mean Square Error
NLOS	Non Line-Of-Sight
ODS	Optimum Distance Spectrum
OFDM	Orthogonal Frequency Division Multiplexing
OFDMA	Orthogonal Frequency Division Multiple Access
P2P	Peer-to-Peer
PCCC	Parallel Concatenated Convolutional Codes
PDF	Probability Density Function
PER	Packet Error Rate
QAM	Quadrature Amplitude Modulation
QC-BLDPCC	Quasi-Cyclic Block LDPC Code
QoS	Quality of Service
QPSK	Quadrature Phase Shift Keying
RAC	Random Access Channel
RAN	Radio Access Network
RAT	Radio Access Technology
RBD	Regularized Block Diagonalisation
RCP	Rate Compatible Punctured
RN	Relay Node.
RRM	Radio Resource Management.
RS	Resource Scheduling
RTU	ReTransmission Unit
SDMA	Spatial Division Multiple Access
SINR	Signal to Interference and Noise Ratio
SISO	Single-Input Single-Output
SMMSE	Successive Minimum Mean Square Error precoding
SNR	Signal to Noise Ratio
SRM	Spectrum Resource Management
SSC	Spectrum Sharing and Coexistence
ST	Short Term
TCP	Transmission Control Protocol
TDD	Time Division Duplex
TDMA	Time Division Multiple Access
UDP	User Datagram Protocol
UT	User Terminal
VS	Vertical Sharing
WA	Wide Area
WLAN	Wireless Local Area Network

1. Introduction

Concept groups coordinate the definition of a proof of concept among the various expert tasks in the WINNER project. A proof of concept is a WINNER system tuned to a specific deployment scenario. Three scenarios have been defined: Local Area (LA), Metropolitan Area (MA), Wide Area (WA), corresponding to different environments, traffic patterns, bandwidth, etc. Concept groups are also a vehicle to investigate innovative techniques as key differentiators compared to existing or forthcoming systems. For example, a key differentiator of WINNER is its flexibility and its ability to adapt to any kind of environment.

This deliverable addresses the Local Area scenario and presents the performance assessment of the WINNER system concept derived for local area use. This deliverable also focuses on the enablers of self-adaptation at each layer, and shows the performance evaluation of their benefits. Due to the complexity of each technique, the document does not aim at providing an exhaustive description and evaluation but rather provides an overview with links to other WINNER deliverables for further reading.

The document is structured as follows. Section 2 describes the scenarios related to Local Area concept group. Section 3 presents the self-adaptation techniques that are investigated. Section 4 summarises the reference set of parameters of LA deployment that is used in the following sections for performance assessment. Sections 5 to 12 describe and evaluate the techniques used in the radio interface for local area deployment or for self-adaptation capabilities. Finally section 13 concludes the deliverable.

2. Local Area deployment scenarios

2.1 WINNER Local Area as a solution for in-home communications

High data rate wireless communications in a house could be provided thanks to a WINNER base station (BS), connected to a high data rate communication backbone (Figure 2.1). User equipments are then connected to the backbone by the WINNER base station. The WINNER base station controls a single cell, encountering limited interference from other systems as it can be assumed that the house represents a well-protected environment. Within the cell, concurrent accesses can be prioritised by the BS thanks to both user preferences, previously set and operator global policy. The operator should have the possibility to remotely control the BS in order to register the latest policy or provide the latest firmware.

Within the cell, user equipments could establish direct communication that could be controlled or not controlled by the BS. A typical example could be to stream a video from the house multimedia centre data storage (located for instance in a garage) to the large screen located in the living room. For that purpose, the multimedia centre and the screen establish a direct communication link.

The WINNER BS should be connected to a high data rate backbone. For that purpose, it could either use a wired connection (cable, ADSL) or use a wireless feeder connection, typically running a WINNER Metropolitan or Wide Area mode. In that context, the WINNER BS in the house acts as a relay between the WINNER Metropolitan / Wide Area base station to the user equipments in the house.

At last, the user equipments could initiate a session in the house and terminate it outside (or conversely). For that purpose, the WINNER LA system should support seamless handover to WINNER Metropolitan or Wide area systems, as well as with legacy systems.
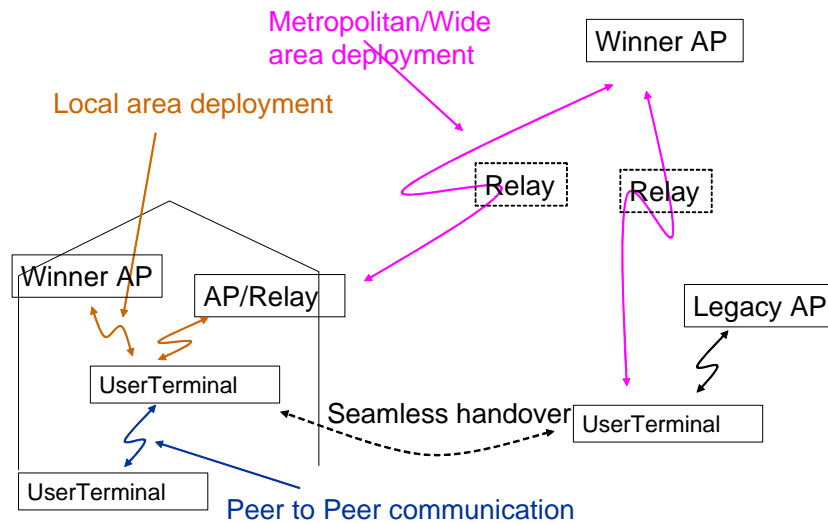

Figure 2.1: Illustration of home use of WINNER Local Area

2.2 WINNER Local Area as a solution for hot-spot (hotel, small office, shopping centre) deployment

In that scenario, the coverage area is higher than the home deployment. Several WINNER BSs may be required and thus the assumption of limited interference may be not anymore relevant.

For the hotel/small office deployment, it could be assumed that a single operator operates the various BSs, and thus the BSs could cooperate with each other. On the other hand, in case of shopping center deployment, each store may want to provide its own wireless high data rate access using WINNER LA systems. As a result, little/no cooperation between the various WINNER BSs can be assumed and coexistence issues between WINNER LA systems must be tackled.

Moreover, for "Internet coffees" types of deployment, coverage should be extended to outdoor (terrace).

Direct communication between user equipments can be imagined in both cases. In the small office environment, two colleagues would like to exchange a file in a meeting room in a peer-to-peer manner. In the shopping mall environment, peer-to-peer communication can be driven by the user equipment context, which could sense its direct neighbourhood and initiate a communication with a peer device.

Distributed base stations (many antennas, spatially distributed connected to a BS via optical fibre) could be used to extend the coverage (for a given quality) as indoor is often a challenging propagation environment.
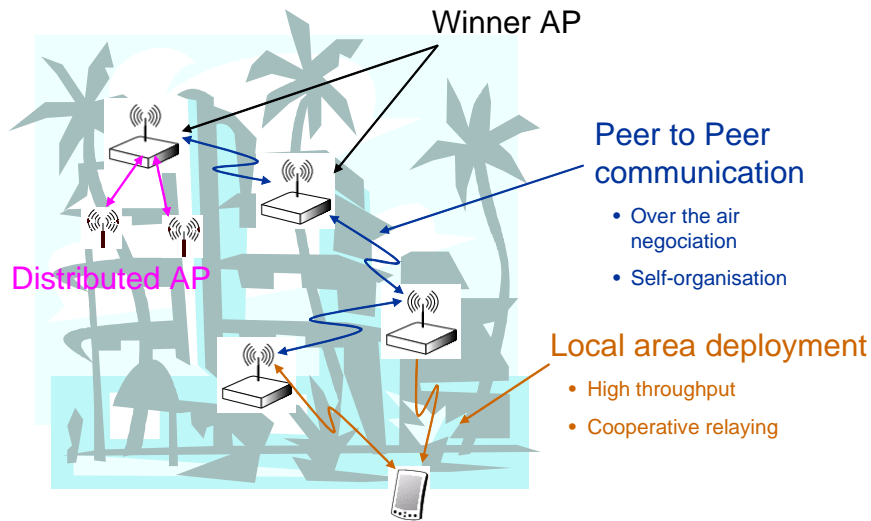

Figure 2.2: Illustration of hot-spot use of WINNER Local Area

For this kind of deployment, the LA concept group focuses on the indoor case while the metropolitan concept group considers outdoor and outdoor to indoor cases.

2.3 Example of usage scenario

In order to illustrate an use case of the WINNER system in context of LA deployment, a typical usage script is proposed in the following [WIN2D6112]. Each step addresses different aspects that could be related to the LA proof of concept, therefore the script is followed by a table that decomposes each step into the relevant aspects.

Both environments (residential – hot spot) that fall within the scope of LA-CG are depicted in the scenario while the major (relevant) implications are also incorporated within the script steps.

Main actor: John, male, 18 years old

Location: Urban area (a city of Europe)

Occupation: Student

Date: A day in 2015

1. John is woken up by the ringing on his portable device; he has received a multimedia message (video message), sent to him by the relevant service of his university, informing him about some change in the daily class schedule.

2. Having woke up, he surfs on the Internet using his laptop, while making a voice call to his girlfriend.

3. He turns on the next generation WINNER LA BS he bough yesterday. The new BS detects the other BSs of John's house, as well as neighbouring ones, and all the BSs coordinate with each other to refarm the available frequency and optimize the wireless resource usage.

4. Visiting an online music store, he selects some new tunes. The songs are purchased and transferred directly to his online music server.

5. He tries to communicate his roommate that sleeps in the next room, establishing a direct connection with his device.

6. His roommate is not responding so John sends him a short video message.

7. While having his breakfast, John streams TV news on his device.

8. He initiates a voice call (using a VoIP service), while he leaves the house and enters the car to drive to the mall, where he is supposed to meet with a fellow student.

9. During his drive through the city, the VoIP call is continued, and after entering a cafeteria in the mall he decides to terminate this session.

10. The cafeteria offers online menu, so John selects what to order after browsing on the relevant locally available web site.

Obviously the scenario tries to address most of the important aspects involved within typical LA proof-of-concepts, rather than being exhaustive in terms of service usages. The elements of interest regarding the scenario composition are depicted in Table 2-1. User mobility is low (0 – 5 km/h) throughout the whole example.

Table 2.1: Representative scenario of Local Area proof of concept

Script Extract	Service Class	User Density	Associated Traffic Model	Environment	Coverage	Implication
he has received a multimedia message	Multimedia messaging	High (residential)	File Transfer	Residential	3 – 100 m	Connectivity between BS and WINNER backbone
he surfs the Internet	Lightweight browsing	High (residential)	Internet / Browsing	Residential	3 – 100 m	Connectivity between BS and WINNER backbone
while making a voice call to his girlfriend	Simple Telephony and Messaging	High (residential)	Conversational	Residential	3 – 100 m	Connectivity between BS and WINNER backbone
he turns on the next generation WINNER LA BS... *the BS detects the other BSs of John's house...* *all BSs coordinate*	Short control messages and signalling	High (residential)	Signalling	Residential	3 – 100 m	Self-Organisation between WINNER BSs
visiting an online music store *...the songs are purchased*	Lightweight browsing	High (residential)	Internet / Browsing	Residential	3 – 100 m	Connectivity between BS and WINNER backbone
and transferred directly to his online music server	File exchange	High (residential)	File Transfer	Residential	3 – 100 m	Connectivity between BS and WINNER backbone / self organisation

Script Extract	Service Class	User Density	Associated Traffic Model	Environ ment	Coverage	Implication
						between residential WINNER devices
He tries to communicate his roommate ...establishing a direct connection with his device.	Simple telephony and messaging	High (residential)	Conversational	Residential (P2P mode)	3 – 100 m	P2P communication between WINNER enabled devices
so John sends him a short video message	File exchange	High (residential)	File Transfer	Residential (P2P mode)	3 – 100 m	P2P communication between WINNER enabled devices
John streams TV news on his device	Video streaming	High (residential)	Video Streaming	Residential	3 – 100 m	Connectivity between BS and WINNER backbone
He initiates a voice call (using a VoIP service), while he leaves the house...During his drive through the city, the VoIP call is continued, and after entering a cafeteria in the mall he decides to terminate this session	Simple telephony and messaging	High (residential) (for as long as the actor is still at home)	Conversational	Residential (for as long as the actor is still at home)	3 – 100 m (for as long as the actor is still at home)	Handover between WINNER modes
The cafeteria offers online menu, so John selects what to order after browsing on the relevant locally available web site	Lightweight browsing	Medium (hotspot)	Internet / Browsing	Hotspot	20 – 100 m	Coordination between co-existing BSs / cooperation between WINNER system modes so as to complement for coverage areas

In these examples of deployment and usage scenarios, it is quite obvious that the ability of WINNER equipment to be self-configurable is a need, in order to minimise human intervention. In addition, self-configuration is also a means to meet the specific challenges of LA deployments. The next section presents the self-configuration techniques that are addressed in this document.

3. Self-organisation in WINNER

In the specific case of LA deployment, the WINNER system raises the following challenges: high data rate links, efficient radio resource management, coexistence with other systems, cost efficiency, and peer-to-peer communication. Obviously, some challenges are also fully appropriate for the other deployment scenarios (Wide Area, Metropolitan Area).

Self-organisation and distributed approaches are foreseen to become key enablers to meet these challenges. By self-organisation, we mean that the system is able to adapt itself to a varying environment. This inherently assumes that the equipments in the system have means to sense their environment, to learn and to act based on some heuristics to ensure efficient operation. Self-organisation is often linked to distributed intelligence where there is no or little central control entity. Base stations and user equipments interact directly among each other. These interactions are often localised in space and time.

In this document, self-adaptation is addressed by the presentation and the evaluation of the following techniques:

- **Adaptive modulation and coding.** Optimising the link between transmitter and receiver is required to provide high data rate links. Two approaches, frequency-adaptive transmission and non-frequency adaptive transmission, are proposed for adaptation to the propagation conditions. They can be applied in any type of deployment scenario.

- **Self-organised network synchronisation.** A self-organised network synchronisation algorithm is particularly important in the local area scenario where no GPS signal, which would provide a global timing reference, is available. Consequently a self-organised scheme is needed: no central entity is responsible for inter-cell synchronisation, and user terminals and base stations align their time reference by following simple rules, so that all agree on a common time slot structure. The proposed approach is inspired from the studies of synchronisation phenomena of fireflies in South-East Asia.

- **Multi-User MIMO processing**. In Local Area scenario, the base station relies on four distributed antenna arrays that are connected through fibre links. In downlink, adaptive multi-user MIMO precoding based on instantaneous Channel State Information (CSI) is applied to efficiently exploit the spatial degrees of freedom while still being rather robust against CSI errors. In uplink frequency-adaptive transmissions, the optimum transmit antenna weights are computed by the base station and then sent to the user terminals via feedback. However cancelling the multi-user interference is still performed at the base station.

- **Cooperative relaying**. In order to benefit from cooperative relaying in Local Area scenario, e.g. an airport or a shopping centre, a specific algorithm (Static Routing information Enhanced Algorithm for Cooperative Transmission) is investigated to adapt the cooperation between source and relays to the topology of the environment. The selection of the cooperating relays is based on the observation of the received power by the relays and the user terminals.

- **Multiple access**. Multiple access schemes for frequency adaptive transmission and non-frequency adaptive transmission are discussed in the context of the Local Area scenario. The characteristics of this scenario are taken into account in the parameterization and adaptive selection of multiple access schemes.

- **Decentralized dynamic channel allocation.** There is a need for efficient decentralized interference management to deal with the deployment of many distributed base stations and relays that might not even belong to the same operator. To facilitate self-organized interference management, an interference aware dynamic channel allocation algorithm that can be applied to arbitrary network topologies is presented. The performance evaluation is completed for a local area peer-to-peer network.

- **Flexible Spectrum Use (FSU)**. FSU considers the spectrum usage of different Radio Access Networks (RAN) within the same Radio Access Technology (RAT). The spectrum functionalities proposed lead to a better utilization of the spectrum throughout multi-operator solutions, therefore increasing the availability of the spectrum. Long term and short term spectrum assignments are considered.

4. Deployment parameters for performance evaluation

For performance assessment of WINNER reference design, an indoor test scenario has been defined in [WIN2D6137] and is summarized here. The system operates at 5GHz and shall provide a downlink peak data rate of 1Gbps (performance requirement R34 in [WIN2D6114]) using[WIN2D6114] 100MHz bandwidth and time division duplexing. Licensed and unlicensed cases are considered. However, the primary focus is licensed spectrum for consistency with the other types of deployment. User density can be high (hot spot) but with limited user mobility (up to 5 km/h).

The indoor test scenario consists of one floor of a building containing a regular grid of 40 rooms (10m x 10m x 3m) and two corridors (100m x 5m x 3m) as presented in Figure 4.1. 90% of the users are uniformly distributed in rooms and the other 10% are uniformly distributed in corridors. Such a scenario is characterised by high shadowing and considerable signal attenuation due to the existence of rooms separated by walls. As a result of its isolated characteristic it also features low interference from other cells when compared to the outdoor cases. Four antenna arrays are operated as remote radio heads and each of them contains 8 antennas. Each antenna array is rotated by 45°.
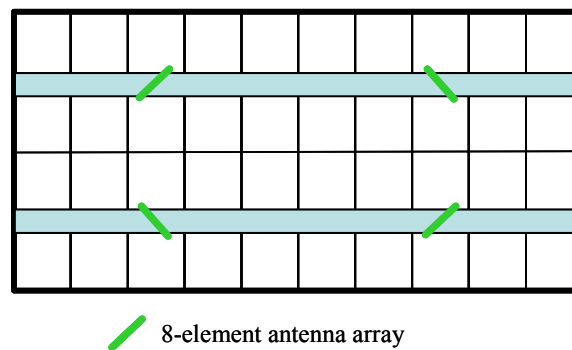

8-element antenna array

Figure 4.1: Sketch of indoor environment (one floor)

Following WINNER I denomination, the scenarios of Local Area CG are covered by the scenarios A1, A2, B1 and B3 (see [WIND72], [WIND54]), and summarized in the Table 4.1. The description of these scenarios and of the corresponding channel models can be found in [WIN2D112].

Table 4.1: High level scenarios investigated in LA CG

Scenario	Definition	LOS/NLOS	Mob.	Distance range
A1 In building	Indoor small office / residential	LOS/ NLOS	0–5 km/h	3 - 100 m
A2 In building	Indoor to outdoor	NLOS	0–5 km/h	
B1 Hotspot	Typical urban micro-cell	LOS/ NLOS	0–5 km/h	20 - 100 m
B3 Hotspot	Indoor	LOS	0–5 km/h	

Please note that the scenario B1 considered in LA CG is slightly different from the original one. The difference are the user mobility, limited to 5 km/h (instead of 70 km/h) and the cell range which is limited to a hundred of meters.

The deployment parameters for base stations and user terminals are given in Table 4.2. These parameters are used as default parameters for performance assessment in the following sections except in the case of relaying.

Table 4.2: Base station and user terminal parameters

base station	location/height	3 m
	max. transmit power per sector	21 dBm = 125.9 mW
	number of sectors per BS	4 arrays operated as remote radio heads
	number of antennas per sector	8 elements per array
	antenna configuration[1] (per sector)	Cross polarised linear array X X X X
	antenna element spacing	$0.5\lambda = 0.5c/f_c$ (f_c: DL carrier frequency, c: speed of light)
	azimuth antenna element pattern	$A(\theta) = -\min\left[12\left(\dfrac{\theta}{\theta_{3dB}}\right)^2, A_m\right]$ [dB] $A_m = 12$, $\theta_{3dB} = 70°$
	antenna gain	5 dBi
	receiver noise figure	5 dB
user terminal	Height	1.5 m
	transmit power	21dBm = 125.9mW
	number of antennas	2
	antenna configuration	dual cross polarised antennas: X
	azimuth antenna element pattern	$A(\theta) = 0$ dB
	antenna gain	0 dBi
	receiver noise figure	7 dB

The baseline relay deployment consists of four relay nodes (green ones) coordinated by the base station located in the centre (red node), as presented in Figure 4.2. RNs are placed in the corridors at the same positions as the remote antenna heads in the no-relaying case and are located 25 m and 75 m away from the left/right side of the building, respectively. The performance assessment results presented in Chapter 8 show, however, that this deployment is best suitable for single path relaying and due to the existence of walls it is impossible to observe almost any gain from the RN-RN cooperation.

Figure 4.2: Baseline relay deployment in indoor scenario

---

[1] Since the channel models are essentially two-dimensional, 0° downtilt is assumed.

Therefore it was concluded that different deployment would be more advantageous. Namely, in order to gain from good quality links between the BS and the RNs, the BS should be positioned in the corridor. For this purpose two base stations are necessary and each is proposed to be located in the middle of the corridor and to be assisted by four RNs, two on its left and two on its right side. More details can be found in Section 8.3.

5. Modulation, coding and link adaptation

Modulation and coding determine the overall performance of the WINNER system to a large extent. They both have an impact on:

- The necessary SINR to achieve a certain QoS (e.g. CWER) and through this indirectly on the **average** and **cell edge throughput**, **spectral efficiency** and **coverage**.

- The **delay** which is caused by retransmissions and the trade-off between tolerable delay and throughput.

- The **complexity** of the receiver and transmitter in terms of the **computational effort**, **power consumption** and hence **cost**.

In *state-of-the art* (SoA) systems, the impact of coding and modulation on the overall performance has increased. Adaptive coding and modulation with fine granularity (in time, frequency and spatial dimension), Hybrid ARQ (HARQ) and advanced spatial processing schemes provide a larger degree of freedom, but the large achievable data rates also impose challenges on decoding/encoding complexity.

One can assume that all techniques described within Section 5 are common to all concept scenarios, i.e. *local area* (LA), *metropolitan area* (MA) and *wide area* (WA), except as otherwise stated.

5.1 Modulation and coding

5.1.1 Modulation alphabets

The WINNER reference design uses the following modulation alphabets: BPSK, QPSK, 16-QAM, 64-QAM, and also 256-QAM when applicable[2]. The bit labelling is following a Gray encoding.

The use of non-square QAM constellations, i.e. 8-QAM, 32-QAM and 128-QAM is not considered any further. Evaluations of the frequency adaptive transmission scheme shown that the differences in performance with or without these non-square modulation alphabets are negligible (cf. Section 5.2.1.2).

5.1.2 Forward error correction techniques

During phase I of the WINNER project, three different *forward error correction* (FEC) coding techniques were identified and proposed as main candidates for the WINNER concept: ***duo-binary turbo-codes*** (DBTC) in the form of *parallel concatenated convolutional codes* (PCCC), ***quasi-cyclic block low-density parity check codes*** (QC-BLDPCC) and ***convolutional codes*** (CC) [WIND210]. The former two coding methods, as iterative coding schemes, are able to provide an excellent performance for medium to large block sizes (200 information bits and beyond) while taking implementation simplicity (e.g. parallelisation, memory requirements) into account already in the code design phase. BLDPCC outperform DBTC at large block lengths and/or high code rates (for a detailed assessment and comparison, please refer to Appendix B.2 in [WIND210] and [LZH+06]). The use of convolutional codes was only considered for block lengths below 200 information bits.

In Phase II of the project the above mentioned coding scheme candidates were thoroughly evaluated with respect to link adaptation (cf. Section 5.2), hybrid ARQ (cf. Section 5.3) and encoding of the signalling and broadcast information. The most important extension of the BLDPCC and DBTC from Phase I is the rate-compatibility of the puncturing schemes, which is required for HARQ Type-II with Incremental Redundancy (IR), and proper integration with the Stiglmayr's MI-ACM algorithm [SBC07] used in link adaptation. The current BLDPCC can use a very fine-grained code rate set, starting from R = 1/2. This set can be defined as follows:

$$R = \frac{24}{48 - P}, \qquad P = \{0,2,4,...,22\} \tag{5.1}$$

---

[2] 256-QAM might be difficult to demodulate in some scenarios due to synchronization problems, but currently there is no final evaluation of this issue. Since its use in link adaptation can improve the throughput by 2bits/symbols, compared do 64-QAM, it is still considered in the reference design, at least for the local area scenario.

Additionally, a parity check matrix for $R = 1/3$ BLDPCC is also provided, but this code is not rate-compatible with other rates at the moment. For the DBTC the following compatible code rates can be obtained through puncturing:

$$R = \left\{ \frac{1}{3}, \frac{2}{5}, \frac{1}{2}, \frac{4}{7}, \frac{2}{3}, \frac{3}{4}, \frac{4}{5}, \frac{6}{7} \right\} \tag{5.2}$$

Both the BLDPCC and DBTC have their advantages and disadvantages, but their performance vs. decoding complexity is not a sufficient metric to take the final choice, since more implementation aspects would need to be taken into account. Further complexity comparison can be found in appendix F.2 from [WIND210]. Besides, Table 5.1 from [WIND210] summarises the proposed FEC techniques with respect to their performance, memory requirements, decoding complexity and maturity[3].

Table 5.1: Comparison of the most promising FEC techniques [WIND210]

		CC[4]	DBTC	BLDPCC
Performance[5]	Short blocks	-	<0.5 dB	<1 dB
	Medium blocks	<1–1.5 dB	-	<0.2–0.4 dB
	Large blocks	<2–2.5 dB	<0.2 dB	-
Memory Requirements	Code structure	Very low	Low	Medium
	Decoding	Low	Medium	Medium
Encoding complexity		< 10 ops/info bit		
Decoding complexity		~ 2500 ops/info bit	<1700 ops/info bit	<1200 ops/info bit
Maturity		High	Medium	Medium

Since the reference design of WINNER phase 2 is targeting higher codeword lengths (higher than 5000 information bits), and based on phase I comparisons (cf. Figure B.5 from [WIND210]), it was then decided to recommend **BLDPC codes as a primary FEC technique for the reference design**.

This decision does not diminish the assets of the other considered candidate – DBTC, which might be still considered as a suitable alternative to BLDPCC in the final WINNER system.

Low rate convolutional codes for broadcast information

The modulation and coding requirements for control channel signalling are different than the ones for user data transmission. The information sent through the control channel is very important for proper functioning of the advanced protocols of the WINNER concept. Although the proposed BLDPCC and DBTC provide an excellent coding performance as shown in [WIND210], they can not be used for encoding the control information due to very short packet sizes being considered (25 information bits). Therefore low rate convolutional codes (CC), which can be used for encoding of such a short packets by choosing a *tail-biting* algorithm, are still considered for the WINNER reference design (CC were already proposed in Phase I, cf. [WIND210]).

Instead of the convolutional code defined in the previous proposal for the WINNER reference design with $R = 1/3$ and $G_A = [575, 623, 727]_{oct}$, one of the *optimum distance spectrum* (ODS) convolutional codes [FOO+98] with $R = 1/4$ can be used. The BER and CWER performance results presented in Figure 5.1 and Figure 5.2 have been obtained for the convolutional code with the following generator polynomials: $G_B = [473, 513, 671, 765]_{oct}$. These results are compared with the results for the convolutional code from Phase I. Additionally, $R = \frac{1}{2}$ results have been obtained from the same mother convolutional code using the puncturing matrix from equation (5.3).

---

[3] Although the information in Table 5.1 comes from year 2005, most of the indicators are still valid.

[4] Memory 8 convolutional code, soft Viterbi decoding

[5] Loss with respect to the best technique at codeword sizes 50, 576, 4308 bits (AWGN, BPSK, target CWER 1%)

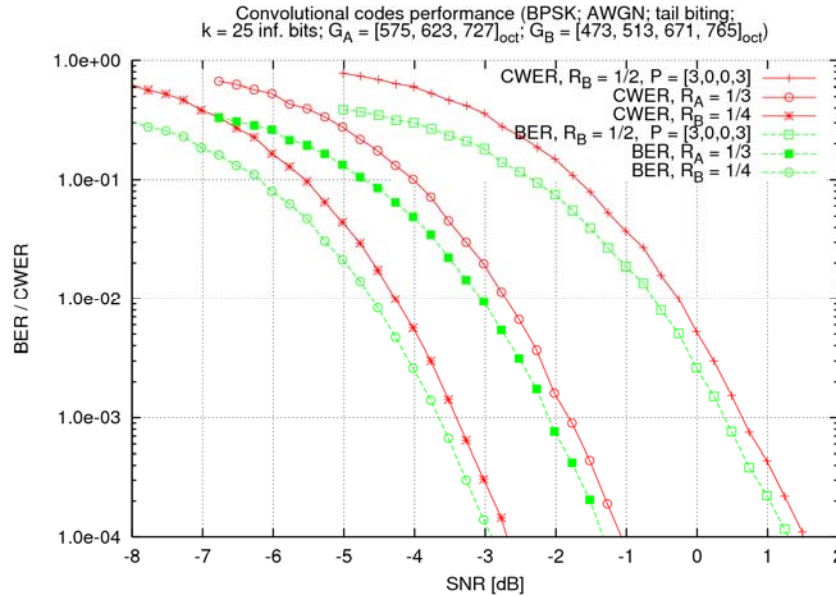$$P = \begin{bmatrix} 1\,1 \\ 0\,0 \\ 0\,0 \\ 1\,1 \end{bmatrix}$$

(5.3)

Figure 5.1: BER and CWER vs. SNR results of R = 1/4 (ODS), R = 1/3 (MFD) and R = 1/2 (ODS, punctured) convolutional codes for K = 25 inf. bits (BPSK, AWGN, tail biting)
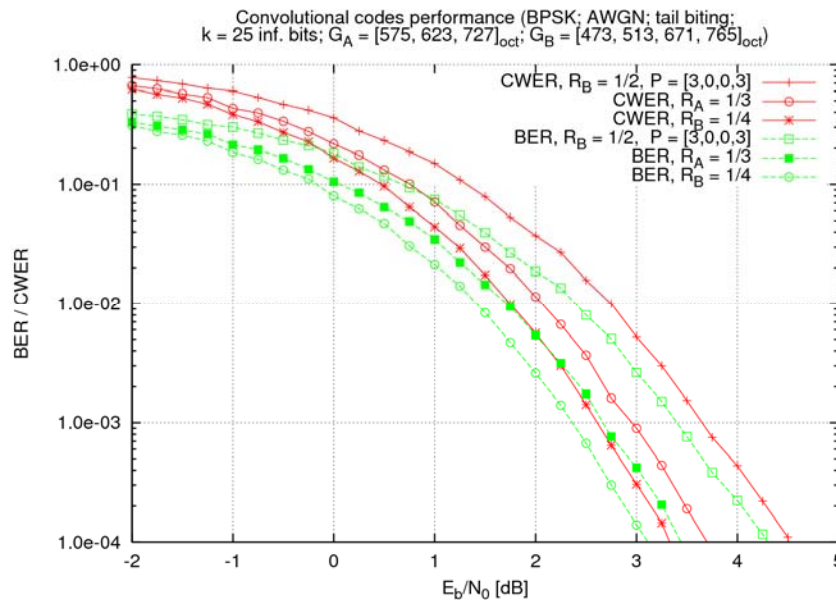

Figure 5.2: BER and CWER vs. E_b/N_0 results of R = 1/4 (ODS), R = 1/3 (MFD) and R = 1/2 (ODS, punctured) convolutional codes for K = 25 inf. bits (BPSK, AWGN, tail biting)

There is one issue related to the tail-biting Viterbi decoding, which needs to be taken into account – complexity. The "brute-force" tail-biting algorithm is $2^{k(L-1)}$ times more complex than a standard Viterbi decoding with a known tail, where k represents the number of inputs of the convolutional code ($R = k/n$)

and L is the constraint length. For a convolutional code with $L = 9$, this means an additional complexity factor of 256. Therefore other convolutional codes with shorter constraint lengths seem to be a good compromise between the decoding complexity and performance figures. Figure 5.3 compares CWER (green curves) and BER (red curves) results of a few $R = 1/4$ ODS convolutional codes with different constraint lengths, i.e. $L = \{6, 7, 8, 9\}$[6]. The CWER performance of the shortest code in this group, i.e. with constraint length $L = 6$ is about 0.5 dB worse than the code with $L = 9$. On the other hand, the decoding complexity of this shortest code is $2^{9-6} = 8$ times lower than the longest one, so it might be a good candidate for the final WINNER concept.
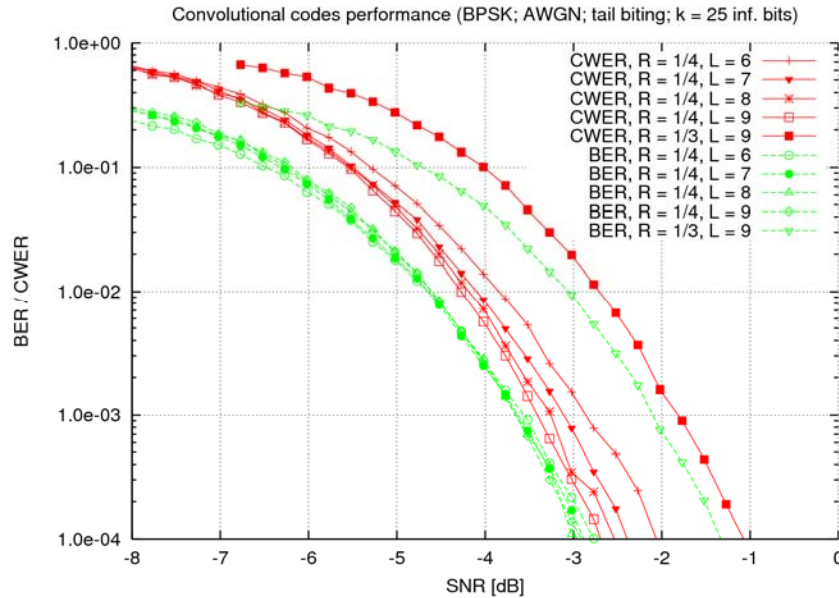

Figure 5.3: BER and CWER vs. SNR results of $R = 1/4$ ODS convolutional codes for various constrain lengths L and $K = 25$ inf. bits (BPSK, AWGN, tail biting)

5.1.3 Performance results of modulation and coding schemes

Bit and codeword error rate performance over the AWGN channel of the two main FEC candidates, i.e. QC-BLDPCC and DBTC, has been thoroughly investigated. The results of these simulations are collected in databases[7], which consist of BER/CWER vs. SNR or E_b/N_0 plots and text files with data for each modulation and coding scheme combination, and various packet sizes.

As an example, the QC-BLDPCC simulation results presented in Figure 5.4 and Figure 5.5 have been obtained through Monte Carlo simulation using the following simulation chain. In the transmitter, each information packet of $K = 288$ or $K = 1152$ random bits[8] have been encoded with the BLDPC code encoder, then rate-compatible punctured, interleaved using a pseudo-random bit interleaver and finally mapped into constellation symbols of b bits. Such a block of symbols has been transmitted through an AWGN channel. In the receiver, a soft demodulation has been performed for each symbol of a block to obtain log-likelihood ratios (LLR). The demodulator assumed Max-Log-MAP approximation. Next, such an LLR block has been deinterleaved, depunctured and sent to the LDPC code decoder. The decoder used a standard belief propagation algorithm in the LLR domain in parallel fashion (flooding schedule), i.e. all

---

[6] The following generator polynomials have been used for R = 1/4 convolutional codes: $G_6 = [51, 55, 67, 77]_{oct}$, $G_7 = [117, 127, 155, 171]_{oct}$, $G_7 = [231, 273, 327, 375]_{oct}$, and $G_7 = [473, 513, 671, 765]_{oct}$. All of them are *optimum distance spectrum* (ODS) convolutional codes [FOO+98].

[7] The databases with the BER/CWER results in the form of text files and plots will be published on the public WINNER website (https://www.ist-winner.org/). Some of these results can also be found in [WIN2D223].

[8] These two particular sizes in information bits are taken from the reference design assumptions.

variable→check node messages updated in one sweep, then all check→variable node messages updated in another sweep. The maximum number of decoding iterations has been set to 50.
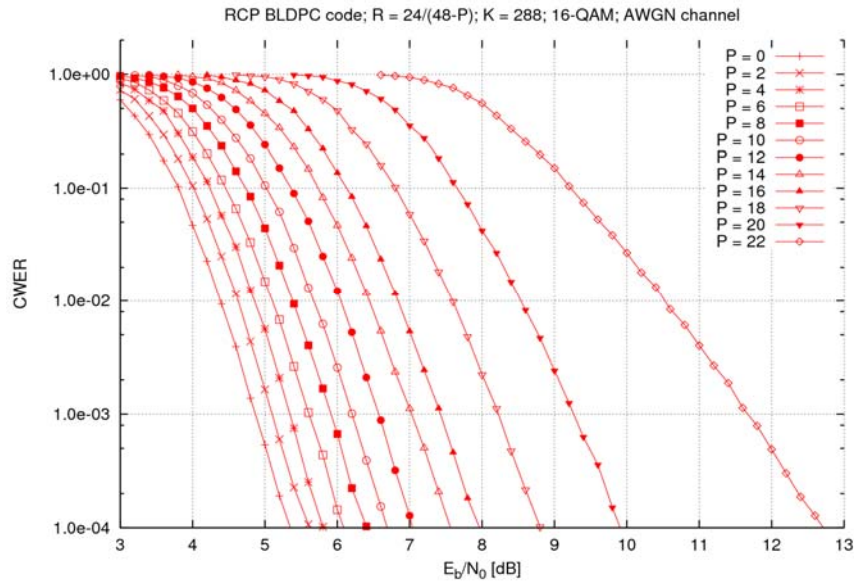
RCP BLDPC code; R = 24/(48-P); K = 288; 16-QAM; AWGN channel

Figure 5.4: CWER curves for 16-QAM and *K* = 288

RCP BLDPC code; R = 24/(48-P); K = 1152; 256-QAM; AWGN channel

Figure 5.5: CWER curves for 256-QAM and *K* = 1152

5.2 Link adaptation

The over-all framework for adaptive modulation and coding within the WINNER concept was described in Section 5 of [WIN2D6135]. Sections 5.2 and 5.3 of that report outlined the reference designs for using link adaptation within frequency-adaptive and non-frequency adaptive transmission, respectively. This chapter extends the description of [WIN2D6135] in three respects.

- The reference design of link adaptation for frequency adaptive transmission is based on using individual adaptive modulation within chunk layers, and map a code block over multiple such

resource unit. The code block is punctured with an appropriate average puncturing rate. The algorithm for performing the adaptive modulation and code rate adjustment is described in more detail in Section 5.2.1 below.

- The reference design for link adaptation for non-frequency adaptive transmission is based on using the same modulation and code rate within all transmission resource units allocated to a code block. The nature of these transmission resource units has been investigated in [WIN2D461] and the proposed mapping schemes (small sub-chunk blocks that are regularly spaced in frequency) are briefly motivated in Section 5.2.2 and also Chapter 9 below.

- Link retransmission schemes, or Hybrid ARQ are an important part of the total link adaptation strategy. Section 5.3 presents the reference design for the retransmission scheme: Incremental redundancy that uses cyclic shift repetition coding if a large number of retransmissions is required.

More details on both coding and link adaptation can be found in [WIN2D223]. A discussion of MAC layer aspects, MAC-and physical layer interactions and control overhead of the proposed schemes can be found in [WIN2D61314].

5.2.1 Frequency adaptive transmission

In the following, the *mutual information based adaptive coding and modulation* (MI-ACM[9]) algorithm [SBC07] used in the frequency adaptive transmission is briefly described.

Figure 5.6 shows the system model for one user which applies frequency-adaptive transmission on N_{ch} chunks which have been previously allocated to him by the scheduler. The input data flow is grouped into N_{cw} packets of K bits. During each time slot (subframe), N_{cw} packets are encoded into $N_{cw} \cdot N$ bits, where $N = K/R$ is the codeword length. The MI-ACM algorithm selects a modulation scheme per chunk with $b_n \in B = \{1,2,4,6,8\}$ bits per QAM symbol, leading to

$$N_{cb} = N_q \sum_{n=1}^{N_{ch}} b_n \tag{5.4}$$

coded bits, where N_q stands for the number of payload symbols per chunk. Since N_{cb} is generally not an integer multiple of the codeword length, the number of codewords is calculated as

$$N_{cw} = \left\lfloor \frac{N_{cb}R}{K} \right\rfloor \tag{5.5}$$

codewords. The missing $N_{pad} = N_{cb} - N_{cw}N$ bits are inserted before interleaving as a cyclic repetition of the first N_{pad} bits of the codeword block. This is more efficient than simple zero-padding and incurs hardly any additional complexity.
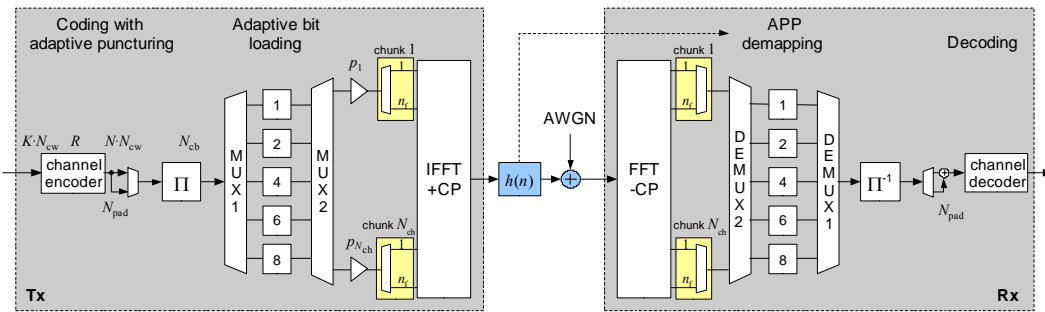

Figure 5.6: System model for frequency-adaptive transmission

---

[9] MI-ACM algorithm is also known as *Stiglmayr's algorithm.* Similar adaptation approach has been also proposed independently in [LR07].

The detailed description of the MI-ACM algorithm steps for the WINNER reference design can be found in [WIN2D223].

The performance of the MI-ACM algorithm is depicted in Figure 5.7, where CWER and throughput results of the proposed algorithm are compared with the reference results of Hughes-Hartogs ([Hug91]) optimum bit and power loading algorithm, and also with the non-frequency adaptive transmission performance. The presented simulation results have been obtained for three different scheduling assumptions: (a) – 21 random chunks scheduled for one user, (b) – 21 best chunks scheduled, and (d) – 5 random chunks scheduled. Two different packet lengths considered in the reference design, i.e. $K = 288$ and $K = 1152$ information bits, have been used to show the narrow-band staircase effect (d) for the latter K value. The WINNER B1 NLOS channel model has been used in all simulations.
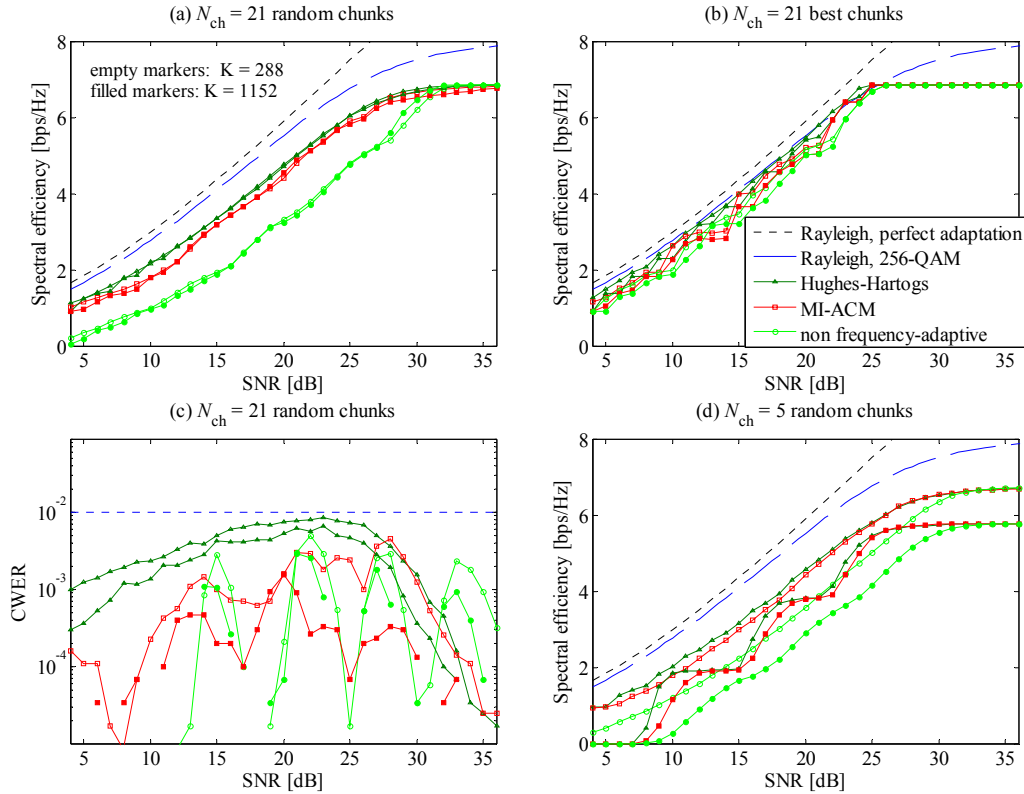

Figure 5.7: Throughput and CWER results of Hughes-Hartogs and MI-ACM algorithms for different chunk allocations (B1 NLOS channel model)

5.2.1.1 Modulation and coding schemes for the reference design

The reference design for the frequency adaptive transmission (cf. Section 5.2 of [WIN2D6135]) assumes the application of Stiglmayr's MI-ACM algorithm [SBC07], [PPS07] with rate-compatible punctured (RCP) BLDPC codes [WIN2D223]. The downlink control signalling overhead consists of **2 bits per each chunk** for indicating the modulation scheme and another **3 bits per each FEC block** (or even per frame) for selecting the code rate (puncturing pattern). This gives in total 32 possible combinations of the modulation and coding schemes (MCS). Table 5.2 presents the constellation sizes, denoted by b, the number of bits per constellation symbol, and the code rates represented by P, the number of punctured subblocks (cf. Equation (5.1)), that were proposed initially for the reference design.

Table 5.2: Overall rates $R \cdot b$ of the original Stiglmayr's MCS for the reference design

$b \setminus P$	0	4	8	12	16	18	20	22
1	0.50	0.55	0.60	0.67	0.75	0.80	0.86	0.92

2	1.00	1.09	1.20	1.33	1.50	1.60	1.71	1.85
4	2.00	2.18	2.40	2.67	3.00	3.20	3.43	3.69
6	3.00	3.27	3.60	4.00	4.50	4.80	5.14	5.54

Table 5.3: SINR thresholds [dB] of the original Stiglmayr's MCS for $K = 288$ and CWER = 0.01

P	0	4	8	12	16	18	20	22
$b \setminus R$	0.50	0.55	0.60	0.67	0.75	0.80	0.86	0.92
1	-1.03	-0.37	0.37	1.28	2.37	3.23	4.33	6.41
2	1.98	2.64	3.38	4.29	5.38	6.24	7.34	9.42
4	7.40	8.26	9.19	10.32	11.62	12.65	13.90	16.20
6	12.01	13.02	14.13	15.56	17.09	18.28	19.64	22.14

The set of SINR thresholds from Table 5.3 was provided for packets of size $K = 288$ information bits and 1% CWER. Please note that the SINR thresholds for the MCS marked with an orange background colour will **never** be used for an average code rate calculation in the Stiglmayr's MI-ACM algorithm. This is because in the first step the algorithm chooses the modulation scheme (picks one row from Table 5.3) for each chunk using the SINR thresholds marked with a green background colour. Moreover, the maximum throughput for the above MCS set is limited by the 64-QAM constellation, which results in a peak overall rate equal to 5.54 information bits per constellation symbol.

In order to optimise the selection of MCS for the WINNER reference design, investigations using a full set of available MCS for RCP BLDPC codes have been performed (cf. Section 3 in [WIN2D223]). To achieve higher throughput than 5.54 information bits per constellation symbol, 256-point QAM modulation should be included in the final MCS selection for the reference design. However, the maximum number of modulations used in adaptation is limited by the signalling overhead in each chunk (currently, only 2 bits are reserved for this purpose). Therefore, an introduction of the fifth modulation scheme is not considered. Instead, there are two solutions that can be used:

1. Assuming that the minimum code rate is $R = 1/3$, BPSK can be omitted from the set of adapted modulations: $b = \{2, 4, 6, 8\}$. In such case the minimum SINR value for which the chunk is used in the transmission increases by 3.01 dB (BPSK -> QPSK) to about 0.24 dB for $K = 288$ and CWER = 0.01. This solution seems to be a good compromise for frequency adaptive transmission, where the minimum SINR value for switching from non-frequency adaptive transmission is assumed as 4-5 dB.

2. Alternatively, the idea of a "sliding window" can be used: the modulation set is $b = \{1, 2, 4, 6, 8\}$, so it includes both BPSK and 256-QAM, but at the same time only 4 leftmost or rightmost constellations are used, depending on the operating SINR.

Figure 5.8 depicts throughput in the form of the number of information bits per constellation symbols for all possible combinations of modulation and rate compatible punctured BLDPC coding schemes.
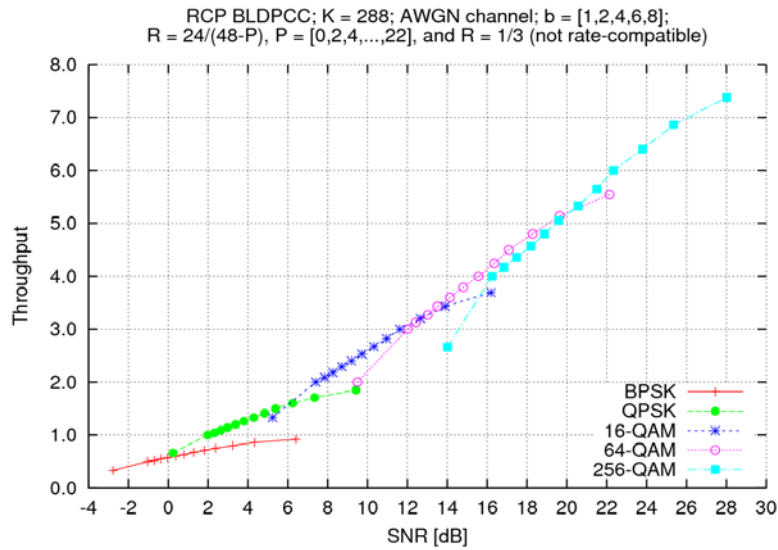
Figure 5.8: Throughput of all MCS for RCP BLDPCC at CWER = 0.01

Evaluations of the optimum subset of only eight code rates have been performed as well (cf. [WIN2D223]). As a result of these evaluations, the following conclusions have been drawn:

- For the most part of the assumed SINR range, i.e. from 5 dB to 25 dB the averaged code rate in the MI-ACM algorithm is between $R = 0.6$ and $R = 0.71$.

- Code rates higher than $R = 0.75$ are only used for very high SINR values (> 25 dB), where peak throughput is achieved for the highest constellation size (256-QAM in this case).

- The highest code rate $R = 0.92$ is almost[10] never chosen, because the proposed RCP BLDPC code can not decode packets with higher rates than $R = 0.92$. Therefore, all locally calculated rates are limited to $R = 0.92$. Since these local rates are averaged and rounded down to the next available code rate, $R = 0.86$ is the highest adapted value in practice.

These three observations suggest that to maximize the throughput a slightly different selection of code rates might be considered for the reference design. Table 5.4 shows the optimised set of MCS for the reference design with RCP BLDPC codes that has been proposed, whereas Table 5.5 and Table 5.6 present the SINR thresholds to achieve 1% CWER for packets sizes $K = 288$ and $K = 1152$ bits.

Table 5.4: Overall rates $R \cdot b$ of the new set of MCS for RCP BLDPC codes

$b \setminus P$	R=1/3	0	8	10	12	14	16	20
2	0.66	1.00	1.20	1.26	1.33	1.41	1.50	1.71
4	1.33	2.00	2.40	2.53	2.67	2.82	3.00	3.43
6	2.00	3.00	3.60	3.79	4.00	4.24	4.50	5.14
	2.66	4.00	4.80	5.05	5.33	5.65	6.00	6.86

Table 5.5: New SINR thresholds [dB] for RCP BLDPC codes (K = 288; CWER = 0.01)

P	R=1/3	0	8	10	12	14	16	20
$b \setminus R$	0.33	0.50	0.60	0.63	0.67	0.71	0.75	0.86
2	0.24	1.98	3.38	3.80	4.29	4.83	5.38	7.34
4	5.24	7.40	9.19	9.71	10.32	10.96	11.62	13.90
6	9.48	12.01	14.13	14.80	15.56	16.36	17.09	19.64

---

[10] *Almost* is used here, because it is theoretically possible to obtain this maximum rate $R = 0.92$, if the channel to noise ratios for all scheduled chunks are greater than or equal to the maximum SINR limit.

8	14.01	16.25	18.87	19.59	20.57	21.50	22.34	25.35

Table 5.6: New SINR thresholds [dB] for RCP BLDPC codes (*K* = 1152; CWER = 0.01)

P	R=1/3	0	8	10	12	14	16	20
b \ R	0.33	0.50	0.60	0.63	0.67	0.71	0.75	0.86
2	0.20	1.36	2.73	3.14	3.6	4.09	4.7	6.52
4	5.17	6.67	8.39	8.93	9.51	10.12	10.84	12.97
6	8.96	11.12	13.21	13.86	14.59	15.36	16.2	18.68
8	13.22	15.31	17.79	18.57	19.44	20.28	21.35	24.25

The comparisons of the throughput and CWER simulation results for various sets of MCS and *K* = 288 are shown in Figure 5.9 and Figure 5.10 (without code rate *R* = 1/3).

Figure 5.9: Throughput results of the Stiglmayr's MI-ACM algorithm for various MCS
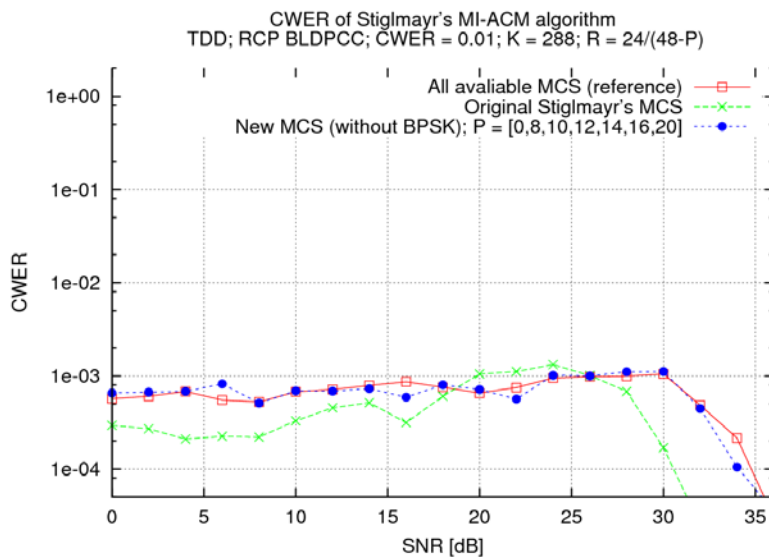

Figure 5.10: CWER results of the Stiglmayr's MI-ACM algorithm for various MCS

5.2.1.2   Possible gains from power-loading and non-square modulation formats

The MI-ACM algorithm does not apply power-loading, i.e. all chunks with $b_n > 0$ have the same transmit power. It is known from theory that power-loading yields an additional gain which is significant for low SINR and marginal for high SINR. Since frequency-adaptive transmission is applied for SINR > 5 dB, no significant gain can be expected from power loading. This has been confirmed by numerous simulations where the achieved rate with the MI-ACM algorithm was compared to the Hughes-Hartogs algorithm, which does apply power-loading and it is known to yield the optimum discrete bit-loading. The rates in Figure 5.7 for both algorithms are very similar, which shows not only that the possible gains from power-loading are insignificant but also that the MI-ACM algorithm is very close to the optimum solution. In Figure 5.7, it can be observed that the resulting CWER with the MI-ACM is even lower and that the CWER of $P_w \leq 0.01$ is fulfilled for all SINR.

From Figure 5.11, we can observe immediately that nothing can be gained from including 8- and 32-QAM. Only 128-QAM has a higher throughput than the adjacent square constellation for the two highest code rates $R = 4/5$ and $R = 6/7$ of DBTC.
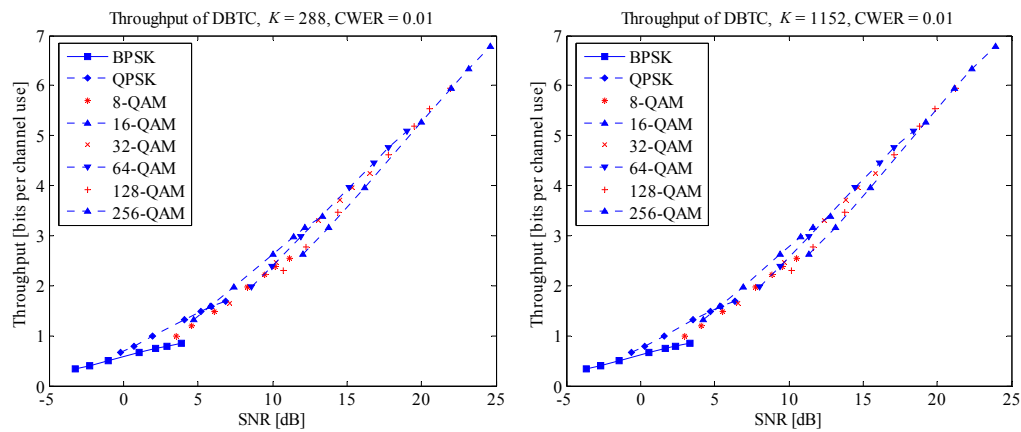

Figure 5.11: Throughput of all MCS at CWER = 0.01. The non-square 8-QAM and 32-QAM constellations result in lower throughput than the square ones. Only 128-QAM, for the two highest code rates, is marginally better than 64- and 256-QAM.

However, this small rate increase is hardly appreciable in the throughput curves in Figure 5.12. Thus, it is clearly not recommendable to consider non-square QAM constellations for the frequency-adaptive mode.
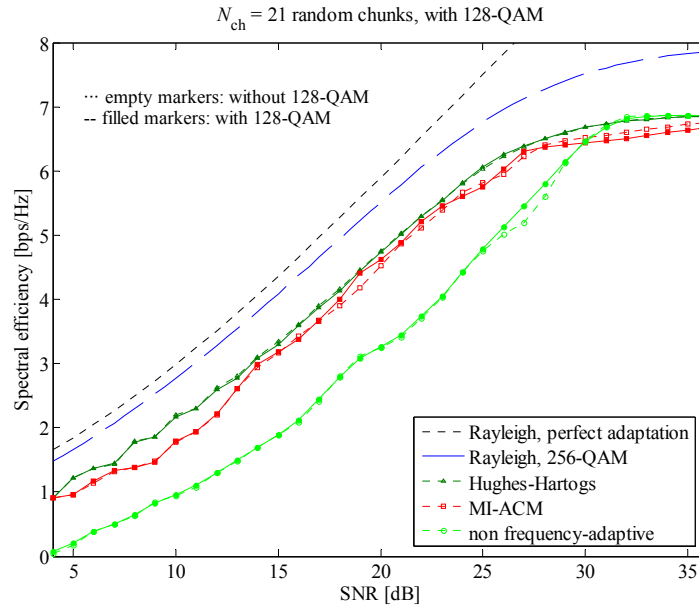
Figure 5.12: Achieved throughput with and without 128-QAM

5.2.2 Non-frequency adaptive transmission

The frequency-adaptive transmission described in the previous section utilizes the channel variability in the frequency domain. It uses individual link adaptation (adaptive modulation) within each chunk [WIN2D6135], and is typically combined with channel-aware scheduling which allocates chunk layers to users, further boosting the performance. In the WINNER reference design, this scheme is complemented by non-frequency adaptive transmission, which instead averages over the frequency-domain channel properties. This scheme is used when and where frequency-adaptive transmission is impractical or impossible. The same modulation is here used within all transmission resources assigned to a code block. The same coding schemes are assumed to be applied for non-frequency adaptive as for frequency-adaptive transmission. From a coding and decoding perspective, non-frequency adaptive transmission therefore just becomes a special case of the more general frequency adaptive transmission scheme, in which resource-individual adaptive modulation is not used.

The reference design for non-frequency adaptive transmission was outlined in section 5.3 of [WIN2D6135]. The downlink frame allocation control scheme for downlink as well as uplink transmissions is presented in [WIN2D61314].

The link adaptation used for non-frequency adaptive transmission is based on the average SINR, averaged over the resource blocks to be used. Such measurements can be collected on a time-scale corresponding to that of the shadow fading. Faster updates of SINR estimates are potentially advantageous in an environment with fast-varying interference whose power stays constant over short time intervals. This would result in better adjustment of the utilized modulation to the instantaneous interference level, thus reducing the need for retransmissions. It would be of particular value in the transmission of urgent control information, for which Hybrid ARQ cannot be used due to timing constraints.

The performance of non-frequency adaptive transmission is illustrated in Figure 5.12 and compared to the use of frequency adaptive transmission for one particular test scenario. The performance of non-frequency adaptive transmission is here much lower than for frequency adaptive transmission. It should be noted that this example uses SISO (single-antenna) transmission. Many multi-antenna schemes, such as beamforming and maximum ratio combining, equalize the frequency-domain properties of channels and tend to reduce their variability. When using such multi-antenna schemes, the performance difference between frequency adaptive and non-frequency adaptive transmission will tend to be smaller than the one illustrated above.

For non-frequency adaptive transmission, a particular mapping of code blocks onto transmission resources was proposed in [WIN2D461]. To harness adequate frequency diversity, it is important to be

able to map also small code blocks onto resource blocks that are widely dispersed in frequency. The current WINNER reference design maps code blocks to/from different users onto small rectangular time-frequency blocks (sub-bins) that are regularly spaced in frequency. This scheme, denoted B-EFDMA in downlinks and B-IFDMA in uplinks, is motivated by the following considerations:

- Use of orthogonal mapping (no code multiplexing) of flows to/from different users onto time-frequency resources simplifies the receivers.

- Use of small resource blocks increases the frequency diversity relative to allocation of whole chunks. It also decreases the padding losses when mapping small code blocks.

- The use of a regular spacing of resource blocks in frequency within a frame reduces the addressing overhead, It also reduces the addressing overhead needed for pre-defining the resources within the super-frame that are pre-allocated for frequency-adaptive and non-frequency adaptive transmission. (This partitioning is denoted *resource division* in the reference design.)

- A regular spacing of blocks in the frequency direction also enables the used of DFT-precoded uplink transmission which lowers the signal envelope variations. This variant is denoted block-IFDMA, or B-IFDMA.

- A short block duration in time (shorter than the chunk duration) enables terminals to restrict their activity to shorter transmit/receive intervals, thus reducing their power consumption. When transmission occurs, it will be concentrated in time. This improves the power amplifier efficiency, which further improves the power consumption budget.

- A short block duration in time furthermore increases robustness w.r.t. channel time variations within blocks. This is of major importance for the highest considered vehicular velocities, 250 km/h in the Wide Area scenario.

The basic B-EFDMA/B-IFDMA block size has for evaluation purposes been set to 4 subcarriers x 3 OFDM symbols. This corresponds to 1/8 of a chunk in the FDD baseline design and 1/10 of a TDD chunk. In uplink, each such block contains one known time-frequency pilot. These smallest blocks are of use for small packets, encoded by convolutional coding. For larger code block sizes, it is advantageous to combine the 4x3 blocks into larger units. Please see [WIN2D61314] for a further discussion on the balancing of the resource block sizes and [WIN2D233] for a discussion of channel estimation aspects.

5.3 Hybrid ARQ

The proposed HARQ scheme allows for a flexible implementation of incremental redundancy (IR) and repetition coding under a unified framework, providing a seamless transition from incremental redundancy to chase combining through the parameterization of the retransmission unit (RTU) size. The motivation has been to focus on minimising the number of required retransmissions to foster one of WINNER's features that is to allow fast retransmissions. On the other hand, the working assumption in WINNER is that modulation is controlled by an independent procedure (e.g. link adaptation), so it is a matter for the HARQ to handle retransmitted packets with different modulation formats. That implies the receiver to handle soft values. During retransmissions, the corresponding likelihoods obtained for the associated modulation are combined in a similar fashion as chase combining combines the proper likelihood values (L-values) of each retransmitted packet (details in [WIN2D223]).

The retransmission scheme sends at each retransmission a certain amount of redundancy, either additional parity bits or repeated bits in a cyclic shift fashion. Such a cyclic shift implementation allows parameterisation with a single parameter: retransmission unit length. The retransmission scheme only requires 1 bit acknowledgement to confirm correct packet transmission or to request a new retransmission. The only additional signalling required is associated to the initialization phase, where the retransmission mode is selected depending on system or service requirements, for instance, delay sensitiveness associated to data flows.

As an example, 2-bit signalling for initialisation allows 4 operating retransmission strategies which are pre-defined in Table 5.7. It will typically include a conservative mode which intends to minimise the number of required retransmissions, and modes that progressively reduce the amount of retransmitted redundancy with the aim of achieving throughput maximisation. In Table 5.7 mode 0 sends the same amount of redundancy data as the initial data packet, whereas mode 4 sends only a fraction of the initial data packet ($0<\alpha_i<1$ with $\alpha_1>\alpha_2>\alpha_3$,).

Table 5.7: Re-transmission operating modes with 2-bit signalling. *L* denotes the initial packet length in bits and $0<\alpha_i<1$.

Mode	RTU size
0	*L*
1	$\alpha_1 L$
2	$\alpha_2 L$
3	$\alpha_3 L$

Next, a description of the cyclic shift incremental redundancy implementation is detailed.

Based on the WINNER channel code candidate the retransmission scheme considers a mother code of rate 1/3. In each transmission the equivalent rate 1/3 codeword is stored in a buffer, then a given number of coded bits are selected according to the selected modulation and coding scheme. Given the selected operating coding rate, the first N_1 bits are selected for transmission: $[c(1) \ldots c(N_1)]$. If an error occurs, the retransmission mechanism will select the next bits in a sequential order: $[c(N_1+1) \ldots c(N_2)]$. The selection mechanism is illustrated in Figure 5.13 and Figure 5.14 for operating mode 0, that is, for the case where the RTU size is equal to the initial packet size. If a second retransmission is required it would send the remainder of the incremental redundancy and would fill up the RTU with repeated bits in a cyclic fashion: $[c(N_2+1) \ldots c(3K) \, c(1) \ldots c(N_3)]$, and so forth.
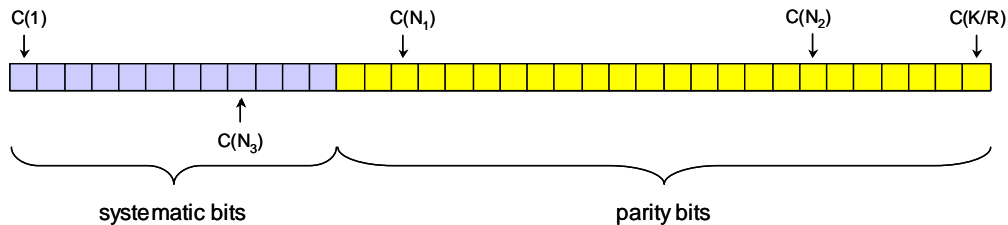

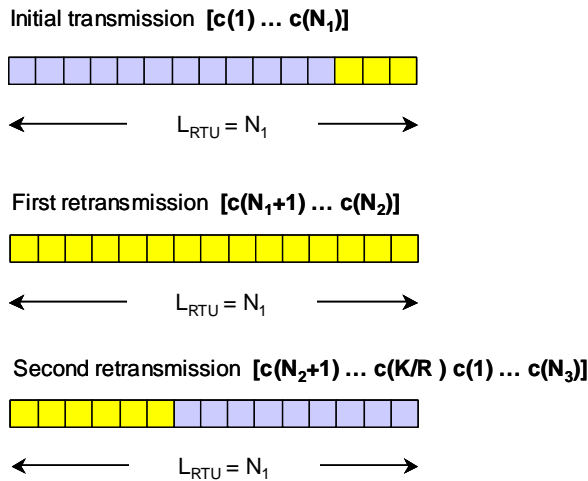**Figure 5.13: Codeword notation for a rate R=1/3 code**

Figure 5.14: Illustration of the generalized HARQ retransmission scheme: example of redundancy data sent in each retransmission, for a fixed RTU size with incremental redundancy and cyclic shift repetition coding

There exists an implementation to extend the rate compatibility of the channel code to include finer granularity. It consist of introducing an interleaver after the channel encoder followed by a buffer and a bit selection block. By properly designing the interleaver, a simple sequential selection of a given amount of the interleaved rate 1/3 codeword bits, results in an equivalent punctured codeword. This is especially

suitable for the proposed retransmission scheme since the HARQ operating modes could be determined independently of the specific modulation and coding schemes, by only specifying the fraction of redundancy bits with respect the packet length for transmission. The scheme is illustrated in Figure 5.15. Details of the particular implementation of the generalised puncturing via interleaving are described in [WIN2D223].
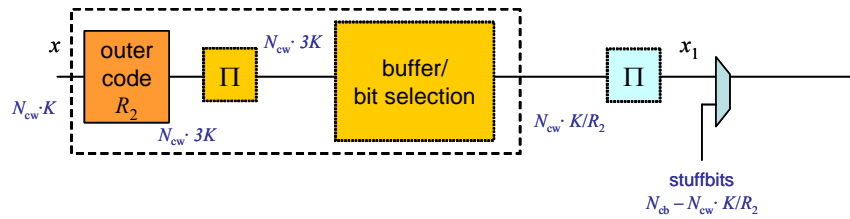

Figure 5.15: Rate compatible coding via interleaving and bit selection

6. Synchronisation procedures

Link level procedures are essential for a wireless system to work properly. Most of the radio access layer techniques rely on estimation of the channel parameters and on the fact that system elements are synchronised. The next paragraphs focus on two synchronisation procedures that are particularly relevant to the local area scenario. Further information on link level procedures, e.g. channel estimation, pilot design, can be found in [WIN2D233].

In Section 6.1 link-level synchronisation in a license-exempt scenario is discussed. Generally the link-level synchronisation problem is defined as estimating at the receiver the mismatch in time, frequency and phase, in order to recover when the message was emitted, at what frequency and with which phase. In Section 6.1 downlink synchronisation is more particularly addressed when narrowband interference or coexistence with other systems occur.

In Section 6.2 a self-organised network synchronisation technique is presented. Slot synchronisation is an enabler for TDD systems. All nodes in the network need to agree on a common time slotted structure, where the start of a time slot corresponds to the start of a super-frame. A self-organised network synchronisation algorithm is particularly important in the local area scenario where no GPS signal, which would provide a global timing reference, is available. Consequently a self-organised scheme is needed: no central entity is responsible for inter-cell synchronisation, and user terminals and base stations align their time reference by following simple rules, so that all agree on a common time slot structure. The proposed approach is inspired from the studies of synchronisation phenomena of fireflies in South-East Asia.

6.1 PHY Layer Synchronisation in License-Exempt Case

Synchronisation algorithms developed for spectrum sharing case are suitable for several spectrum sharing scenarios: horizontal sharing (HS) with or without coordination and vertical sharing (VS) scenario. Note that operation in license exempt bands corresponds to HS scenario without coordination.

In license exempt case transmission signal can be disturbed by narrowband interference (NBI), e.g. caused by Bluetooth signals transmitting simultaneously on overlapping frequencies. The effect of NBI is such that the common approach of using a dedicated training block composed of several repeated parts for timing and frequency acquisition would experience significant degradations. When NBI is present the signal received over the preamble is not any more symmetrical in time domain making it difficult to apply conventional synchronisation algorithms. Thus, in order to achieve good synchronisation in a spectrum sharing scenario, it is necessary to explicitly take care of NBI.

A preamble block composed of $3N$ time domain samples, corresponding to 3 OFDM symbols is used to perform the following operations: detection of NBI sources and timing synchronisation and carrier frequency offset estimation. After that the NBI sources have been detected (NBI detection phase) and the interfered sub-carriers have been set to zero (NBI cancellation phase), the virtually interference-free time domain samples of the preamble are fed to the synchronisation unit. The block diagram of the receiver is shown in Figure 6.1.
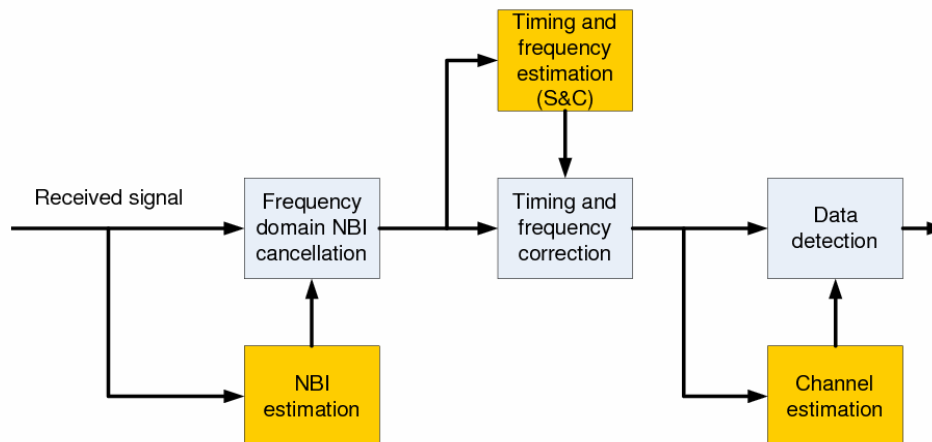

Figure 6.1: Receiver block diagram

The synchronization preamble is divided in two half blocks of size $3N/2$ symbols each (see Figure 6.2). The first half block contains the sequence $\{b_1(n)\}, n = 1, \ldots, 3N/2$ and the second half block contains the sequence $\{b_2(n)\}, n = 1, \ldots, 3N/2$, which is a replica of $b_1(n)$ rotated by a frequency corresponding to the subcarrier spacing $\Delta f = 1/(NT)$, i.e.

$$b_2(n) = b_1(n)e^{j\frac{2\pi n}{N}} \tag{6.1}$$

Thus, indicating with $s(n)$ the time domain samples (tds) transmitted in the preamble, it is

$$s(n) = \begin{cases} b_1(n) & n = 1, \ldots, 3N/2 \\ b_2(n - 3N/2) & n = 3N/2 + 1, \ldots, 3N \end{cases} \tag{6.2}$$
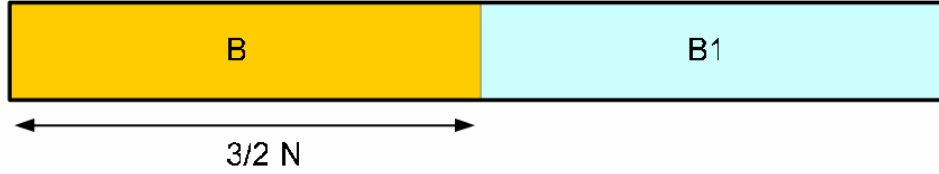

Figure 6.2: Proposed WINNER DL synchronisation preamble structure

The NBI detection algorithm relies on the specific structure of the preamble, which has been built to make the NBI detection algorithm robust to frame-synchronisation error θ up to $N/2$. At the receiver the tds of the preamble are grouped in two N-dimensional blocks $\mathbf{r}^{(0)} = [r(1), \ldots, r(N)]^T$ and $\mathbf{r}^{(1)} = [r(1 + 3N/2), \ldots, r(N + 3N/2)]^T$ where $r(n)$ is defined as

$$r(n) = x_\theta(n) + i(n) + n(n) \tag{6.3}$$

where $x_\theta(n)$ is the useful signal at the receiver delayed by θ samples and $i(n)$ are the time samples of NBI signal.

Neglecting noise and carrier frequency offset, $R^{(0)}(m)$, the m-th outcome of the DFT of $\mathbf{r}^{(0)}$, is

$$R^{(0)}(m) = H(m)S_\theta^{(0)}(m) + I^{(0)}(m), 0 \le m \le N\text{-}1 \tag{6.4}$$

and $R^{(1)}(m)$, the m-th outcome of the DFT of $\mathbf{r}^{(1)}$, is

$$R^{(1)}(m) = H(m)S_\theta^{(1)}(m) + I^{(1)}(m), 0 \le m \le N\text{-}1 \tag{6.5}$$

where $S_\theta^{(0)}(m)$ is the m-th output of the DFT of the vector $\mathbf{s}_\theta^{(0)} = [s(1-\theta), \ldots, s(N-\theta)]^T$, $S_\theta^{(1)}(m)$ is the m-th output of the DFT of the vector $\mathbf{s}_\theta^{(1)} = [s(1+3N/2-\theta), \ldots, s(N+3N/2-\theta)]^T$, and $I^{(0)}(m)$ and $I^{(1)}(m)$ are the DFT of the NBI in the two vectors. The channel $H(m)$ is assumed constant for the duration of the whole preamble.

Since the preamble is built with two sequences that are rotated with respect to each other of a frequency exactly equal to the sub-carrier spacing, there is a cyclic shift of a position between $S_\theta^{(0)}(m)$ and $S_\theta^{(1)}(m)$, i.e.

$$S_\theta^{(1)}(m) = S_\theta^{(0)}(m-1). \tag{6.6}$$

The above property can be exploited to reveal the presence of NBI. The metric $\Lambda(m) = R^{(0)}(m) - R^{(1)}(m-1)$ is

$$\Lambda(m) = S_\theta^{(0)}(m)((H(m) - H(m-1))) + I^{(0)}(m) - I^{(1)}(m-1) \tag{6.7}$$

Assuming that the channel does not exhibit sensible variations between adjacent sub-carriers, i.e. $H(m) \approx H(m-1)$, the desired signal is cancelled in previous equation resulting in

$$\Lambda(m) = I^{(0)}(m) - I^{(1)}(m-1) \tag{6.8}$$

Thus, in the following we compare $\left|\Lambda(m)\right|^2$ with an adequate threshold to detect the presence of NBI.

The synchronisation algorithm has to cope with larger offsets and can be easily adapted to be very robust to any frequency offset. The effect of a frequency offset ν is a fixed phase rotation $\phi = 2\pi \dfrac{3}{2}\nu$ between corresponding elements of the vectors $\mathbf{s}_\theta^{(0)}$ and $\mathbf{s}_\theta^{(1)}$. Thus being the DFT a linear operator, this fixed rotation phase translates also on $\mathbf{S}_\theta^{(0)}$ and $\mathbf{S}_\theta^{(1)}$ and it is

$$S_\theta^{(1)}(m) = S_\theta^{(0)}(m-1)e^{j\phi} \tag{6.9}$$

Therefore, to remove the effect of the phase offset ϕ, the metric $\Lambda(m)$ needs to be modified in

$$\Lambda(m) = \left| R^{(0)}(m) \right| - \left| R^{(1)}(m-1) \right|. \tag{6.10}$$

Let Ψ be the set of the subcarriers that have been detected as interfered, interference is removed by setting to zero the sub-carriers in Ψ so that the timing synchronisation and the carrier frequency estimation algorithms can work reliably. Figure 6.3 shows how NBI cancellation is implemented:

- The tds $r(n), n = 1,\ldots,N_1$ of the received signal are fed to a DFT device that yields $R(m), m = 1,\ldots,N_1$. The DFT length N_1 is chosen to include the whole synchronisation preamble, so that all the interference is removed at the same time.

- Most of the interference is removed by setting to zero all the subcarriers in Ψ. This operation yields $\widetilde{R}(m), m = 1,\ldots,N_1$ such that

$$\widetilde{R}(m) = \begin{cases} 0 & m \in \Psi \\ R(m) & \text{otherwise} \end{cases} \tag{6.11}$$

The symbols $\widetilde{R}(m)$ are fed to an IFFT device to generate the virtually interference-free tds $\widetilde{r}(n)$.
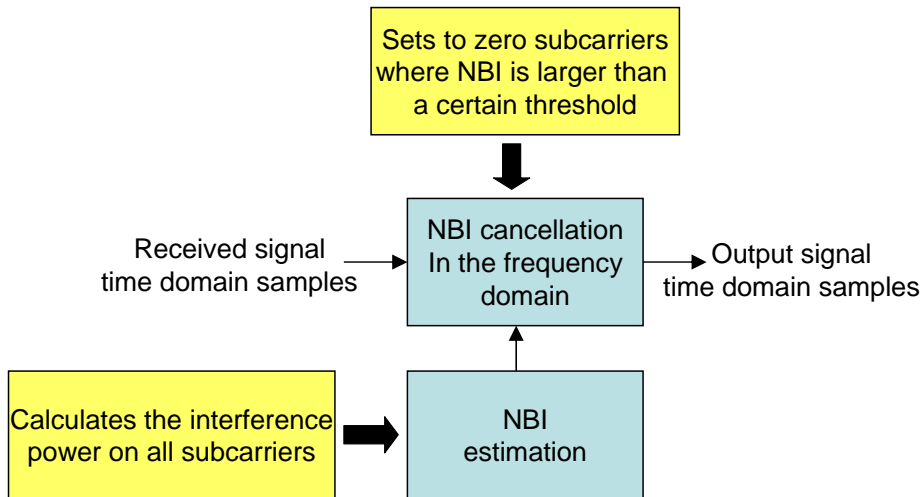

Figure 6.3: NBI cancellation block diagram

In spectrum sharing case, symbol and timing estimation are performed according the algorithm proposed by Schmidl & Cox (S&C). Since we assume to have cancelled all the NBI, interference does not appear explicitly anymore in the received signal equations.

Signal synchronisation is performed using the same preamble block employed for NBI detection, composed by two semi-blocks of size $3N/2$ tds each. As already mentioned, the second semi-block contains the sequence $b_2(n)$ that is a replica of the sequence transmitted in the first semi-block $b_1(n)$ rotated by a frequency corresponding to the subcarrier spacing.

Timing synchronisation is achieved by maximization of the timing metric $\Lambda(d) = |P(d)|^2 / R^2(d)$, i.e.

$$\hat{\theta} = \arg\max\{\Lambda(d)\}. \tag{6.12}$$

The difference with the standard S&C is that the tds of the second semi-block need to be counter-rotated before being correlated with the tds of the first semi-block and thus it is

$$P(d) = \sum_{n=0}^{N-1} \tilde{r}^*(n+d)\tilde{r}(n+d+3N/2)e^{-j2\pi n/N} \tag{6.13}$$

while $R(d)$ normalizes the timing metric with respect to the energy received on the training symbol, i.e.

$$R(d) = \sum_{n=0}^{N-1} |\tilde{r}(n+d)|^2 . \tag{6.14}$$

The frequency estimation algorithm has to deal with the frequency shift $\Delta f = 1/(NT)$ of the sequence $b_2(n)$ with respect to the sequence $b_1(n)$. In fact, after having estimated the correct timing, the N-leg correlation of the tds of the two semi-blocks yields

$$S = \sum_{n=0}^{N-1} \tilde{r}^*(n+\hat{\theta})\tilde{r}(n+\hat{\theta}+3N/2)e^{-j2\pi n/N} = \sum_{n=0}^{N-1} |x(n)|^2 e^{j2\pi(3v/2+d_0/N)} + w_0 . \tag{6.15}$$

where $d_0 = \hat{\theta} - \theta$ introduces a bias on the frequency estimate. To overcome this problem in the following we assume that the $3N/2$ tds of $b_1(n)$ are obtained as the three-fold repetition of a primary sequence $b_0(n)$ of $N/2$ tds, so that $b_1(n) = b_0(\mod(n, N/2))$. Exploiting the periodicity of the training sequence, the carrier frequency offset can be estimated as the mean of $\hat{v}_1$, the offset estimated on the first semi-block and $\hat{v}_2$, the offset estimated on the second semi-block. Thus, let S_1 and S_2 be the $N/2$-leg correlations of the tds of the first and second semi-block, respectively

$$S_1 = \sum_{n=0}^{N/2-1} \tilde{r}^*(n+\hat{\theta})\tilde{r}(n+\hat{\theta}+N/2) = \sum_{n=0}^{N/2-1} |x(n)|^2 e^{j\pi vN} + w_1 . \tag{6.16}$$

and

$$S_2 = \sum_{n=0}^{N/2-1} \tilde{r}^*(n+\hat{\theta}+3N/2)\tilde{r}(n+\hat{\theta}+2N) = \sum_{n=0}^{N/2-1} |x(n)|^2 e^{j\pi(v+1)N} + w_2 . \tag{6.17}$$

Then, the offset calculated on the first semi-block is $\hat{v}_1 = \frac{1}{\pi}\arg\{S_1\}$ and the offset calculated on the second semi-block is $\hat{v}_1 = \frac{1}{\pi}\arg\{S_2\} - 1$ and an unbiased estimate of the frequency offset is

$$\hat{v} = \frac{\hat{v}_1 + \hat{v}_2}{2} . \tag{6.18}$$

Performance Evaluation

This section evaluates the performance of the proposed NBI cancellation algorithm. The results have been obtained in the presence of several randomly located NBI interferers modelled as pulse amplitude modulated signals, each occupying a bandwidth of 1MHz. The signal to interference ratio (SIR) is defined as the ratio of the average power received over a sub-carrier of the desired signal and the power of the interfering signal. An indoor scenario is considered in subsequent simulations.

Figure 6.4-Figure 6.6 show the timing histograms obtained without interference, with interference and with interference cancellation, respectively. Correct synchronisation is achieved if the timing estimate lies inside the range $[CP_{length} - L, 0]$ where L is the channel length. Results show that in absence of interference cancellation, synchronisation in presence of strong interferers is impossible. On the other hand, Figure 6.6 shows that the timing histogram measured after cancellation is very close to the ideal optimum of the interference-free case.
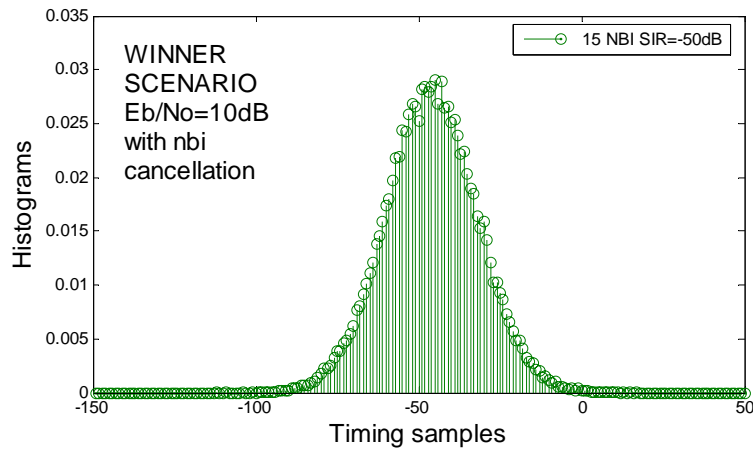
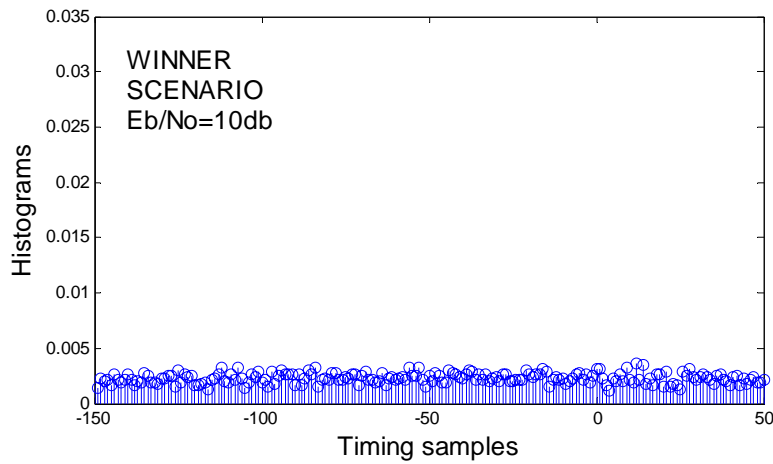**Figure 6.4: Histogram of timing estimator without NBI**

Figure 6.5: Histogram of timing estimator with NBI without cancellation
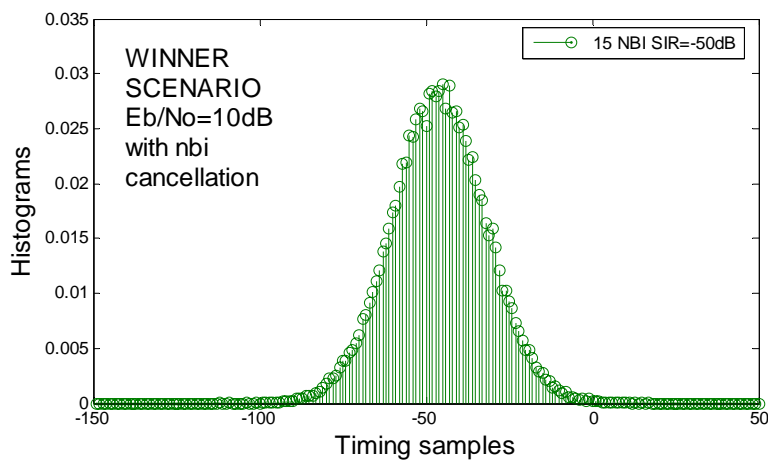

Figure 6.6: Histogram of timing estimator with NBI cancellation

6.2 Self-organised network synchronisation

Network synchronisation is defined as aligning all internal time references within the network, so that all nodes agree on the start and end of a super-frame. To do so in a self-organised manner, similar rules to the ones used in nature by fireflies are applied: each node maintains a time reference, referred to as the phase function, which is updated upon reception of a pulse from other nodes. The update rule is extremely important, and it was shown by Mirollo and Strogatz in their seminal paper [MS90] that the phase increment, which is a function of the internal phase, needs to be always strictly positive.

6.2.1 Firefly Synchronisation

A firefly is modelled as a pulse oscillator that flashes periodically and interacts with other nodes through pulses. This class of oscillators is termed *pulse-coupled oscillators*. These systems are known to show interesting phenomena ranging from perfect synchrony to pattern formation [GDL+00].

This section describes how time synchronisation is achieved between pulse-coupled oscillators, i.e. all oscillators pulse simultaneously. First, a mathematical model is associated with these oscillators. Then the scheme and conditions for a system of N oscillators to synchronise are presented.

Mathematical Model

As a simple mathematical representation, a pulse-coupled oscillator is described by its phase function $\phi_i(t)$. This function evolves linearly over time:

$$\frac{d\phi_i(t)}{dt} = \frac{\phi_{\text{th}}}{T} \quad . \tag{6.19}$$

When the phase reaches a threshold value ϕ_{th}, the oscillator is said to *fire*, meaning that it will transmit a pulse and reset its phase. If not coupled to any other oscillator, it will naturally oscillate and fire with a period T. Figure 6.7(a) plots the evolution of the phase function during one period when the oscillator is isolated.
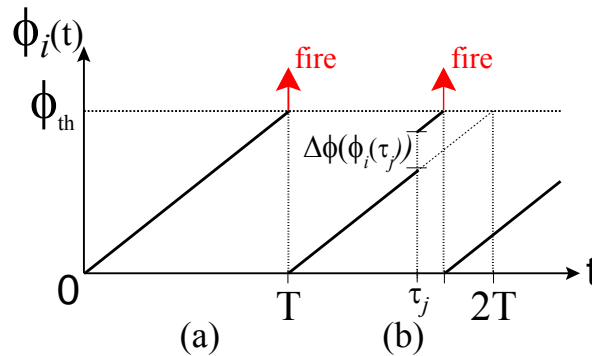

Figure 6.7: Time evolution of the phase function (a) for an isolated node, (b) upon reception of a pulse at instant τ_j

The phase function can be seen as an internal counter that dictates when a pulse should be emitted. The goal of the synchronisation algorithm is to align all internal counters, so that all nodes agree on a common firing instant. To do so, the phase function needs to be adjusted. In the following, we consider that all nodes have the same dynamics, i.e. clock jitter is considered negligible.

Synchronisation of oscillators

When coupled to others, an oscillator i is receptive to the pulses of its neighbours. Phase adjustment is performed upon the reception of a single, and depends on the current phase value at the receiver. When receiving a pulse at instant τ_j, a node instantly increments its phase by an amount that depends on the current value:

$$\phi_i(\tau_j) \rightarrow \phi_i(\tau_j) + \Delta\phi(\phi_i(\tau_j)) \text{ when receiving a pulse.}$$

Figure 6.7(b) plots the time evolution of the phase when receiving a pulse. The received pulse causes the oscillator to fire early. By appropriate selection of $\Delta\phi(\phi_i)$, a system of N identical oscillators forming a fully meshed network is able to synchronise their firing instants within a few periods [MS90].

The phase increment $\Delta\phi(\phi_i(\tau_j))$ is determined by the Phase Response Curve (PRC), which was chosen to be linear in [MS90]:

$$\phi_i(\tau_j) + \Delta\phi(\phi_i(\tau_j)) = \min(\alpha \cdot \phi_i(\tau_j) + \beta, \phi_{th}) \qquad (6.20)$$

where α and β determine the coupling between oscillators. In the following the threshold ϕ_{th} is normalised to 1. It was shown in [MS90] that if the network is fully meshed, the system always converges, i.e. all oscillators will agree on a common firing instant, for $\alpha > 1$ and $\beta > 0$.

An example of the synchronisation of pulse-coupled oscillators is shown in Figure 6.8.
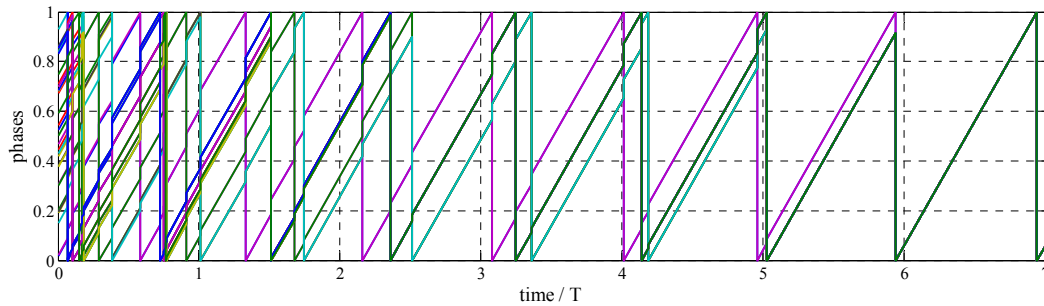

Figure 6.8: Synchronisation emerges from an initially random situation

In Figure 6.8, initially all nodes start with a random phase, which increments until one phase reaches the threshold. At this instant and each time a phase reaches the threshold value ϕ_{th}, all nodes increment their phase. Over time, order emerges from a seemingly chaotic situation where nodes fire randomly, and after 6 periods in Figure 6.8, all nodes fire in synchrony. Thus synchronisation is achieved in a dynamic fashion after several periods.

This synchronisation property is very appealing. Nodes do not need to distinguish between transmitters, and simply need to adjust their internal clock $\phi_i(t)$ by a phase increment when receiving a pulse and transmit a pulse when firing. After some time, synchronisation emerges from an initially unsynchronised situation, and pulses are transmitted synchronously.

Refractory Period

When delays are introduced in the system, such as propagation delays, a system of pulse-coupled oscillators becomes unstable, and the system is unable to synchronise [EPG95]. To regain stability, a refractory period of duration T_{refr} is introduced after transmitting. During this period no phase increment is possible [HS03]. A node's receiver is switched on during this period, but the phase function stays equal to 0 even if a synchronisation message is received.

The appropriate choice of T_{refr} is important, and may be determined through simulations. In general the value of T_{refr} cannot be too small as it helps limiting the number of interactions per period (and thus remain stable) and cannot be too large to enable some interactions between nodes.

In this section, we first review the super-frame preamble structure that is currently defined and used for synchronisation. Then a self-organised network synchronisation scheme derived from the firefly synchronisation principle is extended to fit into the super-frame preamble. Two modes are considered. The first one considers that cells are completely misaligned, e.g. some cells transmit the super-frame preamble when other cells transmit data. The second mode deals with tracking synchronisation offsets and keeping the network synchronised. More detailed description of the firefly synchronisation and simulation results are available in [WIN2D233].

6.2.2 Synchronisation Rules and Process for WINNER

Initially when a UT accesses the network, it needs to synchronise with its base station by following its timing reference, so that it does not disturb ongoing transmissions. This Master-Slave type of synchronisation is fine for intra-cell synchronisation, and is currently deployed in GSM and UMTS networks.

The synchronisation of pulse-coupled oscillators presents the advantage that synchronisation emerges from *any* random initial situation, and does not have pre-requisites regarding the distribution of initial firing instants. Thus self-organised synchronisation enables to cope with changes in the topology, which is especially interesting in mobile systems, where wireless communications do not guarantee that all nodes in the network are connected.

Given the super-frame structure, Figure 6.9 presents the two state machines defined for BSs and UTs as well as the super-frame preamble structure, when nodes are synchronised. To force the formation of two groups, one formed by BSs and the other by UTs, the phase function of BSs is adjusted when detecting a transmission from UTs, and vice versa. Hence two distinct synchronisation sequences "UL Synch" and "DL Synch" are used.
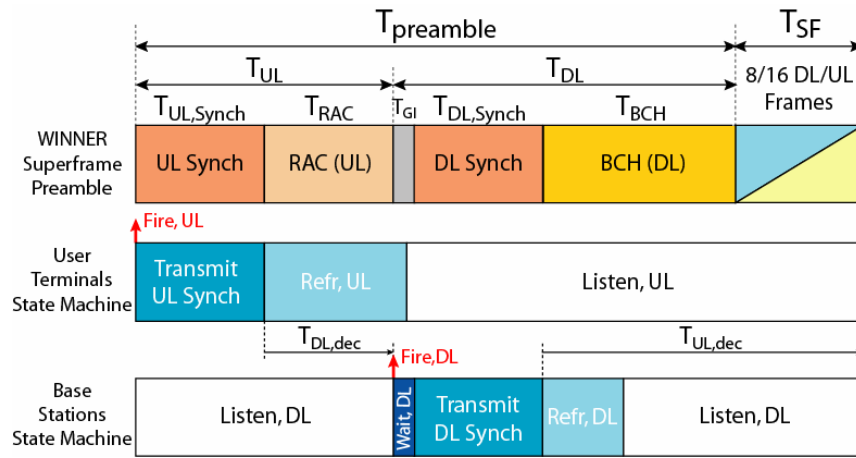

Figure 6.9: State Machines of Network Synchronisation units for coarse misalignments

Based on the two state machines of Figure 6.9, interactions occur between the two groups (BSs and UTs) when a node transmits and nodes from the other group detect this transmission. Detection of the distinct synchronisation words is done by the PHY link synchronisation. This allows for robust detection and avoids too much additional processing at the receiver.

Based on the super-frame structure, the listening time for user terminals and base stations is equal to:

$$T_{\text{UL,Rx}} = (T_{\text{preamble}} + T_{\text{SF}}) - (T_{\text{UL,Sync}} + T_{\text{refr,UL}})$$ (6.21)

$$T_{\text{DL,Rx}} = (T_{\text{preamble}} + T_{\text{SF}}) - (T_{\text{DL,Sync}} + T_{\text{refr,DL}})$$ (6.22)

Based on the firefly synchronisation rules presented earlier, slot synchronisation requires all nodes to maintain a phase function that is adjusted. Thus all user terminals maintain a phase function, which increments linearly over time:

$$\frac{d\phi_i(t)}{dt} = \frac{1}{T_{\text{UL,Rx}}}$$ (6.23)

where $T_{\text{UL,Rx}}$ is the listening period of a user terminal and is to be defined later.

Similarly all base stations maintain a phase function:

$$\frac{d\phi_i(t)}{dt} = \frac{1}{T_{\text{DL,Rx}}}$$ (6.24)

where $T_{\text{DL,Rx}}$ is the listening period of a user terminal and is to be defined later.

Key to separating nodes into two predefined groups is done in two parts:

- Coupling at Base Stations: if at instant τ_j, a BS node i is in 'Listen' state, where its phase function ϕ_i linearly increments over time, and a UT node j, which can communicate with i, started transmitting $T_{\text{UL,Synch}} + T_{\text{DL,dec}}$ before, then the receiving BS node i increments its current phase ϕ_i:

$$\phi_i(\tau_j) \rightarrow \phi_i(\tau_j) + \Delta\phi_{\text{BS}}(\phi_i(\tau_j)) \text{ where } \phi + \Delta\phi_{\text{BS}}(\phi) = \alpha_{\text{BS}} \cdot \phi + \beta_{\text{BS}} \qquad (6.25)$$

- Coupling at User Terminals: if at instant τ_i, a UT node j is in 'Listen' state, where its phase function ϕ_j linearly increments over time, and a BS node i, which can communicate with j, started transmitting $T_{\text{DL,Synch}} + T_{\text{UL,dec}}$ before, then the receiving UT node j increments its current phase ϕ_j:

$$\phi_j(\tau_i) \rightarrow \phi_j(\tau_i) + \Delta\phi_{\text{UT}}(\phi_j(\tau_i)) \text{ where } \phi + \Delta\phi_{\text{UT}}(\phi) = \alpha_{\text{UT}} \cdot \phi + \beta_{\text{UT}} \qquad (6.26)$$

Thanks to this strategy, the formation of two groups is controlled: starting from a random initial state, where all nodes fire randomly, after following the simple coupling rules, UTs and BSs separate over time into two groups, all BSs firing T_{UL} after UTs and all UTs firing T_{DL} after BSs. This state corresponds to a synchronised state.

6.2.3 Time to Synchrony in the Local Area Scenario

To validate the proposed scheme, further Monte-Carlo based simulations are conducted. Thanks to those simulations the convergence of the algorithm is evaluated, and more precisely the time taken by a given network to perform slot synchronisation.

The local area scenario considers that four antenna arrays are placed within corridors. The network topology considered for simulations for 15 user terminals participating to the network synchronisation is depicted in Figure 6.10.
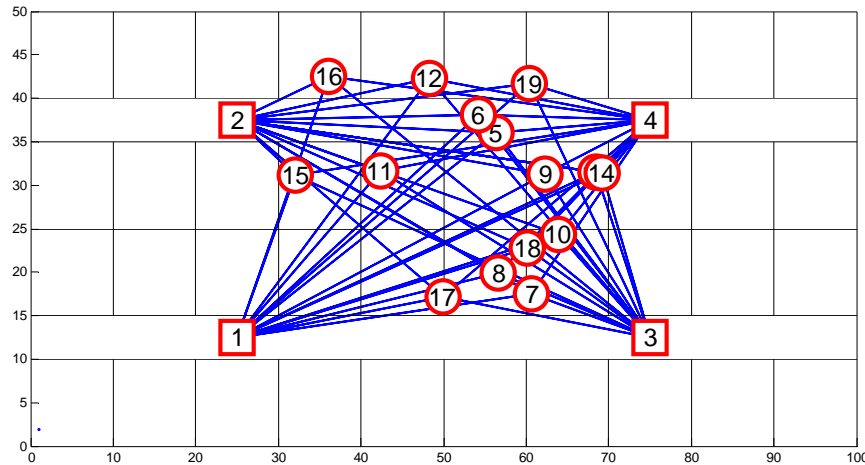

Figure 6.10: Considered Network Topology for 15 UTs

To accelerate the synchronisation process, it is useful to limit the number of user terminals that participate to the synchronisation process. In Figure 6.10 user terminals, which are marked as circles, can communicate directly with all base stations, which are marked as squares, and cannot communicate directly. User terminals that do not participate to the network synchronisation procedure do not transmit the "UL Sync" word, and adjust their slot oscillator based on received "DL Sync" words.

The following simulation results look at the time needed for the entire network to synchronise, i.e. all user terminals fire simultaneously before all base stations fire simultaneously. The time to synchrony T_{sync} is

normalised to the duration a super-frame T_{SF}, and is evaluated for 5,000 sets of initial conditions, i.e. all participants initially commence with a uniformly distributed random clock value, as the coupling value at user terminals α_{UT} varies. Base stations parameters are set to: $\alpha_{BS} = 1.1$, $\beta_{BS} = 0.01$ for the coupling, and $T_{refr,DL} = 10 \cdot T_s$ where T_s is the duration of an OFDM symbol. User terminal parameters are set to $\beta_{UT} = 0.01$ and $T_{refr,UL} = 10 \cdot T_s$. Figure 6.11 and Figure 6.12 show the cumulative distribution function of the normalised time to synchrony for 10 and 25 participating user terminals.
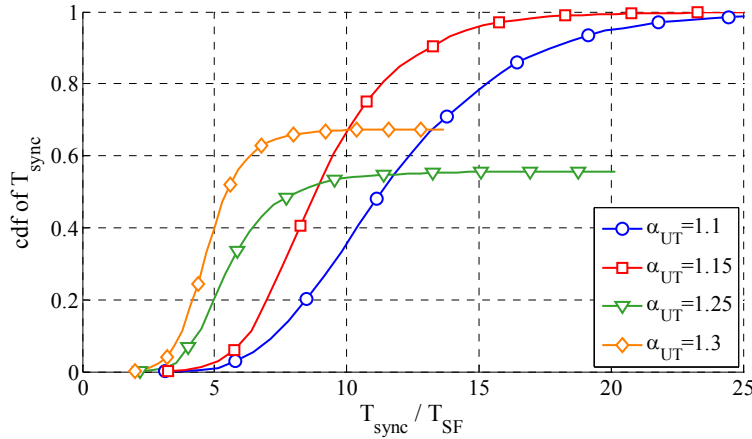

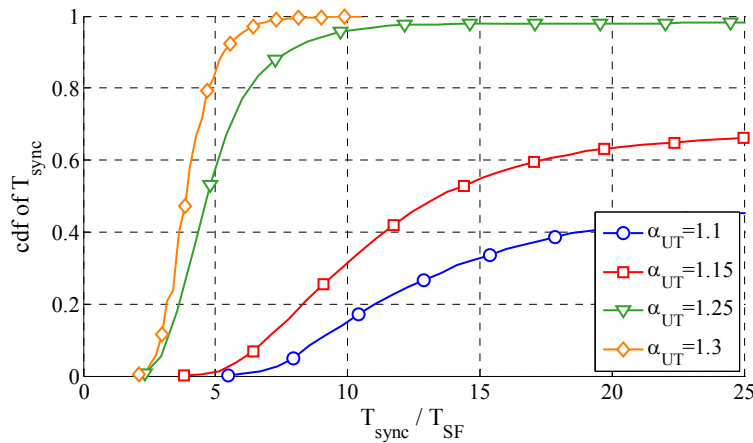Figure 6.11: Local Area Results for 10 UTs

Figure 6.12: Local Area Results for 25 UTs

From these figures, the performance of the proposed slot synchronisation algorithm augments as the number of nodes in the system increases.

For 10 user terminals, low coupling values is preferable, as synchronisation is always reached for $\alpha = 1.1$ and $\alpha = 1.15$. For higher coupling values, synchronisation is not always reached, but convergence is quicker.

As the number of user terminals increases, the results for high coupling improve: synchronisation is always reached for $\alpha = 1.25$ and $\alpha = 1.3$ and the time to synchrony is always below 10 super-frames. For 90% of initial conditions, T_{sync} is equal to 5 periods when $\alpha = 1.3$.

7. Spatio-temporal processing

In this section, performance evaluation results of the reference design for the spatio-temporal processing schemes are presented. We first review the main aspects of the reference design and then discuss the performance of the schemes.

In order to obtain a realistic impression of the actual performance of the proposed schemes, simulations were aligned to the base line local area scenario setup as described in section 4. Deviations from the base line configuration will explicitly be stated. Also, if not stated otherwise, the simulations account for overhead in terms of pilots and feedback as well as imperfections such as CSI errors or RF impairments.

7.1 Multi-user MIMO reference design

From the multi-antenna perspective, the local area scenario has a number of specific characteristics that enable us to efficiently exploit the spatial degrees of freedom of the MIMO channel. First of all, the user mobility is expected to be low which results in relatively large coherence times. Therefore channel state information is valid over larger time intervals. Secondly, the time division duplexing allows to acquire downlink channel state information from uplink transmissions by relying on the reciprocity of the MIMO channel. Finally, the coverage area is expected to be rather small which enables us to deploy distributed antenna arrays at the base station which can be synchronized through fibre links. This deployment will lead to a more even distribution of transmit power and it will decorrelate the users' channels, which allows having several users sharing the same time and frequency resources.

For the downlink transmissions the reference design is therefore chunk-wise adaptive multi-user MIMO precoding based on instantaneous CSI. In particular, the linear precoding techniques Successive MMSE [HSG05] and Regularized Block Diagonalization [SH07] are able to efficiently exploit the spatial degrees of freedom while still being rather robust against channel state information errors. The performance assessment demonstrates that even with imperfect CSI a large number of terminals can be served on the same time/frequency resources, resulting in significantly increased spectral efficiencies.

For the uplink transmissions the major effort in suppressing multi-user interference resides at the base station. Here, we propose a combination of successive interference cancellation with linear receivers where the SMMSE and RBD techniques can again be used efficiently. At the user terminals in the non-frequency adaptive mode open-loop Alamouti space-time coding can be used to exploit the two UT antennas without requiring any channel state information. In the frequency-adaptive mode the optimum transmit antenna weights can be precomputed by the base station and then sent to the user terminals via feedback.

7.1.1 Downlink reference design

The downlink reference design is based on exploiting the instantaneous channel state information that is available at the base station due to the combination of TDD with low user mobility. It enables us to perform chunk-wise adaptive multi-user MIMO precoding. We have to take into account that we do not have perfect CSI due to a limited number of pilots available for channel estimation and due to imperfections in the RF components which violate the reciprocity assumption. Since non-linear precoding schemes are in general rather sensitive to CSI imperfections we focus our attention on linear precoding schemes. It has been shown that by successively optimizing the users' subspaces we can extract the full antenna diversity of the MIMO channel by means of SMMSE [HSG05] or RBD [SH07] precoding. At the user terminals, MMSE filtering should be used to combine the signals from the two receive antennas.

7.1.1.1 System model and linear precoding

The system model is shown in Figure 4.1. The base station is equipped with M_T antennas, each user terminal with $M_{\mathrm{R},k} = 2$ antennas. There are K users in total out of which K_cc are served simultaneously within one chunk via SDMA. Consequently, the total number of receiving antennas is equal to $M_\mathrm{R} = \sum_{k=1}^{K_\mathrm{cc}} M_{\mathrm{R},k} = 2 \cdot K$. Each user receives $r_k = 1$ data stream, the total number of data streams is therefore equal to $r = \sum_{k=1}^{K_\mathrm{cc}} r_k = K_\mathrm{cc}$.

The data model can be summarized as

$$y = D \cdot \left(H \cdot F \cdot x + n \right)$$

where $D \in \mathbb{C}^{r \times M_R}$ is a block-diagonal matrix containing the receive filters $D_k \in \mathbb{C}^{r_k \times M_{R,k}}$, the matrix $H \in \mathbb{C}^{M_R \times M_T}$ represents the MIMO channel matrix, $F = [F_1, \cdots, F_K] \in \mathbb{C}^{M_T \times r}$ denotes the overall precoding matrix and the vectors x, y and n represent the vectors of sent symbols, received symbols and additive noise at the receive antennas, respectively.
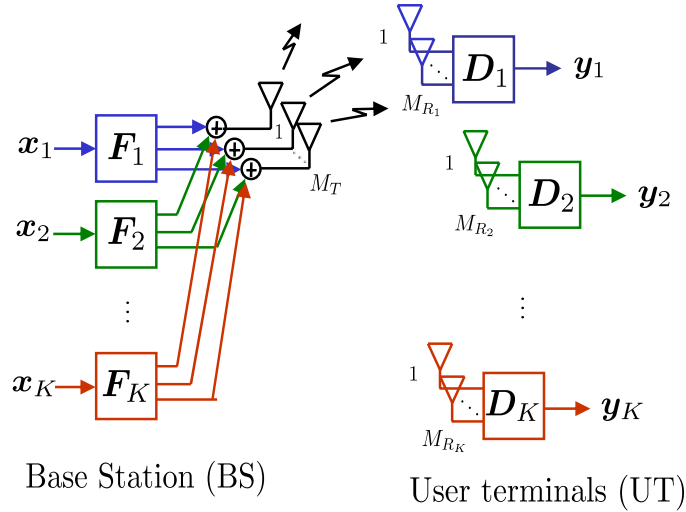

Figure 7.1: System model for the downlink

We assume that the base station has acquired channel state information from K users through dedicated pilots in the users' uplink transmission. Note that in case the users were divided into contention bands to reduce the pilot overhead, K refers to the number of users per contention band, i.e. the number of users that compete for assignment of the resources of one chunk. It is the task of the scheduler to find a group of K_{cc} out of K users that is optimum in terms of a suitable criterion (such as maximum sum throughput under fairness constraints). In the Local Area scenario the number of possible combinations can be very large which renders an exhaustive search infeasible. We propose to use the low-complexity approach ProSched, which is described in detail in [WIN2D341].

The task of the linear precoder is to compute the precoding matrices $F_k \in \mathbb{C}^{M_T \times r_k}$ such that the multi-user interference is minimized while balancing it with noise enhancement. The linear precoding techniques Successive Minimum Mean Square Error (SMMSE) precoding and Regularized Block Diagonalization (RBD) are able to extract the full antenna diversity by successively optimizing the users' subspaces. Details on these algorithms are described in [WIN2D341].

If distributed antennas are deployed, the spatial correlation of the users can become very low, in which case the scheduler may decide for very large SDMA group sizes. For example, for 32 transmit antennas, group sizes of up to 30 were observed. In this case, the channel matrix H has more rows than columns (i.e. it is "tall") which makes it impossible for the precoder to block-diagonalize it. We can however make use of the fact that the user terminals will apply MMSE filters to combine their signals, since the combined matrix $D \cdot H$ is always "flat" and can therefore be block-diagonalized. The difficulty is that we are trying to optimize the precoding matrix F for the combined matrix $D \cdot H$ even though the user terminals will tune their receive MMSE filters D from the estimated effective downlink channels given by $H \cdot F$. As a solution we propose the following iterative method

1. Initialize the receive filters $\boldsymbol{D}_k^{(0)}$ to the MRC solution obtained from the SVD of the channel matrix.

2. Set $n = 0$.

3. Compute the precoding matrices $\boldsymbol{F}_k^{(n)}$ from the combined channel $\boldsymbol{H}_{\mathrm{c}}^{(n)} = \boldsymbol{D}^{(n)} \cdot \boldsymbol{H}$.

4. Compute the MMSE receive filters $\boldsymbol{D}_k^{(n)}$ from the effective downlink channel matrix $\boldsymbol{H}_{\mathrm{e}}^{(n)} = \boldsymbol{H} \cdot \boldsymbol{F}^{(n)}$.

5. Test for convergence, e.g., by comparing the precoding matrices between iterations. If they do not change significantly between iterations, stop. Otherwise, set $n = n + 1$ and jump to step 3.

Note that this iterative method is not required if the total number of receive antennas M_{R} is less than the total number of transmit antennas M_{T}. In our setup this is true when the scheduler decides for a user group with $K_{\mathrm{cc}} \leq M_{\mathrm{T}} / 2$.

7.1.1.2 Signalling requirements

The chunk-wise adaptive multi user MIMO precoding requires instantaneous channel state information at the base station. To acquire it, we rely on the reciprocity of the TDD system. We therefore require the user terminals to transmit dedicated pilots per antenna in the uplink. Since the coherence time is rather big, a set of pilots every few superframes should be sufficient. To reduce the overhead further, the users may be divided into groups that share competition bands. For example, if we divide the users into four groups and let each group share one competition band, the pilot overhead is reduced to ¼. Certainly, the more competition bands we use, the more frequency diversity is lost.

For the downlink transmissions we additionally require dedicated pilots per spatial layer. The user terminals will use these pilots to tune their MMSE receive filters. Since the spatial separation is usually reasonably well, spatial pilot reuse can be applied. Therefore, a certain number of pilot symbols (i.e. four) should be reserved in every chunk and then filled with pilots in all the spatial layers. This introduces some multi-user interference on the pilot symbols which deteriorates the estimation of the effective downlink channel. Due to the good spatial separation, this loss is rather low.

The benefit of this pilot design is that the pilot overhead is entirely independent of the number of antennas at the base station. This enables us to deploy a larger number of antennas without ending up in prohibitive pilot overhead figures. Moreover, due to the reciprocity we do not require any feedback.

7.1.2 Uplink reference design

For the uplink transmissions, many of the benefits we could exploit in the downlink also apply. Again, the large number of antennas can be used efficiently, if they are deployed as distributed antenna arrays. For the uplink transmissions this deployment reduces the near-far problem and again decorrelates the users.

A major difference to the downlink transmission is that the antennas of the simultaneously transmitting users cannot be coordinated. For the downlink transmission, the major processing effort was spent in preprocessing the data as to avoid multi-user interference at the user terminals. In the uplink the goal is to keep the preprocessing step simple in order to enable low-cost user terminals. Therefore, the postprocessing done at the base station has to combat the interference of simultaneously transmitting user terminals.

Successive interference cancellation (SIC) is known in the literature as an efficient approach for multi-user detection. In this scheme, each user is decoded successively. His signal is then reconstructed and subtracted from the received signal in order to cancel the multi-user interference. SIC can be combined with linear techniques to cancel multi-user interference. The SMMSE and the RBD technique proposed for the downlink can be reversed to also operate in the uplink. The advantage of the linear techniques is that they are more robust against imperfect channel state information. If the CSI is not very accurate, the performance of SIC becomes worse due to error propagation. In this case we may also use the linear techniques without the SIC step, which still result in an acceptable performance.

It is wise to assume that the user terminals do not have any channel state information. Acquiring it would be very expensive both in terms of pilot overhead (due to the large number of antennas) as well as in complexity. For the preprocessing of the data at the terminals there are two proposals: As a non-frequency adaptive version we propose to use open-loop space-time coding techniques, such as Alamouti space-time

coding. Its advantages are that it is suitable for two antennas, easy to implement at the terminals and still enables us to extract the antenna diversity. As a frequency-adaptive version, the base station can precompute the optimum beamforming weights for the user terminals and send them to the terminals by feedback. To reduce the feedback overhead, this adaptation can be done on frequency bands larger than the base line definition of a chunk. The optimum trade-off between feedback rate and adaptivity is discussed in [WIN2IR343].

7.1.2.1 System model

The system model is depicted in Figure 7.2. Here, Ala/BF symbolizes the fact that we may use either Alamouti or beamforming to preprocess the data at the user terminals. The input data streams are symbolized by x_k, the decoded streams at the base station as y_k. The base station can use either SMMSE or RBD decoding to cancel multi-user interference. Additionally, SIC may be used on top. More details on computing the receive filters as well as on the feedback scheme can be found in [WIN2IR343] and [WIN2D341].
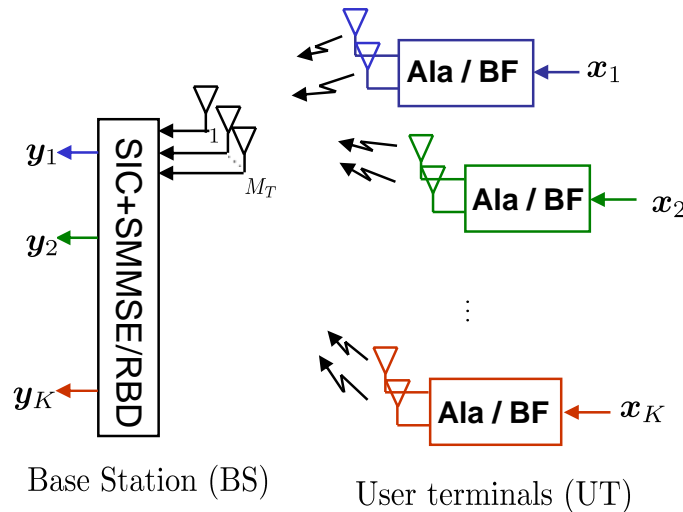

Figure 7.2: System model for the uplink

7.1.2.2 Signalling requirements

One of the goals in the downlink and the uplink reference design were that they operate well together. We therefore decided to choose schemes which have the same requirements in terms of signalling. We can therefore benefit from the same pilot requirements we introduced in the downlink reference design also for the uplink.

In particular, the channel state information the base station requires is obtained from uplink dedicated pilots per user antenna. The same comments as for the downlink apply: Due to the large coherence time, the CSI is expected to be valid for a few superframes. Also, to reduce the overhead, the users may be divided into groups that share competition bands.

At the user terminals we do not require any channel state information. For the non-frequency adaptive transmission, the terminals simply apply the Alamouti scheme. For the frequency-adaptive beamforming approach, the beamforming weights are sent to the user terminals via feedback. The feedback rate depends on the granularity of the adaptation. More details can be found in [WIN2IR343].

7.2 Performance assessment of the uplink reference design

This section summarizes the performance assessment results for the uplink reference design. First, the frequency-adaptive uplink beamforming results are shown. It should be noted that for this simulation, only 8 antennas at the base station (i.e., only one out of the four distributed antenna arrays) was used.

Moreover, the signal to noise ratio was set by hand. Link budget calculations suggest a larger signal to noise ratio in the actual local area base line configuration.

In the second part of this section the non-frequency adaptive scheme with Alamouti precoding at the user terminals is evaluated. For these simulations the parameters are aligned with the local area base line configuration.

7.2.1 UL Adaptive Multiuser beamforming

The system parameters are according to the definition in [WIN2D6.13.7] for the local area scenario, i.e. eight cross-polarized base station antennas and two dual cross polarized antennas at the user terminal. 1840 out of 2048 carriers and a signal bandwidth of 81.25MHz out of a system bandwidth of 100MHz are used. The chunk sizes are varied between $16 \leq B \leq 1840$. The transmitters perform linear precoding based on quantized feedback from the base station. Random vector quantization and $2^{(n_T-1)q}$ bits for the power quantization and the remaining bits for beamformer quantization are used. The receiver performs optimum combining and SIC. The linear precoding matrices are found by convex optimization for Gaussian codebooks. Then, the resulting SINR values per stream and user are computed and mapped to a MCS.

In the following Table 7.1, the impact of finite MCS defined in [WIN2D6.13.7] on the average sum rate is shown. The conversion from the rates achievable with Gaussian code-books to finite MCS via the SINR values of the individual data streams is performed under the assumption that the receiver applies the optimum combining method. The cases with Gaussian input signals and ideal quantization of the feedback are compared to finite MCS and quantized feedback.

The effective rate is computed according to the following model: the amount of feedback as a function of the number of transmit antennas n_T, the number of users K, the quantization q, the coherence time T, the number of carriers N, the chunk size B and feedback channel data rate R_d is defined by $\alpha = \dfrac{N \cdot K \cdot \zeta}{B \cdot R_d \cdot T}$ with ζ as the number of feedback bits for one transmit covariance matrix. In our approach, the control overhead reduces the transmission rate R to the effective transmission rate R_θ $R_{\theta} = R(1 - \alpha) = R\left(1 - \dfrac{N \cdot K \cdot \zeta}{B \cdot R_d \cdot T}\right)$. This approach considers only the uplink and the feedback reduces the transmission rate directly.

Table 7.1: Average sum spectral efficiency [bit/s/Hz] for ideal CE and ideal link-adaptation in WIM A1 for 8 BS antennas and 5 users with 2 receive antennas. The average received SNR is varied between -5 and 15 dB. No pilot and control overhead is subtracted (except the feedback overhead).

SNR	MCS	Quant	B=16	B=40	B=80	B=115	B=230	B=460	B=920	B=1840
15	Gaussian	Ideal	8,001	9,991	10,605	10,737	10,720	10,254	9,684	9,021
15	Finite	Ideal	6,311	7,854	8,388	8,478	8,498	7,987	7,480	6,543
5	Gaussian	Ideal	3,675	4,586	4,855	4,902	4,835	4,556	4,250	3,949
5	Finite	Ideal	2,245	2,806	2,975	3,005	2,997	2,837	2,638	2,659
5	Gaussian	2^16	3,035				3,886			3,138
5	Finite	2^16	1,673				2,177			2,234
5	Gaussian	2^8	2,432				3,080			2,565
5	Finite	2^8	1,397				1,815			1,898
-5	Gaussian	Ideal	0,961	1,199	1,267	1,277	1,243	1,132	1,008	0,897
-5	Finite	Ideal	0,673	0,841	0,890	0,901	0,897	0,850	0,832	0,787

The optimal chunk size is marked for each row in red. The loss due to finite MCS is between 20% (for high SNRs) and 40% (for medium or low SNRs). The impact of quantization of the feedback can also be

observed in Table 7.1. For every transmit covariance matrix 2^{16} bits or 2^8 bits are allocated. Note that the simulations have been carrierd out for different transmit SNR values (first column of Table 7.1).

7.2.2 UL Alamouti precoding and SMMSE/RBD decoding

In this section, we discuss the system level simulation results with the MU-MIMO uplink reference scheme. At the user terminals we use Alamouti space time precoding. The base station is performing regularized block diagonalization or successive MMSE decoding to cancel the multi user interference and then decoding the Alamouti transmissions user by user.

For the sake of simplicity and due to its inherent fairness we use a Round Robin scheduling scheme to decide which users should belong to one SDMA group. For the baseline design with 32 distributed antennas, the optimum group size was found through system level simulations to be in the range of 12 to 15 depending on the placement of the users. For the simulations the SDMA group size K_{cc} was set to 13.

The results of system level simulations with the proposed scheme are shown in Figure 7.3and Figure 7.4. The simulation parameters were chosen according to the LA baseline assumptions (32 distributed antennas). The total number of users in the system K is set to 32 from which K_{cc}=13 are served at the same time and frequency resource through SDMA. These groups are rotated in a round robin fashion over all available chunks.

At the user terminals, no channel state information is required. At the base station, the CSI is assumed to be imperfect. CSI imperfections were modelled according to [WIN2D6.13.7]. Concerning the overhead, the superframe control overhead was subtracted from the throughput and twelve symbols per chunk were reserved for in-chunk control overhead. The guard band overhead is also taken into account in the spectral efficiency computation. Since the density and structure of the uplink (full band) dedicated pilots was not decided yet when the simulations were carried out, the pilot overhead is not subtracted.

The results show that the performance degrades under imperfect CSI. This is mostly due to the sensitivity of the Alamouti precoding scheme to CSI errors. We also notice that the performance of SMMSE and RBD decoding is very similar. The comparison with TDMA/FDMA shows the gain from exploiting the spatial degrees of freedom of the MIMO channel.
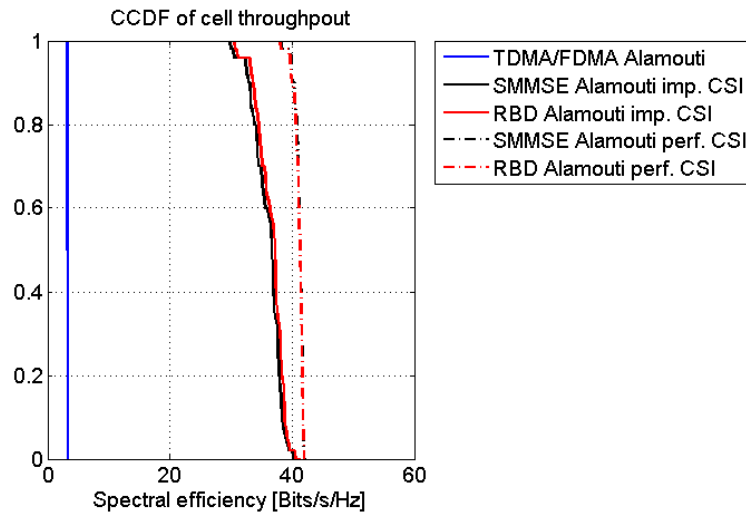

Figure 7.3: Cell throughput for the Local Area uplink with RBD decoding and Alamouti precoding. Round Robin scheduling. Pilot overhead not subtracted.
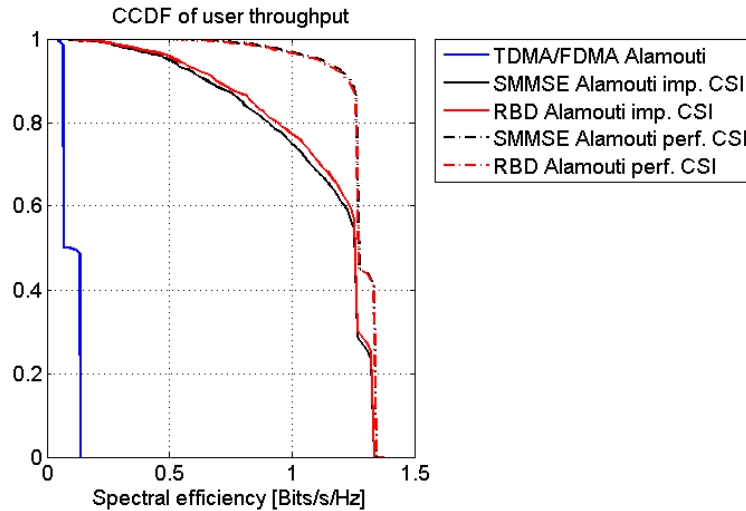
Figure 7.4: User throughput for the Local Area uplink with RBD decoding and Alamouti precoding. Round Robin scheduling. Pilot overhead not subtracted.

7.3 Performance assessment of the downlink reference design

In this section we evaluate the performance of the proposed MU-MIMO scheme for Local Area deployments under realistic assumptions. The CSI imperfections we considered include channel estimation and interpolation errors modelled according to [WIN2D6.13.7] as well as calibration errors due to RF impairments following the self-calibration approach from [BCK03]. The BS and UT antenna setup and the deployment was also aligned with the Local Area baseline assumptions from [WIN2D6.13.7] (i.e., 32 distributed antennas).

At the base station SMMSE or RBD precoding is performed. Since the instantaneous CSI is imperfect, the user terminals will suffer from a certain degree of multi user interference. At the user terminals, MMSE receivers are assumed.

In order to find suitable groups of users that we can serve jointly using SDMA, we need a scheduling decision for each chunk. It is infeasible to find the best groups through an exhaustive search since for 32 antennas at the base station and 50 users in the system, the total number of possible combinations that would have to be tested for every chunk is $\approx 10^{15}$. A very well suitable alternative is given by the ProSched, which reduces the complexity by replacing the exhaustive search through a tree-based greedy search. We compare two versions of the ProSched. The first version always selects the best group in order to maximize the total system throughput (MaxTP). This may result in scenarios where users with bad channel conditions do not get served and therefore a bad user outage behaviour. We therefore also developed a version that includes fairness following a Proportional Fair approach (PF).

The spectral efficiency figures consider guard band overhead, superframe control overhead and in-chunk pilot and control overhead. Eight (twelve) symbols are reserved for pilots (control) within each chunk. For TDMA/FDMA only four pilot symbols are subtracted as overhead.

The system level simulation results are shown in Figure 7.5 and Figure 7.6. The results demonstrate that the performance of SMMSE and RBD is similar. The comparison with the pure TDMA/FDMA case demonstrates the gain achieved from applying SDMA. From Figure 7.5 we can clearly see that including the fairness constraint reduces the total cell throughput slightly. However, the corresponding curves in Figure 7.6 demonstrates the improvement in terms of fairness: while the maximum throughput version of the scheduler does not assign any resources to approximately 10% of the users, the proportional fair version guarantees that every terminal gets served on some of the resources, which were previously assigned to users with higher throughputs.
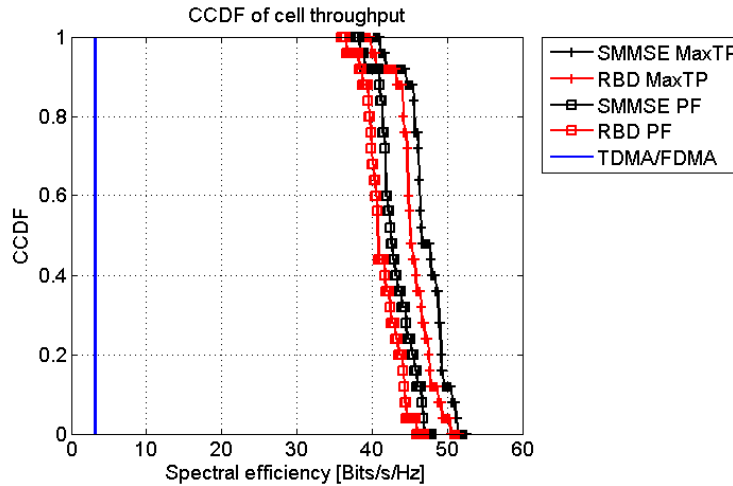
Figure 7.5: Cell throughput for Local Area downlink, SMMSE and RBD precoding. ProSched scheduling with maximum throughput (MaxTP) vs. Proportional Fair (PF). Including CSI errors, including pilot overhead.
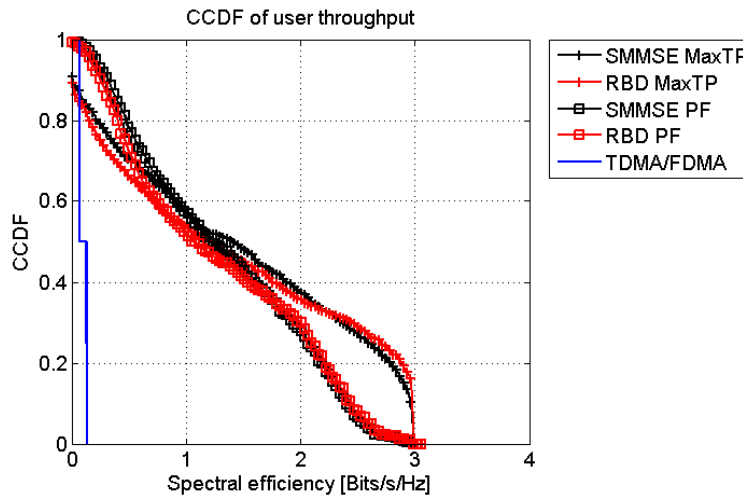

Figure 7.6: User throughput for Local Area downlink, SMMSE and RBD precoding. ProSched scheduling with maximum throughput (MaxTP) vs. Proportional Fair (PF). Including CSI errors, including pilot overhead.

7.4 Conclusions

In this chapter the reference design for the Local Area spatio-temporal processing algorithms was evaluated through simulations. It was demonstrated that a large number of antennas at the base station can effectively be used to achieve very high spectral efficiencies. This is due to the combination of low user mobility, time division duplexing and rather small coverage areas. The distributed antennas additionally increase the potential value of the MIMO techniques since the transmit power is distributed more evenly and the correlation of the users' channels is reduced. When 32 distributed antennas at the base station are used, the overall system should be capable of providing above 30 Bits/s/Hz in the uplink and above 40 Bits/s/Hz in the downlink, i.e. more than required in [WIN2D6114] (requirement R40).

8. Relaying

It is foreseen that new spectrum in different frequency bands will be allocated for future radio communication systems. The main part of these (IMT) candidate bands are beyond 3 GHz. The high carrier frequencies of these bands together with regulatory constraints on the transmission power will limit the range for broadband services. Relay based deployments are a promising technology to save costs while achieving a similar service level or coverage as compared to a base station only deployment.

Relaying technologies have been studied in WINNER since the very beginning of the project with the purpose of providing an efficient relaying concept able to guarantee the envisaged broadband radio coverage under the assumption of cost efficiency. Although the common effort was made to design a consistent solution, the work was structured accordingly in order to cover the requirements of all three concept groups: wide area, metropolitan area and local area. Thanks to this approach a significant dose of flexibility was introduced to the resulting relaying concept such as, among other, the support for single path and cooperative relaying, MIMO relaying and cooperating RAPs selection. Following, the relaying concept was verified with the aid of simulations and proved to be well tailored to work efficiently for all the investigated scenarios.

As a result, in the following sections the aspects of the relaying concept that are relevant to the local area concept group scenario are presented. In particular the performance analysis for the local area scenario is presented following the baseline assumptions for relaying given in Section 4. Three cases are analysed: direct transmission (single-hop), single path (conventional) relaying and relay node to relay node cooperation (cooperative relaying). Based on the achieved results the applicability of the latter transmission type to the local area scenario is evaluated and the preferred relay deployment is suggested.

8.1 Assumptions and parameters

Simulations were performed according to the assumptions for indoor environment given in [D6.13.7] and taking into account the specific parameters outlined in Table 8.1. Since the scenario under investigation is symmetric, the simulation area was limited to a set of 10 rooms located in the right bottom part of Figure 4.2, i.e. around RN3. For this reason solely this region will be presented and referred to in all the following figures and descriptions. Two RNs (green squares number 2 and 3) were used and they were coordinated by the BS (red square number 0) located in the centre. Fixed modulation and coding scheme was employed consisting of QPSK modulation and (4, 5, 7) convolutional code. Channel modelling was limited to AWGN channel and A1 NLOS propagation model was used not only between RNs and UTs, but also in the case of the links between BS and RNs. This remains in contrast with [D6.13.7] but seems well justified due to the existence of walls. Additionally no outdoor users were taken into account and an average interference power level of -125 dBm per subcarrier was assumed.

Table 8.1: Simulation parameters

Parameter	Value	Comments
Carrier frequency	5.0 GHz	
Channel bandwidth	100 MHz	
Number of cells	1	Indoor scenario
Distance BS – RN	27,95 m	
Spatial processing	Distributed OSTBC	RN-RN cooperation case
BS number of antenna per sector	1	
RN number of antenna	1	
UT number of antenna	1	
BS transmission power	21 dBm	
RN transmission power	21 dBm	

UT transmission power	21 dBm	
Retransmissions (ARQ, HARQ)	No	
Segmentation and Reassembly	No	
Link adaptation	Fixed code and modulation scheme	QPSK and (4, 5, 7) convolutional code
Channel modelling	AWGN channel	A1 NLOS Room-Room model used for both BS-RN and RN-UT links (also for Room-Corridor transmission)
Mobility	Yes	
Resource scheduling	Fixed	Each user was assigned 1 chunk (8 subcarriers and 15 OFDM symbols)
Resource partitioning	Fixed	see Figure 8.1
Selection of best RAP	Signal strength	
Traffic model	Constant Bit Rate (CBR)	

As regards the deployment presented in Figure 4.2, each user was assigned one chunk, i.e. 8 subcarriers and 15 OFDM symbols and resources were partitioned according to the scheme depicted in Figure 8.1. The structure of the superframe was defined according to [D6.13.7] and radio resources were partitioned in both the temporal and spectral domains. Similar pattern was repeated twice within the duration of a superframe. First, the resources were assigned to the base station and then to different combinations of RNs. As a result a maximum of 3 RNs could have been active at the same time.
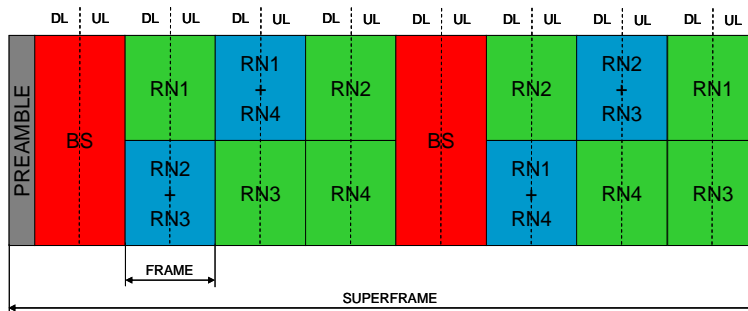

Figure 8.1: Radio resource partitioning

This contribution is a follow-up to the description of the Static REACT algorithm based on [Wod07] and presented in [D3.5.2] and [D3.5.3], where BS selects RAP or cooperating RAPs and is responsible for resource partitioning and scheduling. The results presented in the next subsection pertain to the following cases: direct transmission, single path (conventional) relaying and relay node to relay node cooperation (cooperative relaying).

8.2 Performance evaluation and results

After having the capabilities of the simulator extended as indicated in [D3.5.3] a number of detailed simulation experiments was performed. The relative user throughput for direct transmission, single path relaying and RN-RN cooperation, according to RAP deployment outlined in Figure 4.2, was evaluated as the reference case (Figure 8.2). Those results were obtained assuming the aforementioned average power level of interference and they show that it is possible to make up for the performance degradation visible in Figure 8.2A with the aid of single path relaying. Unfortunately the gain provided by RN-RN cooperation seems almost invisible as compared to the single path relaying case. The reason is that the signal coming to the destination UT from cooperating relay node RN2 is usually more heavily attenuated by a higher number of walls. According to the A1 NLOS propagation model each wall between rooms attenuates the transmitted signal by 5dB (see also Section 8.1 for the specific assumptions). As a result the

power levels of the signals received be the destination UT from both cooperating RNs may differ e.g. by 15 dB. It means that quite often the signal coming from the other relay node (i.e. RN2 in Figure 8.2A) is not strong enough to provide the expected improvement in throughput. Consequently, in this case, it is impossible to gain from spatial-temporal processing provided by the cooperating RNs.
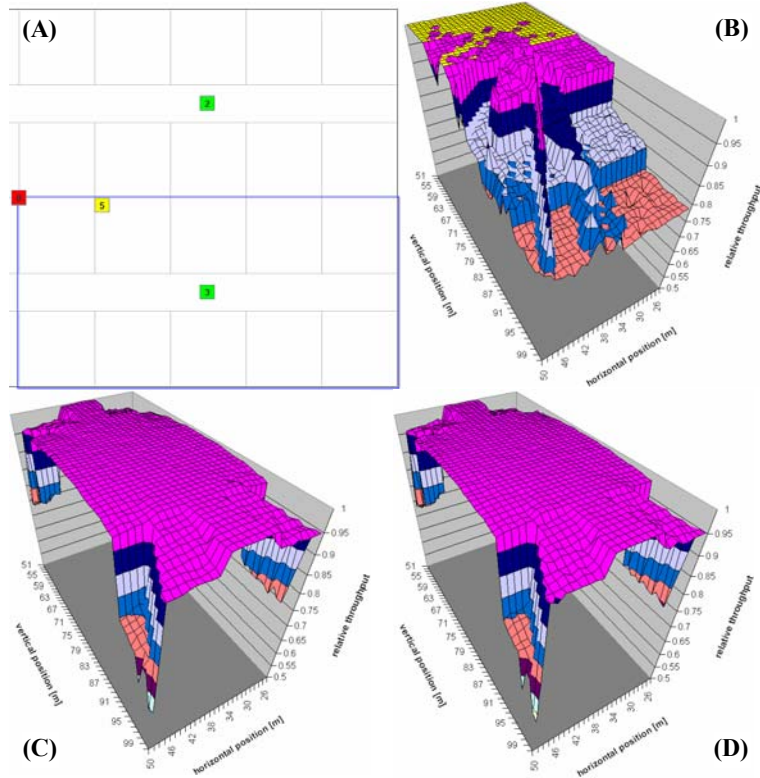

Figure 8.2: Deployment of RNs (A) and relative user throughput for direct transmission (B), single path relaying via RN3 (C) and RN2-RN3 cooperation (D)

For this reason some other RN positioning approaches were verified in order to find out when the RN-RN cooperation could be advantageous in the local area scenario. All the results presented in this section were obtained assuming that a given RN takes part in cooperation even if decoding was unsuccessful. This way the degradation in performance introduced by a wrongly positioned RN was easily noticeable, whereas otherwise such a RN would have to remain silent and no direct indication about its wrong influence would be visible. One should also note that starting from Figure 8.3 up to Figure 8.6 there is always the RN2-RN3 cooperation performance shown in part B, whereas the relative throughputs achievable by single path relaying via RN2 and RN3 are shown in parts C and D respectively. The yellow node indicates a UT at a random position.

First, the position of the RN3 was left unchanged and the cooperating relay node (RN2) was moved to the area of interest (see Figure 8.3 and Figure 8.4). In the case of Figure 8.3, RN2 was placed closer to the BS and an improvement could have been observed as compared to Figure 8.2. Although the throughput attainable by the RN-RN cooperation was higher in some regions as compared to the reference case (Figure 8.2D), one could also consider using both RNs separately to cover different parts of the area of interest. This way the single path relaying via the RN2 could provide even higher throughput in the rooms located in the immediate vicinity of the BS and in the corridor (Figure 8.3C), whereas the RN3 could serve the users located in the remaining area.

Next, the RN2 was placed farther from the BS in order to verify if it is possible to make up for the throughput degradation visible in the distant corners of the area of interest (Figure 8.4). Unfortunately, due to a significant distance from the BS this RN was performing rather poor (Figure 8.4C) and despite the reasonable performance of the RN3 (Figure 8.4D), the RN-RN cooperation was highly affected.
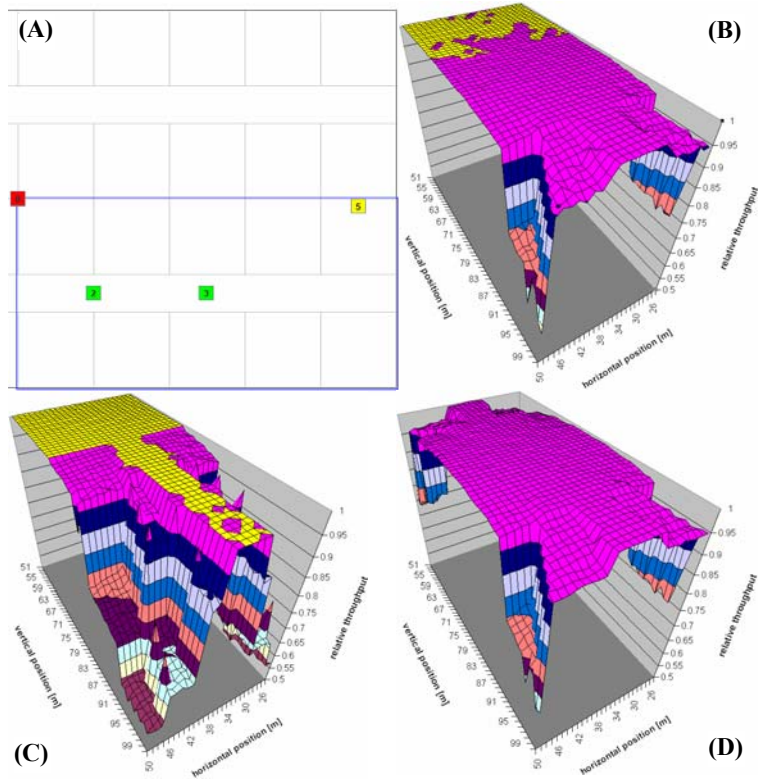
Figure 8.3: Deployment of RNs (A) and relative user throughput for RN2-RN3 cooperation (B), single path relaying via RN2 (C) and single path relaying via RN3 (D)
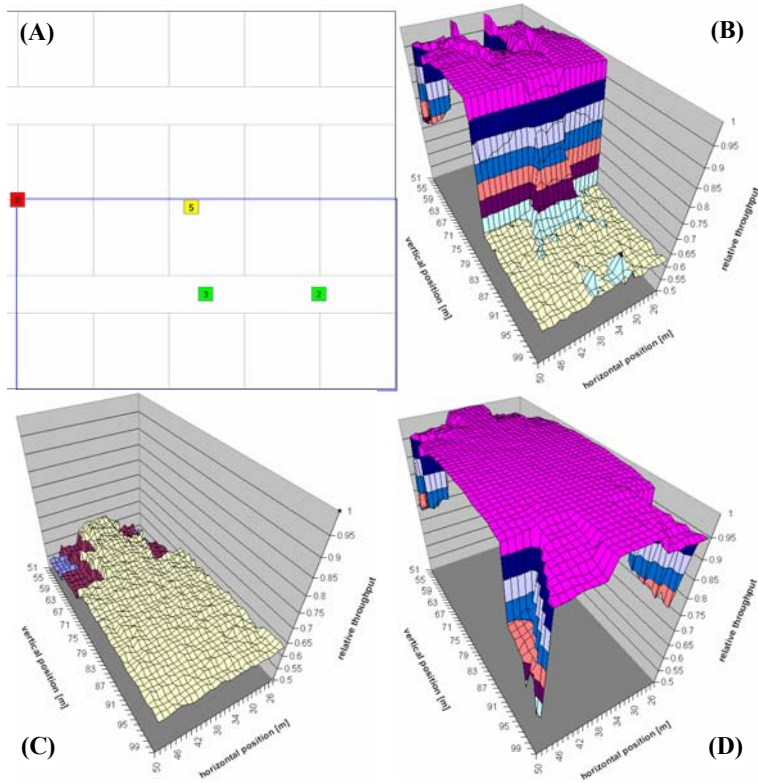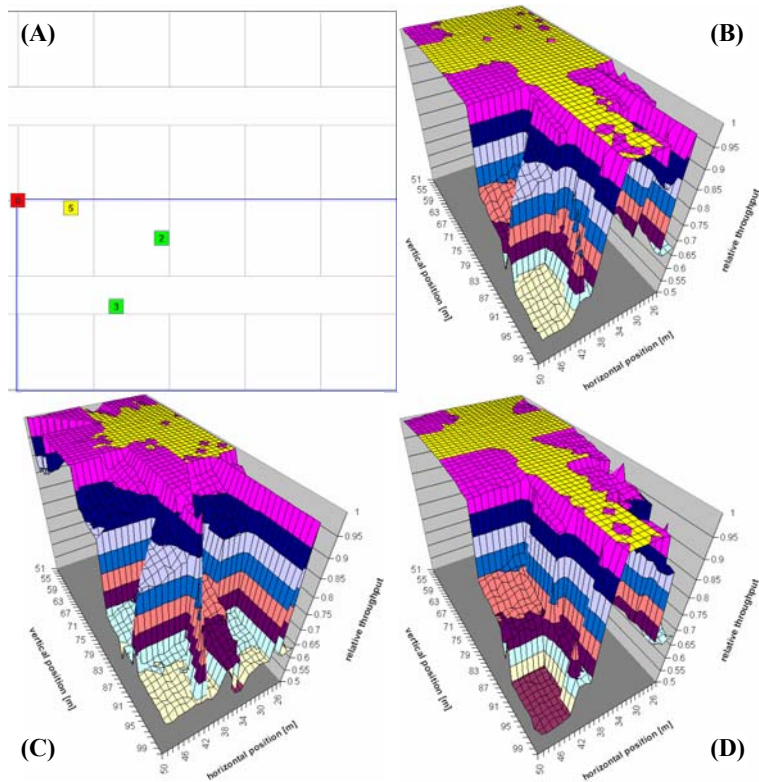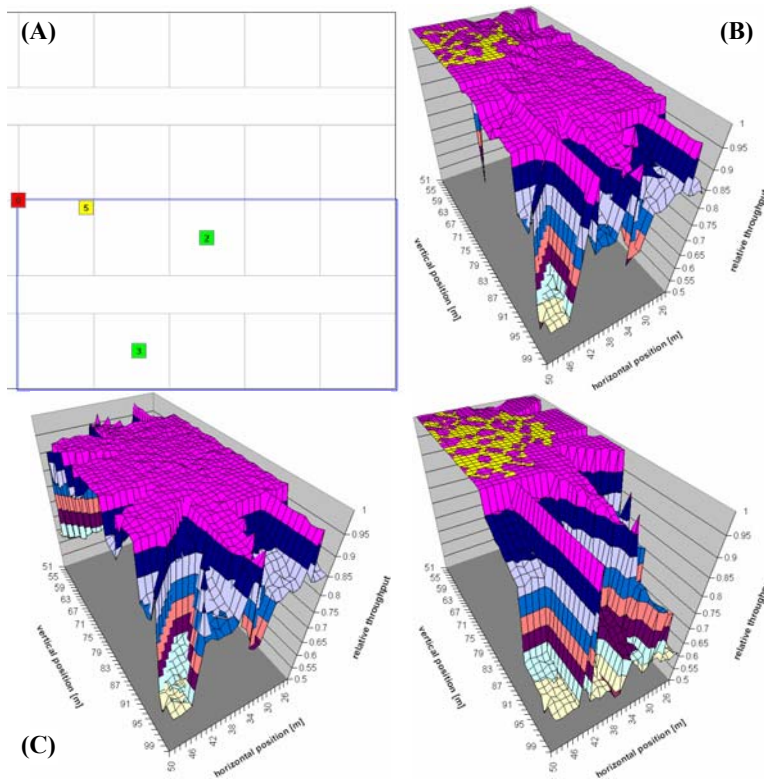

Figure 8.4: Deployment of RNs (A) and relative user throughput for RN2-RN3 cooperation (B), single path relaying via RN2 (C) and single path relaying via RN3 (D)

Figure 8.5: Deployment of RNs (A) and relative user throughput for RN2-RN3 cooperation (B), single path relaying via RN2 (C) and single path relaying via RN3 (D)

Figure 8.6: Deployment of RNs (A) and relative user throughput for RN2-RN3 cooperation (B), single path relaying via RN2 (C) and single path relaying via RN3 (D)

It means that placing a RN at this position would be very ineffective from the cost perspective, because this node would have to remain silent almost of the time in order not to deteriorate the achievable throughput.

Keeping in mind that in the aforementioned two cases the distance and therefore the number of obstacles between the BS and each of the RNs in Figure 8.3 and Figure 8.4 was differing, two other deployments were evaluated (Figure 8.5 and Figure 8.6). This time the number of walls in-between the aforementioned BS-RN pairs was kept the same and the distances were similar. The throughput attainable in the vicinity of the BS (Figure 8.5) seemed also reasonable but the rest of the area was covered rather poorly. The same held true for the set-up presented in Figure 8.6. Also there the single path and cooperative relaying offered lower throughput as compared to the reference scenario (Figure 8.2).

8.3 Preferred deployment and cooperation type

Analysing the results presented in the previous section one should keep in mind two aspects. First, it was assumed that the RNs took part in the transmission even if the packet to be retransmitted was in error. Thanks to this approach it was easily visible when the RN-RN cooperation was not effective due to wrong positioning of the RNs (see Figure 8.4). One should note, however, that in general after having received a packet in error, such a wrongly positioned RN would remain silent. This way the cooperation between the RNs would not spoil the performance but improve it when possible. It is clearly visible e.g. in Figure 8.5, where the performances of both the RNs in the single path relaying case do not differ too much. As a result the other RN does not introduce degradation and the overall achievable throughput increases. Second, one should also remember that at this stage the fixed modulation and coding scheme was used. This suggests that e.g. in some regions of the yellow area which indicates the maximum relative throughput one could possibly achieve better value after choosing a less strong coding and/or higher modulation order. This comment also holds true for all the other results presented in this section.

The main outcome from all the evaluations presented in the previous section is that the local area scenario is a very specific one and it is difficult to show that one can gain significantly from the RN-RN cooperation. The reason is that in [D6.13.7] the A1 LOS propagation model was suggested between BS and RNs, whereas those nodes are separated by walls. As a result the signal received by RNs is attenuated far more severely and it is impossible to gain from a very high quality first-hop links. Additionally there are walls all around and it is difficult to use RNs in order to omit them. This way or another it was shown that in some cases it is possible to gain from the RN-RN cooperation and especially in the immediate vicinity of the BS assuming that both the RNs perform equally well. Different deployments proved to outperform the reference one in some special cases only, but the general feeling is that the latter one offered the most reliable performance over the whole area of interest (but the distant corners). In this case, however, no RN-RN cooperation gain was observed.

Two approaches are then possible as regards the selection of the preferred scenario and cooperation type. The most straightforward one is to keep the reference scenario as it is and to not use the cooperative mode. This way the BS serves UTs in its immediate vicinity and each of the RNs serves the remaining part of the area (Figure 8.2). The other option is to place additional RNs (as depicted in Figure 8.3 and Figure 8.5) for the purpose of improving the performance in the vicinity of the BS and in the corridors. The rest of the area could be still served by the RNs relays placed according to the reference scenario (Figure 8.2). In spite of providing higher throughput in some regions this approach would, however, be more demanding from the cost perspective.
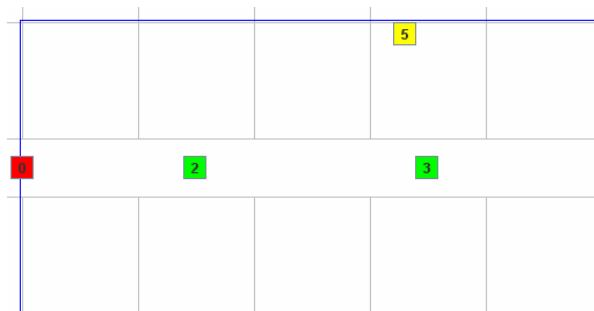

Figure 8.7: The region of interest in the case of the modified deployment consisting of two base stations and eight relay nodes

One could also go one step further and try to modify the baseline relay deployment given in Figure 4.2. This modification would require inclusion of an additional BS and placing each of them in the middle of the corridor. Each BS would be also assisted by four RNs, two on their left and two on their right side so the region of interest would look as depicted in Figure 8.7.
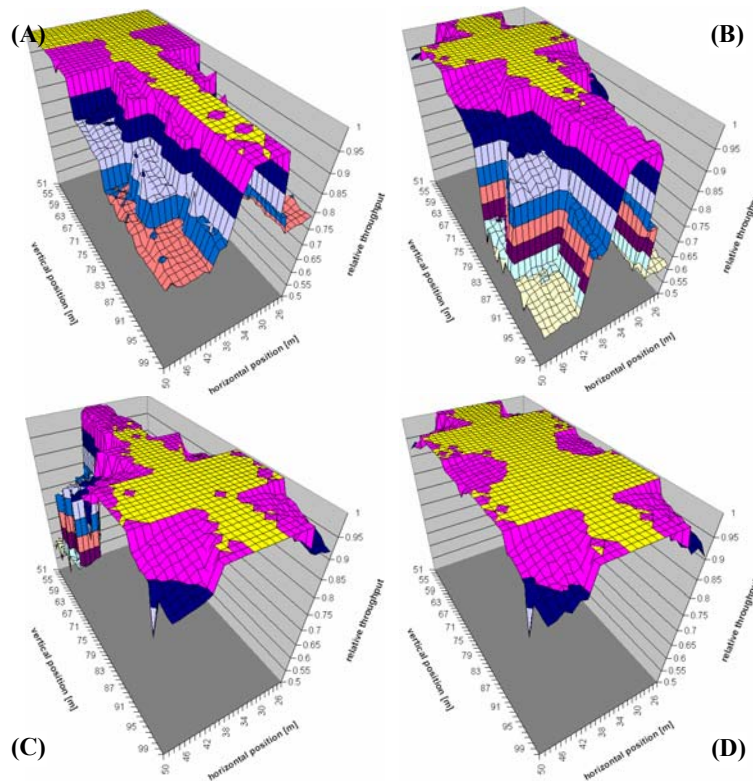

Figure 8.8: Relative user throughput in the modified deployment for direct transmission (A), single path relaying via RN2 (B), single path relaying via RN3 (C) and RN2-RN3 cooperation (D)

Analysing the simulation results depicted in Figure 8.8 one can conclude that this time the RN-RN cooperation performs best. The reason is that BS is able to provide maximum throughput almost in the whole corridor and as a result both cooperating RNs are fed with a signal of a very good quality. Consequently they can retransmit the received packets cooperatively and provide a better coverage as compared to the case when BS is switching between two RNs working in the single path mode. Obviously, this deployment requires a more sophisticated radio resource partitioning. Additionally any losses in the effective throughput resulting from the interference would have to be avoided. One could, however, make use of the fact that both base stations are separated by three walls when trying to make up for this impairment.

8.4 Conclusion

In this section the performance of direct transmission, single path and cooperative relaying was evaluated. Different set-ups were analysed in order to find out when it is possible to gain from RN-RN cooperation in the baseline relay deployment for the local area scenario. It was finally confirmed that due to the existence of significant number of walls it is impossible to have high quality links between the BS and RNs and as a result the RN-RN cooperation might not offer any visible gain.

Consequently the best solution for the baseline relay deployment would be to use the BS to serve the UTs in its immediate vicinity and apply the singe path relaying in the remaining area. This is determined by the nature of the scenario and does not necessarily hold true for other configurations. For this reason one could also consider placing additional RNs in order to improve the performance in the immediate vicinity of the BS. This would be more costly and would require additional cost analysis.

The final conclusion is that in order to achieve a real gain from cooperative transmission one would have to consider another deployment consisting of two base stations and eight relay nodes. This deployment could offer the best performance but it would also require a more sophisticated radio resource partitioning. One would also have to avoid any effective throughput losses that could result from the increased interference.

9. Multiple Access

The WINNER MAC must be capable of supporting users with different needs and provide efficient data transfer over radio links of varying quality and characteristics. The WINNER system must hence support the co-existence of different transmission and multiple access schemes.

The efficiency and flexibility of co-existence of different multiple access schemes depend on the characteristics of the multiple access schemes, the frequency reuse strategy, and the system bandwidth. The co-existence solutions may further look different in the uplink and in the downlink. In addition whenever possible, the adaptation of multiple access schemes should be coordinated between cells to enable a mitigation of intercell interference, especially in low loaded scenarios where not all resources are needed. However, the system should be operational even if such coordination is not possible.

This section discusses the multiple access adaptation in the context of the Local Area scenario.

9.1 Multiple access solutions in the Local Area scenario

The two basic classes of transmission schemes defined in the WINNER system concept are frequency-adaptive resource scheduling and non-frequency adaptive resource scheduling. These basic transmission techniques are used for the two distinct multiple access schemes for scheduled flows in the WINNER system concept. They were briefly discussed in chapter 5.2, but see [WIN2D461] for an in-depth discussion of these multiple access methods. The strategy for link adaptation, resource scheduling and resource mapping is based on tight collaboration between layers that traditionally are more separated. See [WIN2D61314] for a further discussion of the multiple access concept in the WINNER system concept, especially related to the incorporation of the above transmission methods in the system concept.

A flow destined for many users can be mapped on the multicast or broadcast support in the MAC. Both multicasting and broadcasting use the multiple access schemes for non-frequency adaptive transmission; in multicasting adapted to the worst user in the multicast group and in broadcasting adapted to a predefined cell edge user. Thus this transmission mode does not need explicit resources, but the option of macro-diversity gains by coordinated scheduling in adjacent cells is identified as an important topic for further investigations. The initial concept for multicasting and broadcasting support is further described in [WIN2D461].

In the local area deployment scenario, the parameterization and adaptive selection of multiple access schemes have several special characteristics:

- Due to low terminal speeds, the accuracy of CQI information will be quite high in local area scenarios. Therefore, most chunks can be dedicated to frequency-adaptive transmission using chunk-based TDMA/OFDMA in uplinks and downlinks.

- The large frequency-diversity available in the non-frequency-adaptive scheme is useful mainly for local area users with bad SINR (e.g. buildings with many walls to penetrate) with deployment using a small number of antennas or in low scattering scenarios.

- In the multiple access schemes for non-frequency adaptive transmission, it is possible to trade-off the requirement for power amplifier backoff and battery power gains due to "intra-chunk" sleep mode, see [WIN2D461] Appendix B4.3. The short ranges in the Local Area scenario could imply that sleep mode gains are more important than maintaining a low signal envelope in the uplink, which can be obtained by adapting the Resource Scheduler to this requirement.

SDMA in Local Area deployments can benefit from a potentially more accurate CSI feedback. Therefore, if the rate of feedback is sufficiently high or the mobility of users is as low as expected, dedicated precoding matrices can be applied which can drastically increase the throughput, see chapter 7 for further discussion on SDMA in the local area scenario.

9.2 Multiple access adaptation in the Local Area scenario

Resources for frequency adaptive and non-frequency adaptive transmissions may be time or frequency multiplexed, as illustrated in Figure 9.1. Time multiplexing is easy and straightforward, but it may imply a higher delay and it has lower granularity compared to frequency multiplexing. It is also possible to perform spatial multiplexing of the MA schemes by using different MA schemes in different layers of the

same chunk [WIND210]. Sectorization is a simple example, but it is in principle possible to do more advanced spatial multiplexing.

Both adaptive and non-frequency adaptive transmission modes benefit from wide bandwidth, multi-user scheduling gain ('multi-user diversity') and diversity gain towards small scale fading respectively. This is an argument for time-multiplexing of the MA schemes, but this is mainly noticeable for small system bandwidths. Since short delay over the WINNER RAN is set to be one of the most important goals, enabling (H)ARQ and two-hop relaying also for delay-sensitive flows for reliability, support of real-time services, high TCP throughput and good coverage, chunk based frequency multiplexing is the most reasonable way to multiplex different MA schemes.

In the local area case, only the TDD mode is considered. The chunk parameters are the same in 100 MHz as for the metropolitan case, which gives us 128 chunks. This number of chunks is enough to allow frequency multiplexing of the adaptive and non-frequency adaptive MA schemes.
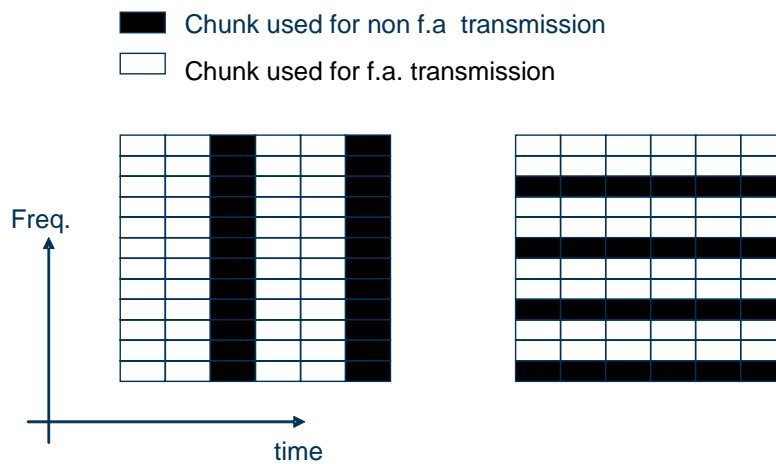

Figure 9.1: Time and frequency multiplexing of resources used for frequency adaptive and non-frequency adaptive transmission

In the local area case, more users are likely to be slowly moving. Since also smaller cells can be expected, adaptive transmission should be the normal transmission mode and most resources should normally be allocated for this mode. However, a specific aspect for local area is the requirement for deployment in unlicensed spectrum. In this scenario, the non-adaptive transmission becomes more important. Strong protection towards interference of the control channels and also optimized diversity techniques in the non-adaptive transmission towards bursty interference become important. Here, spatial diversity and frequency diversity is attractive with e.g. frequency hopping techniques, and should be feasible, especially in isolated hot spots, since less chunks need to be restricted for constraint processing (for a discussion on constraint processing, see [WIND210]).

A time-multiplexing component of users within the allocated frequency resources for the non-frequency adaptive transmission is introduced within chunks to enable power saving sleep mode for UTs: "intra-chunk" sleep mode (see [WIN2D461]). In addition, the Resource Scheduler in the MAC layer can support UTs to obtain sleep mode gains during full chunk durations: "inter-chunk" sleep mode (see [WIN2D461]), in both adaptive and non-frequency adaptive transmission modes. Intra-chunk sleep mode is not supported for adaptive transmission, but that MA scheme will be used for high data rate flows. Since low speed of the UT is expected in the Local Area scenarios, channel prediction could work for long prediction horizons even with long periods of inter-chunk sleep mode. Thus, in a Local Area scenario the Resource Scheduler can support large inter-chunk sleep mode gains also for adaptive transmission, provided the delay requirement of the flow is fulfilled.

The mapping criteria between unicast and multicast in the MAC layer should be to improve the spectral efficiency of the system. In a local area context, many flows can be mapped onto adaptive transmission, whereas the multicast transport channel will use non-frequency adaptive transmission. Thus, the number of users needed in the multicast group in order to gain in spectral efficiency compared to unicast

transmission is larger than in e.g. a wide area scenario. On the other hand, in an isolated cell macro-diversity gains [WIN2D461] cannot be obtained. The exact threshold in number of users is a parameter in the configuration, and can be tuned by measurements in a deployed system or by simulations prior to deployment.

Finally, the peer-to-peer MAC should also co-exist efficiently with the other transmission modes in the local area case. In [WIND210] the peer-to-peer transmission mode was described, and it was located in the DAC frequency bandwidth. Since the DAC channel is not envisioned in the final system concept [WIN2D61314], resources for the peer-to-peer mode as described in [WIND210] has to be accommodated in a dedicated frequency sub-band. No further work on integration and refinement of the peer-to-peer mode has been carried out in WINNER II.

10. Decentralized Interference Management

In self-organizing wireless networks sophisticated network planning that minimizes the interference towards adjacent cells is not feasible. In particular, big buildings where many people gather, such as shopping malls, airports or train stations may have many distributed base stations and relays deployed. As these base stations might not even belong to the same operator, there is a need for efficient decentralized interference management. In this section an interference aware dynamic channel allocation algorithm is presented, and its performance is assessed for a local area peer-to-peer network. The algorithm facilitates self-organized interference management and is applicable to arbitrary network topologies.

10.1 Decentralized dynamic channel allocation for the WINNER TDD mode

In [WIN2D472] section 5.3, a decentralized MAC protocol to dynamic and interference aware chunk selection is applied to the WINNER TDD mode. The proposed scheme enables the transmitter to determine the level of interference it would cause to already active links prior to any transmission. This is achieved through busy-slot signalling that exploits the channel reciprocity offered by the TDD mode. The busy signal concept is implemented by a time-multiplexed feedback channel that also establishes a low-rate feedback link.

The ability to facilitate self-organized interference management is demonstrated for a local area peer-to-peer network. There an indoor deployment environment as defined as scenario A1 in [WIN2D111] was implemented where UTs are randomly placed. Instead of communicating with a base station the UTs directly communicate in a peer-to-peer fashion.

By letting receivers transmit a busy-signal in an associated mini-slot [OH04], [OHA07], two important goals are accomplished. First, the own transmitter is informed about the level of interference at the receiver. Second, at the same time other nodes intending to establish a transmission are notified about ongoing transmissions, so that these nodes can take appropriate steps to avoid interference. Therefore, both channel sensing and reservation are accomplished. Since there is no central controller which coordinates the individual links, network operation in a decentralized, self organized manner is maintained. Moreover, a method for interference management is established so that time-frequency slots (chunks) can be dynamically assigned on a short-term basis. In effect the proposed protocol termed busy tone OFDMA (BT-OFDMA) establishes a decentralized dynamic resource partitioning. Unlike static resource partitioning, non-uniform distribution of user locations and/or bursty traffic loads can be exploited.

The attainable improvements of BT-OFDMA are offset by the required additional signalling overhead, which is in our studies one OFDM symbol per uplink and downlink slot, which results in 6.7% signalling overhead. On the other hand, instead of simply dismissing the busy-tone as overhead, an alternative interpretation is to view the busy-slot as a feedback link from the receiver to the transmitter. To this end, the considered MU-MIMO schemes considered for local area require instantaneous CSI at the transmitter, which typically requires the UT to transmit pilots. For instance, in the mobile WiMAX standard 802.16e, for uplink channel sounding the BS can request a mobile to transmit pilots. Provided that these pilots are located on the busy slot both goals are accomplished: transfer of CSI from receiver to transmitter; and interference management. Moreover, with the use of hybrid ARQ and adaptive modulation and coding schemes, the provision of a reliable feedback link with low latency is becoming increasingly important. To this end, various types of feedback information may be 'piggy packed' on the busy-slot.
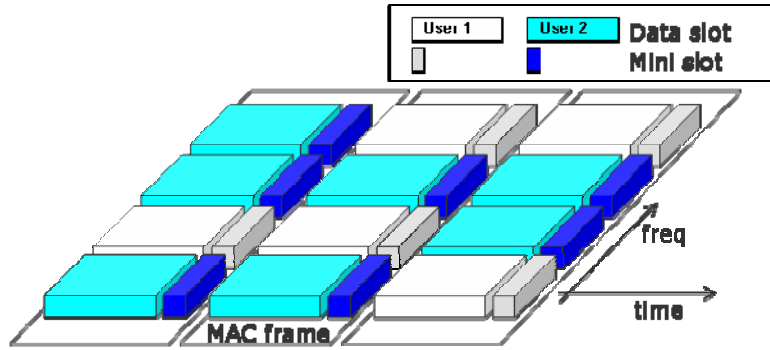
Figure 10.1: MAC frame structure including in-band minislots for busy-tone signalling and low-rate feedback

The MAC frame structure of the busy tone concept proposed in [HNO06] is depicted in Figure 10.1. Associated to each chunk carrying data are so-called *busy-slots* dedicated to interference management and for low rate feedback. So, any chunk scheduled for a certain UT has a busy-slot reserved for the feedback link from the receiver to the transmitter. A busy-slot always occupies the same number of subcarriers as the corresponding data chunk, but spans typically only over one OFDM symbol in time.

10.2 Performance evaluation for LA peer-to-peer network

The simulation is carried out in an indoor deployment environment as defined as scenario A1 in [WIN2D111]. It consists of one floor of a building consisting of 40 rooms of size 10m x 10m x 3m and two corridors of size 100m x 5m x 3m. The UTs are assumed to be distributed uniformly inside the rooms and the corridors with a probability of 90% and 10% respectively. If N_L is the targeted number of links in the system, $2N_L$ mobiles are distributed in the indoor environment. The relevant parameters considered in simulation are presented in Table 10.1.

Table 10.1: List of simulation parameters

Parameters	Value
Channel model	Indoor scenario (A1)
Number of links	15
Environment characteristics	One floor of a building with regular grid of rooms, walls and corridors [WIN2D6137] (see Figure 10.2) Number of rooms: 40 (size 10 m x 10 m x 3 m) Number of corridors: 2 (size 100 m x 5 m x 3 m)
Wrap-around	No
Interference modelling	All links modelled
MS transmit power	21 dBm
MS height	1.5m
Symbol length	20.48 μs
Guard interval	1.28 μs
Total symbol length	21.76 μs
Total bandwidth	100 MHz

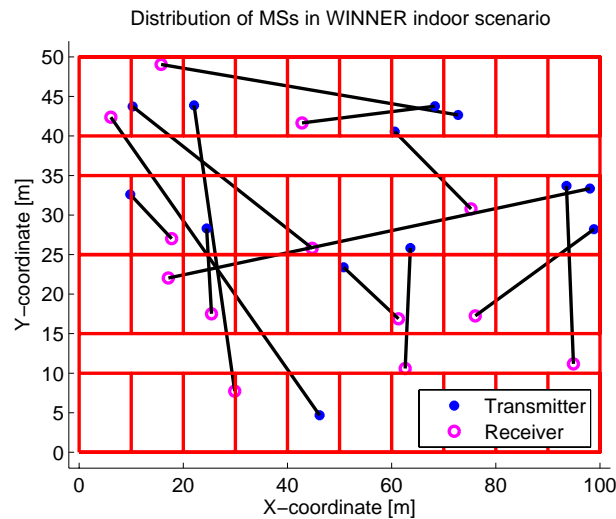|	
Total number of subcarriers (SCs)	2048
Number of SCs used for data transmission	1664
Chunk size	15 (time) × 8 (frequency) = 120
Number of chunks/frame	2 (time) × 208 (frequency)
Packet size	12208 bits
Modulation scheme	QPSK, rate ½ convolutional code
SINR target	5 dB

Figure 10.2: Indoor scenario with randomly distributed UTs. Each transmitter selects its receiver randomly from the distribution.

The deployment scenario and the distribution of UTs are illustrated in Figure 10.2. For forming the links, two mobiles *A* and *B* are randomly selected from the mobiles distributed in the system, forming a peer-to-peer (P2P) link.

At the beginning of a snapshot, each transmitter has a buffer which queues a fixed number of packets of constant length. The offered load to the system is changed by modifying the packet arrival rate which is assumed to be the same for all UTs. The packets in the buffer are characterized by linearly increasing expiration time, $k \Delta t$, where k is the position of the packet in the queue, corresponding to the equidistant inter-packet arrival by rate $1/\Delta t$.

The performance of BT-OFDMA applied to local area peer-to-peer (P2P) networks is evaluated on the basis of four metrics: throughput, data rejection rate, delay and packet expiration rate. Throughput is the number of bits that are transmitted successfully. A transmission is considered successful if the received SINR is greater than or equal to the SINR target. The data rejection rate corresponds to the average number of bits transmitted per unit time but fail to meet the SINR target. Delay is the time elapsed between the beginning of the snapshot to the time the packet is completely transmitted. The packets that expire before fully transmitted are assumed to have infinite delay, which for simulation purposes is made equal to the snapshot duration (100 ms). The packets are assumed to expire if the transmission of the entire packet is not completed before the expiration deadline. The optimum value for the interference threshold is determined by simulations as $I_{thres} = 100$dBm.

The performance of the above algorithm is compared against the random allocation scheme. The random allocation scheme schedules transmission on any chunk with probability *p* if there is data to be transmitted.
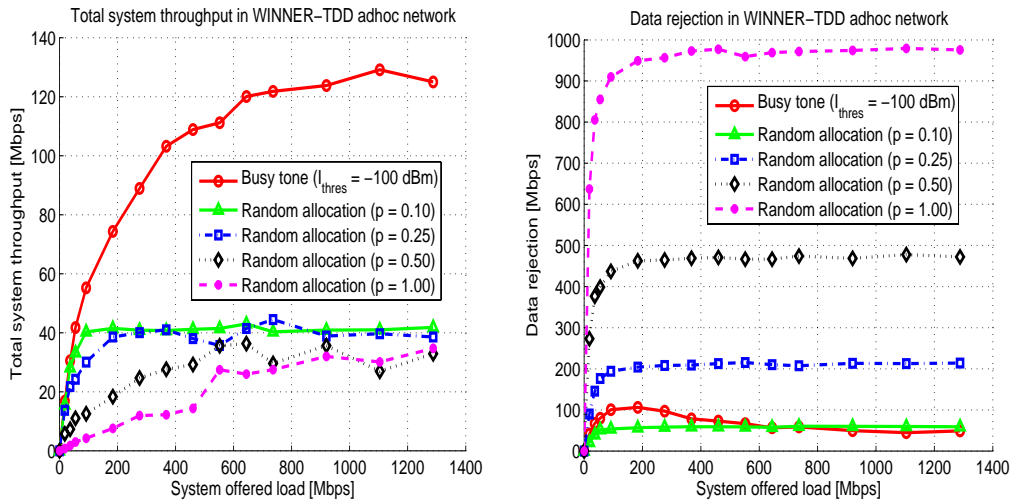
Figure 10.3: Total system throughput (left) and data rejection rate (right) in WINNER–TDD *ad hoc* network.

The simulation results show that the busy tone concept achieves approximately a three-fold gain in throughput compared to the benchmark systems, as can be seen in Figure 10.3. A maximum throughput of approximately 130 Mbps is achieved with busy tone scheme whereas the random allocation scheme with $p = 0.1$ and $p = 0.25$ only give a maximum throughput of only 40 Mbps. Using fixed allocation scheme in which the total number of chunks per timeslot are divided by the number of links in the system, the maximum system throughput that can be obtained would be 67.4 Mbps. In this case, the system is free of interference as no chunk is re-used. From this it can be found that BT-OFDMA achieves approximately an effective frequency re-use of two as the maximum throughput is about 130Mbps.

Finally, as can be seen from Figure 10.4, the busy tone algorithm performs better than the benchmark systems also in terms of delay and packet success rate. The lower delay and packet expiration rate is of paramount importance for time sensitive traffic and therefore establishes the busy tone as a preferred choice among the methods studied here.
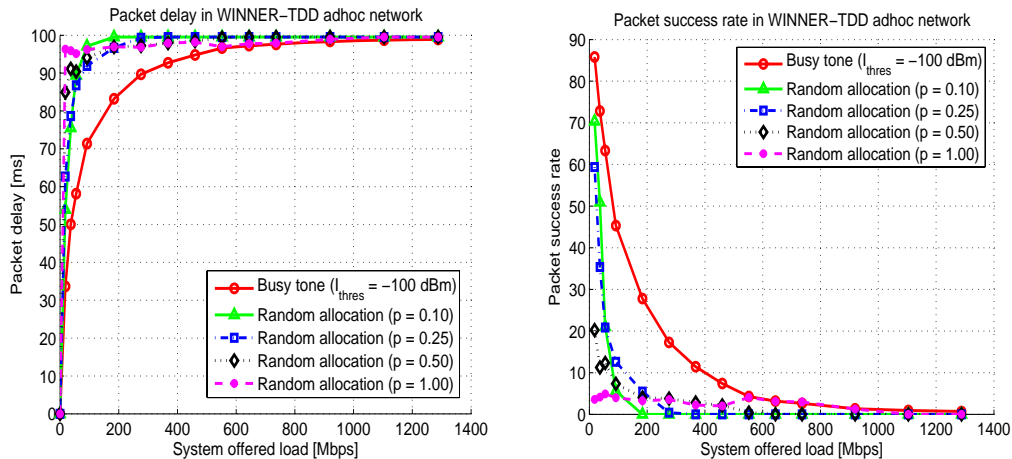

Figure 10.4: Delay performance (left) and packet success rate (right) in WINNER–TDD *ad hoc* network.

11. Mobility and radio access cooperation

In this section we evaluate the performance of the WINNER handover algorithm, focusing on intra-mode (i.e. between LA cells) and inter-mode (i.e. between LA and WA cells) handovers[11]. In the following, we first describe the handover trigger, then the simulator we used to derive performance results reported in Section 11.3.

11.1 Handover Triggers

The algorithm we propose combines all the available quality parameters (SINR, estimated instantaneous throughput and network load) and consists of two independent triggers, one for maintaining the wireless connection, and another for maximizing the network performance.

The wireless connection trigger aims at guaranteeing an available wireless connection for the mobile station and only takes place when the actual connection degrades and is likely to be lost. This algorithm is reported in Figure 11.1. A SINR target is defined, to obtain a PER < 0.01 with packets of 1500 bytes on the basic modulation scheme. By default the period of evaluation for the SINR is 0.2s, but, when the SINR becomes lower than the target, it can be decreased to 0.02s for an intensive evaluation. From the collected values an average SINR is determined. If the average SINR is lower than the target, the handover is triggered.

The network performance trigger instead combines the measured SINR and the network load in order to maximize MAC layer performance. The metric used to activate the trigger is called "Residual throughput" and it is defined as: Data Rate * (1 – PER) * (1 – Channel Occupation). The word "residual" means that a part of network resource is already occupied by other users, then the handover decision is only based on the remaining bandwidth at the user disposal. The handover trigger is based on a comparison between the estimation of the residual throughput on the current cell (namely, Current_residual_throughput) with the one that could be achieved on another cell (namely, Target_residual_throughput). If the ratio between Target_residual_throughput and Current_residual_throughput is bigger that a threshold,

$$Target\_residualt\_throughput / Current\_residual\_throughput > throughput\_margin$$

then the handover is triggered.

After extensive simulations we decided to set the *throughput_margin* to 1.1, a value that avoids ping-pong effects and at the same time does not limit the gain that can be achieved with handovers.

Compared to the wireless connectivity trigger which periodically evaluates the link quality for maintaining the connection, evaluations of the network performance trigger are less frequent. A time average of more samples can better express long-term network performance.

To derive the Data Rate, the Channel Occupation and the PER, the UT performs measurements in the used cells and on broadcast messages sent by the BSs of neighbouring cells. For detailed description please refer to [WIN2D472].

---

[11] Handovers among LA and MA cells are considered behaving similarly as the ones among LA and WA cells, so we only consider this second scenario in this section.
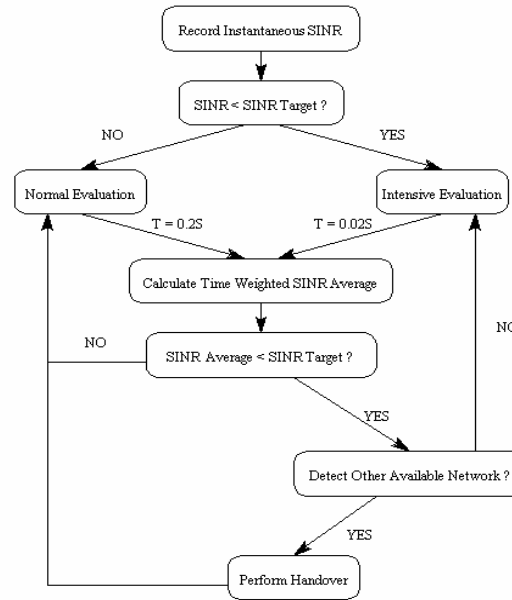
Figure 11.1: Wireless Connection trigger

Moreover, in order to restrict the number of cells to measure, we assume that the user terminal is supplied with a list of the neighbouring cells, that are the most likely to fulfil the SINR or quality requirements at the user terminal location. In this way, measurements are performed only on the cells included in the neighbours list.

11.2 Simulator description

We evaluate the performance of the proposed algorithm providing simulation results derived with OPNET, by modifying the simulator distribution to implement the considered handover criteria.

In our simulations all user terminals have two radio interfaces with different physical layers, MAC stacks and IP addresses corresponding to the wide area and the local area modes. These two interfaces constantly monitor the link quality of each mode and forward this information to a "mobility management" process implemented on the mobile device, which controls continuously the performance of each wireless connection and triggers the inter-mode handover if needed.

It must be highlighted that:

- In one instant only one interface is used for *data* transmission.
- Both stacks (MAC and physical) are always on, and are able to receive and send *control* packets (e.g. to probe the channel quality).
- Each interface (WA and LA) has its own IP address, thus an IP handover is performed switching from WA to LA modes.
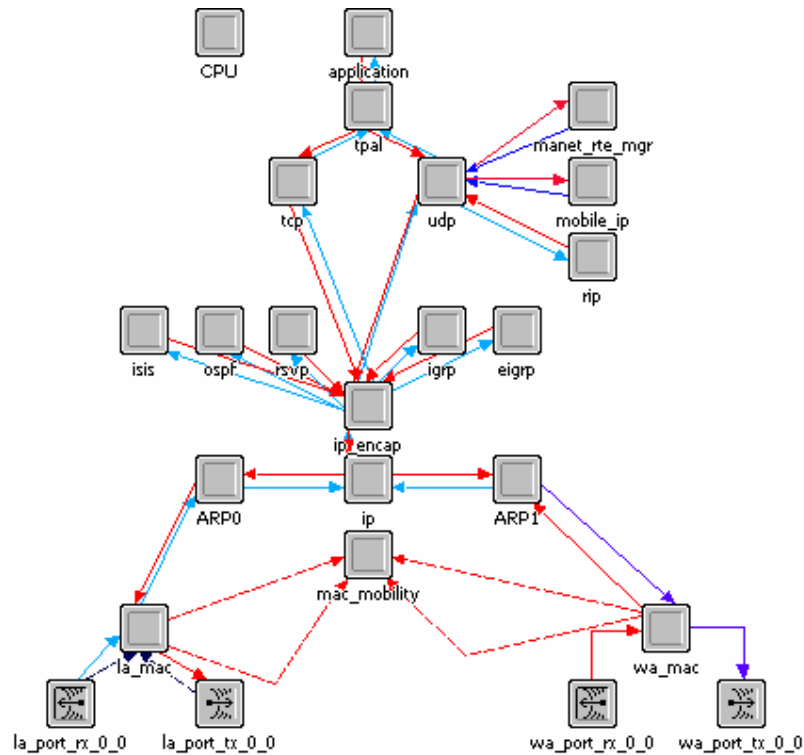
Figure 11.2: Hybrid station structure with two interfaces, WA and LA

Figure 11.2 reports a schematic representation of the user terminal, as implemented in the OPNET simulator. Each multi-mode terminal, able to transmit and receive on the WA and LA WINNER modes, is characterized by double Physical and MAC layers in the protocol stack. Since the PHY and MAC WINNER layers are not totally defined yet and an implementation in the OPNET simulator is not available, we represent the wide area mode with IEEE 802.16e and the local area mode with IEEE 802.11g. The 802.16e addresses LOS and NLOS operations within the 2 to 11GHz frequency range and provides some mobility support capabilities. It has almost 400 meters of radius with 20 Mbps of theoretical throughput. The 802.11g operates in the 2.4GHz licensed band and offers coverage of 70-80 meters with a theoretical throughput of 54Mbps.

The architecture of the upper layers is the reference one. On top of the IP layer, we find all the possible routing protocols and resources reservation protocols: *rsvp* (Resource ReSerVation Protocol), developed for supporting different QoS classes in IP applications; *ospf* (Open Shortest Path First), a routing protocol that determines the best path for routing IP traffic over a TCP/IP network; *eigrp* (Enhanced Interior Gateway Routing Protocol), *rip* (Routing Interchange Protocol), *isis* (Intermediate System - Intermediate System) and *igrp* (Internet Gateway Routing Protocol) that are distance vector routing protocols.

The transport layer is either TCP or UDP, and a process model called TPAL connects the transport layer to the application layer.

The UT implementation includes also the Mobile IP process and the *mac_mobility* entity, needed to perform inter-mode handover. The *mac_mobility* entity is the key element of the dual stack mobile station: it continuously controls the performance of each mode and triggers the inter-mode handover if needed.

11.3 Simulation results

In this section we present some results obtained with simulation and that show the effectiveness of the proposed handover trigger. We consider different scenarios for intra-mode and inter-mode handover, with one or more UTs.

The first scenario we refer to is represented in Figure 11.3. Two BSs operating in the local area mode are available and one user terminal, initially connected to BS1, moves away at 5m/s thus entering the coverage of BS2. Different positions of the BSs have been considered: results reported hereafter are averaged over all the simulations performed.
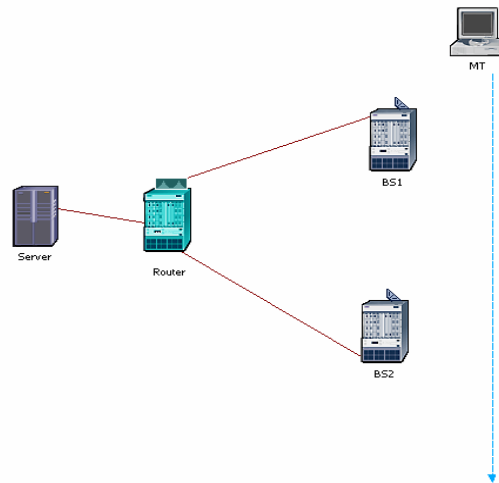

Figure 11.3: Reference scenario for the evaluation of the trigger without cell congestion

In the first simulation set we considered long-lived ftp connections generated at the Server node with a rate of 50Mbps.

We considered both the proposed trigger, as well as the trigger implemented in the legacy WLAN, activated at the disconnection from the current AP due to lack of connectivity. In the case of the legacy WLAN trigger, the search of an available BS is performed only when the connectivity toward BS1 is going to be lost. Conversely, when the WINNER trigger is implemented, the user terminal continuously performs measurements on the neighbouring cells. Without attending the loss of coverage, as soon as the target residual throughput increases the current residual throughput, the handover is performed.

Now, referring to the scenario presented in Figure 11.3, we evaluate the handover latency of the WINNER system and we compare it with the latency of handover in WLANs. We considered two different deployment scenarios, with layer-2 and layer-3 handover respectively.

A layer-2 handover is performed when the UT hands over between BSs controlled by the same gateway. In this case the IP address does not change and, as a consequence, the use of Mobile IP to maintain the connection is not necessary.

In this context, the handover latency is due to the scanning procedure, the handover decision and the authentication/reassociation phase. Since our simulator does not implement the exchange of signalling messages the values reported in the figure do not include exchange of messages with current/target BS and the authentication/reassociation delay. As reported in several work of measurements in WLANs, that delay usually varies between 5 and 15 ms, depending on the used card. The signalling time in WINNER should be shorter since authentication/reassociation is no longer necessary. To have a complete overview of the handover latency, these values have to be added to the simulation results.

A layer-3 (plus layer-2) handover is instead performed when the UT hands over between BSs controlled by different gateways. In this case, the latency accounts also for the binding updates of the Mobile IP protocol.
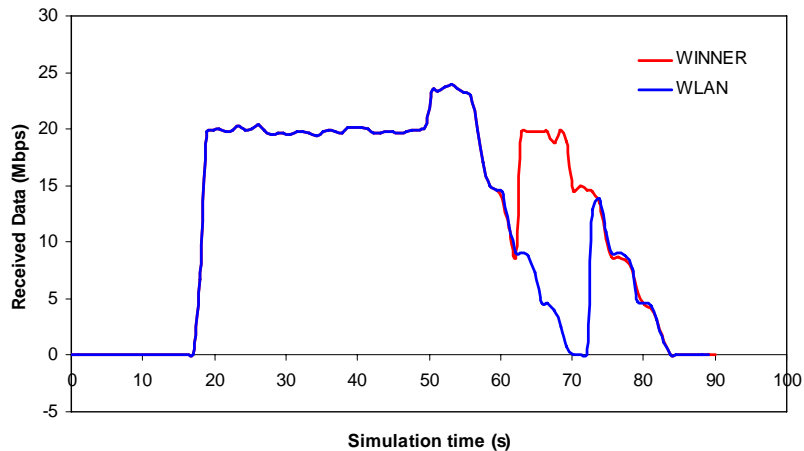
The simulations results are reported in Table 11.1. We can notice that also in case of layer-2 handover, the latency of a WLAN handover is too high to offer seamless mobility. In the WINNER system instead it is equal to zero, since scanning and measurements are done rapidly and periodically on the cells of the neighbouring lists only and no more at the handover time. We have to remember that the signalling delay has to be added to the values reported in the table.

Table 11.1: Handover latencies

	WINNER	WLAN
Layer2 HO	0	90 ms
Layer2+Layer3 HO	680 ms	780 ms

When Mobile IP has to be used to perform a layer-3 handover, the latency dramatically increases, even if the WINNER case still offers better performance.

Note that, besides a reduced latency, the WINNER system offers further advantages: the introduction of the pool of gateway (see D4.8.2) frequently lets to perform layer-2 rather than layer-3 handover, introducing a gain of hundreds of milliseconds.

Figure 11.4: Received data as a function of the simulation time

We report now in Figure 11.4 the amount of received data as a function of the simulation time. We consider again the WINNER and the WLAN triggers. As you can see in the figure, the gain achieved with the proposed trigger is not only in terms of latency, but also of achieved throughput: the UT, exploiting information already collected, is able to select the BS that can provide better performance. Without attending the loss of coverage, as soon as the target residual throughput increases the current residual throughput, the handover is performed. Thus, the handover to another cell allows the use of higher data rates, related to the higher SINR, since an adaptive Modulation and Coding Scheme (MCS) is adopted.

Finally we considered an interactive application like Voice over IP and we study how the two different triggers impact on the quality of the communication.

We compare the performance derived by WINNER with that of legacy WLAN. Figure 11.5 reports the packet delay at the application layer as a function of the simulation time. At the beginning of the communication, that happens 13 seconds after the start of the simulation (see Figure 11.5), the UT is in the coverage of BS1 and the delay of the voice packets is about 80 ms. From that moment on, the UT moves in directions of BS2. In the case of legacy WLAN, the handover to BS2 is triggered only when the coverage of BS1 is almost lost, that is at 68 sec. The poor quality of the communication before the handover and the time necessary to scan all the channels to find the new BS introduce a high delay: you can observe the peak in the delay, that reaches 500 ms. Then the UT continues to move and exits from the coverage of BS2 at 85 sec. There are not others available local area BS, *BSla*, so that at 85 sec the communication is interrupted. This explains the new arise in the delay between 80 and 85 sec.

The behaviour of the UT in the WINNER case is the same. The difference in the experienced delay depends only on the handover from BS1 to BS2. Indeed, with the WINNER trigger, the handover is performed immediately at 65 sec, without degradation in the communication.

This figure clearly shows that the WINNER handover avoids the peaks in the delay due to the interruption of the communication in the classical handover process.
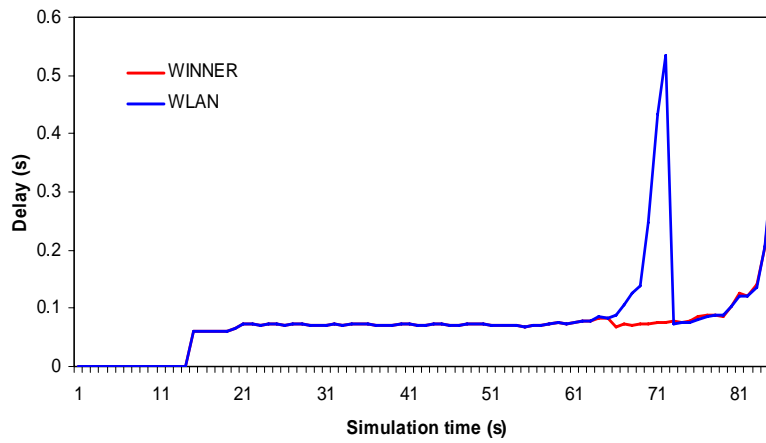

Figure 11.5: VoIP delay

Now we show the impact of the two different combined WINNER triggers, that is the wireless trigger and the throughput based, focusing on inter-mode handover. We consider the scenario represented in Figure 11.6: a mobile station crosses the wide area cell passing through two different local area cells. The mobile station activates the wireless interfaces in the following order: LA – WA – LA – WA.
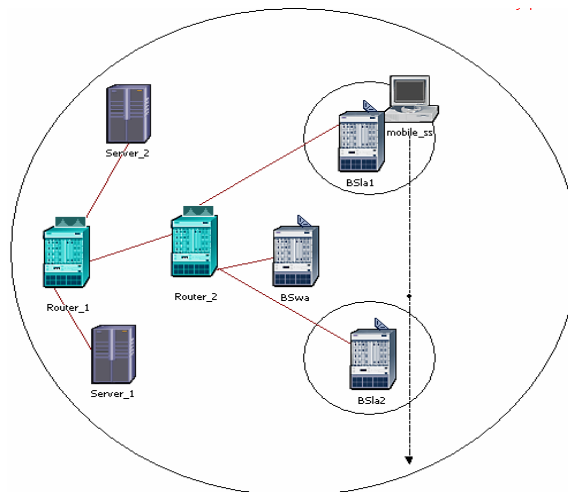

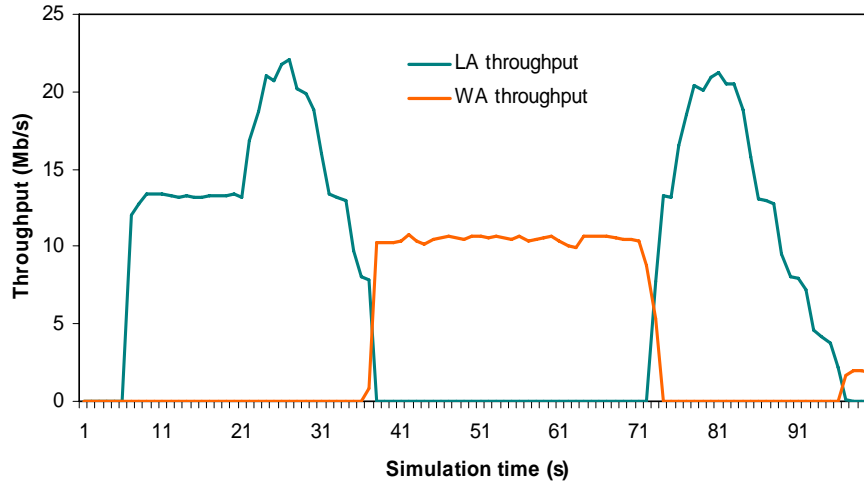**Figure 11.6: Handover scenario with residual throughput criterion**

Figure 11.7: Estimated throughput of mobile_ss

Figure 11.7 depicts the throughput achieved by the station *mobile_ss* when using LA or WA modes. The station, initially in the local area coverage, performs a handover to wide area when the throughput estimate on the wide area overcomes the one in the local area. Then, it enters the coverage of the second *BSla* and, when the LA throughput increases over the WA one, the second handover, from wide area to local area, is performed. Finally, the third handover from LA to WA is triggered by the wireless connectivity criterion. Indeed, the wide area throughput is lower than the local area throughput because the station is fare away from the *BSwa*. For this reason the network performance trigger is not activated. In this case the wireless connectivity trigger lets maintain the connection and avoid packets loss.
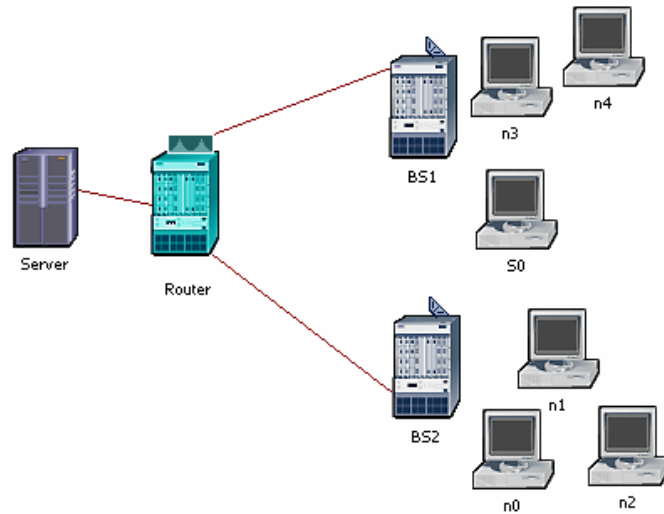

Figure 11.8: Reference scenario for the evaluation of the trigger with cell congestion
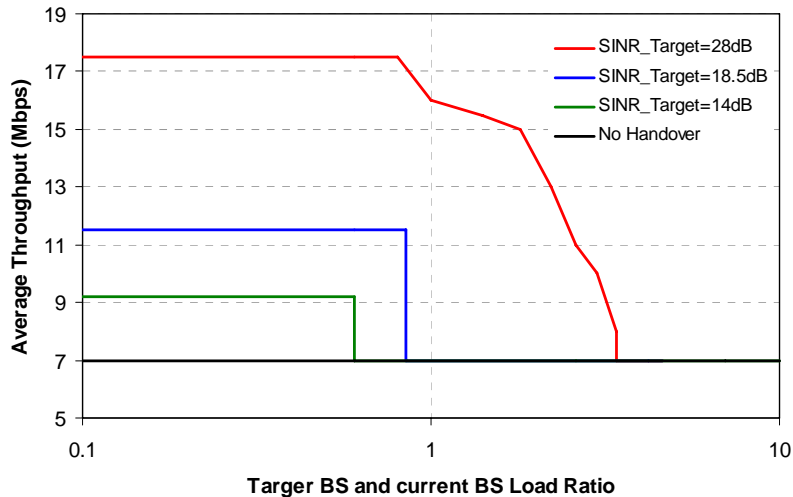
Figure 11.9: Average throughput of the user terminal S0 as a function of the load on the target channel for different SINR values

Finally we show the performance gain that can be achieved performing handovers triggered by the residual throughput in different load conditions. Consider as an example the topology presented in Figure 11.8. The user terminal S0 is under the coverage of both *BSla* BS1 and BS2 and it is initially connected to BS1. Assume that, due to its placement, the SINR of the radio channel to BS1 perceived by S0 is 18.5dB. Then we vary the position of BS2 to achieve SINR in the second cell equal, lower and higher than that in the first cell. Moreover, we assume the other nodes connected to BS1 generate a load of 5 Mbps, while the load of BS2 is varying.

Figure 11.9 reports the layer 2 throughput achieved by station S0, as a function of the load ratio between the two cells, for different values of the SINR on the target channel (to BS2). The throughput achieved transmitting towards BS1, that is, if no handover is performed, is reported as a reference.

First of all, note that all the handovers result in a throughput gain. The estimation of the residual throughput indeed let the user correctly judge if advantages in performance can be achieved handing over. Moreover, we can gather that when the SINR on the target cell is higher than that one the current cell, the handover is performed until high values of load of the target cells. Otherwise, if there if no gain in the signal strength and thus in the used data rate, the handover is performed only when the load on the target cell is lower than that on the current cell.

As a conclusion, the handover strategy implemented in the WINNER system offer several advantages:

- The time necessary to scan the other channels is reduced by the use of the neighbouring cell lists and performed periodically, offering an up-to-date evaluation of available cells.
- The use of Mobile IP and the layer-3 handover cases are dramatically reduced by the introduction of the pool of gateways sharing resources, offering a reduction of the latency of 2–3 sec.
- The handover is not triggered only by the loss of connectivity, but also by the availability of better resources, resulting in a higher achieved throughput.

12. Spectrum Resource Management

In this chapter, we address the performance evaluation of Spectrum Resource Management (SRM) developed in WINNER, where we mainly focus on the short-term spectrum assignment. After providing a general overview of the spectrum resource management, performance results regarding inter-cell interference issue in short term spectrum assignment are presented.

12.1 General overview of the Spectrum Resource Management (SRM)

In order to propose high spectrum efficiency, future mobile short range systems will have to coexist and probably share spectrum in an efficient manner. For that reason two mechanisms for spectrum management are developed inside WINNER: Spectrum Sharing and Coexistence (SSC) and Flexible Spectrum Use (FSU).

- SSC aims at facilitating the coexistence of WINNER with other systems in the same frequency band. The requirement of sharing the spectrum is without a doubt a constraining factor for the system concept, especially if it is assigned a secondary, non-prioritized position in accessing the spectrum. The expected gains from SSC will depend substantially on the properties of the involved systems and also on the regulatory environment. When considering the system requirements, especially Quality-of-Service (QoS) guarantees, operation in shared spectrum (from a secondary system position) can only be seen as a possibility for capacity enhancement.

- FSU considers the spectrum usage of different Radio Access networks (RAN) between the same RATs. The major advantages of FSU result from the enhanced spectral scalability of the system. Prior results from a simplified assessment model [HTL+06] showed that significant benefits can be expected from FSU between the RANs, even when the RANs carry partially correlated traffic patterns and knowing that FSU implementation involves considerable use of guard bands. The spectrum functionalities proposed will lead to a better utilization of the spectrum throughout multi-operator solutions, therefore increasing the availability of the spectrum.

The spectrum functionalities blocks are presented in Figure 12.1. The most feasible localization of these functionalities is indicated between brackets. It may be noticed that SSC and FSU functions are not separated ones, as they have interrelations and common blocks to manage the WINNER spectrum usage.
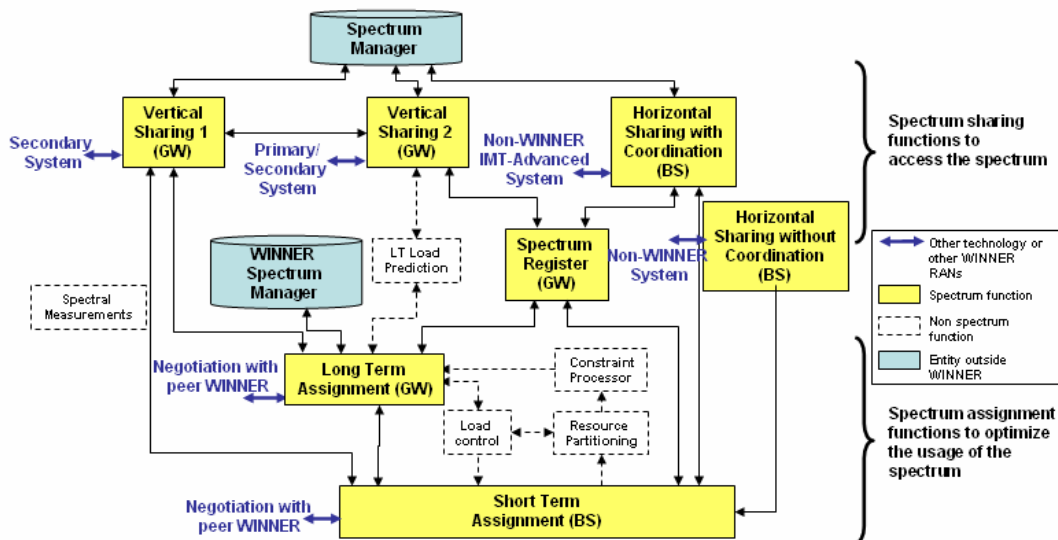

Figure 12.1: Illustration of the interactivity between the spectrum sharing and spectrum assignment functions in the WINNER concept

In general, spectrum functions consist of concurrently triggered procedures. A normal spectrum control procedure (e.g. actualization of a given resource set measurement collection) is the result of several individual action calls

The WINNER system with its dynamic spectrum management features will be considered as a step towards a cognitive radio network. WINNER system captures some aspects of cognitive radio networks, where base stations and radio network are capable of determining the available spectrum resources from other negotiating parties.

Figure 12.1 introduces several functional components to enable the different spectrum functions as depicted in Table 12.1.

Table 12.1: Illustration of the interactivity between the spectrum sharing and spectrum assignment functions in the WINNER concept

Spectrum Sharing and Coexistence (SSC)	Flexible Spectrum Use (FSU)
Spectrum sharing functions	Spectrum assignment functions
This group includes: • Vertical Sharing 1 (VS_1). • Vertical Sharing 2 (VS_2). • Horizontal Sharing with Coordination (HwC). • Horizontal Sharing without Coordination (HwoC).	This group includes: • Long Term Assignment (LT). • Short Term Assignment (ST)

The main functions needed for **Spectrum Sharing and Coexistence** are:

- Vertical Sharing 1 (VS_1): WINNER system has the access to the spectrum and it may assist a secondary system by sharing its spectrum resources (primary or not) when they are not needed.

  Vertical Sharing 2 (VS_2): If WINNER system has a secondary access to the spectrum, it has to implement mechanisms not to interfere with the primary system. For that purpose, considerable knowledge about the deployed primary system may be required.

- Horizontal Sharing with Coordination (HwC): WINNER and other system (i.e. other IMT-Advanced system RATs) have the same priority in access spectrum, and they coordinate their spectrum access based on a set of predefined rules (SSC rules) that all the involved systems are submitted to.

- Horizontal Sharing without Coordination (HwoC): Unlike the previous case, there are no possibilities of coordination (e.g. in license exempt RLAN bands within 5GHz). Each system needs to come up with its own methods of sensing of spectrum holes or spectrum opportunity.

The main functions needed for **Flexible Spectrum Use** are:

- Long Term Spectrum Assignment: The function coordinates and negotiates the spectrum assignments between multiple WINNER RANs for large geographical areas (this function resides inside a GW). It takes into account the average traffic demand and predictions. The spectrum assignments are updated periodically at a slow rate, i.e. in time frame of several tens of minutes and above.

- Short Term Spectrum Assignment: On the other hand, the ST spectrum assignment function controls the short-term and local, i.e. cell-specific, variations of the large-scale spectrum assignments. Hence, it enables faster adaptation to the local traffic load variations and geographically more accurate spectrum assignments than the LT assignment. The assignments are performed in the time scale of several super-frames, i.e. 100 ms to several minutes. The ST assignment requests spectrum resources from other RANs after being triggered by the LT assignment or by preventive load control.

12.2 Spectral Resource Management Performance Evaluation

In this section, the performance evaluation of SRM concerns the short-term spectrum assignment. The task at hand is to efficiently exchange spectrum resources between different RANs of the same technology on a fast basis while managing the interference inflicted to neighbouring cells.

12.2.1 Scenario

Short term spectrum assignment between two different WINNER RANs (RAN_1 and RAN_2) at the cell level is investigated here as shown in Figure 12.2. The focus is on the downlink of the multi-cellular OFDMA system as in WINNER RANs. WINNER MA is considered with TDD as the preferred mode. Therefore the ST assignment in this study investigates spectrum resource negotiation between TDD modes within MA deployment. It is assumed that two separate distinct spectrum bands are assigned for two RANs during LT assignment. The LT spectrum assignment is based on longer timescales and deals with average or expected spectrum resources. Within LT assignment, average spectrum resources are taken into account from traffic demand curves to assign spectrum resources at cell level. But the actual spectrum resources or the spectrum resources demand varies from the average value depending on the dynamicity of spectrum usage in each RAN. Therefore, to efficiently assign these spectrum resources during ST assignment period, spectrum resources are assigned based on the actual spectrum resources rather than on the average values. The difference between the actual usage of spectrum resources against the average assignment of spectrum resources results in an additional or insufficient usage of resources at each cell. This results in spectrum boundaries changes in both RANs (RAN_1 and RAN_2).

In this scenario during ST assignment cell C_1 of RAN_1 has extra spectrum resources to negotiate with cell C_{11} of RAN_2. In this case C_1 is considered as the generous cell and C_{11} is considered as the greedy cell. For an efficient spectrum assignment during each ST assignment period, the impact of interference between new spectrum usages of cell C_{11} in RAN_2 on the cell cluster of cell C_1 in RAN_1 needs to be measured. Figure 12.2 illustrates the impact of inter-cell interference on cell clusters in ST assignment once cells C_1 and C_{11} are in the negotiation of spectrum resources. This negotiation will automatically impact the neighbouring cells of C_1 (C_2, C_3, C_4, C_5, C_6 and C_7). In this scenario it is assumed the interference is only imposed towards the cells in the first tier.
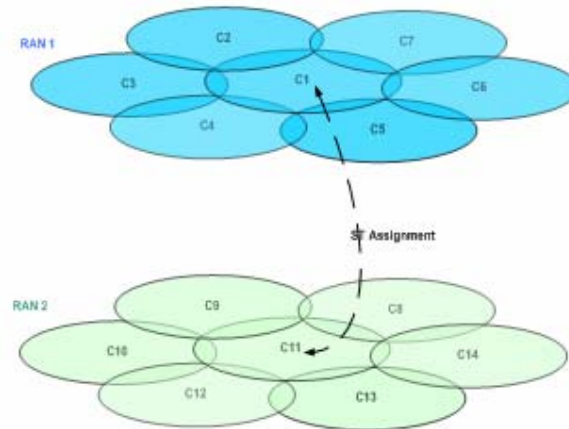

Figure 12.2: Illustration of ST spectrum assignment between cells from RAN1 and RAN2

It is important to know the resource allocation patterns of each cell when investigating the interference between two negotiating cells. Since the objective of this work is to investigate the change of spectrum boundaries during ST assignment, resource allocation in each cell is assumed as in Costas arrays. ST assignment period is considered as the TDD super-frame duration of around 6ms. The minimum time-frequency unit in WINNER downlink OFDMA access is called a chunk. Within WINNER TDD mode of operation the super frame size is 230 chunks in frequency and 16 chunks in time. Each super-frame contains 230*16 = 3680 chunks. Therefore the time-frequency (T-F) mapping (or chunk mapping) is based on a truncated Costas sequence of length 230. Costas arrays are n*n arrays consisting of dots and blanks with exactly one dot in each row and column [14]. According to Costas array representation, Figure 12.3 illustrates the chunk resource allocation pattern for cell C_i (where i =2, 3, 4, 5, 6, 7) and chunk resource allocation pattern of C_{11} respectively, in time and frequency domains. The initial chunk

allocation pattern is a random allocation of any cell C_i (where $i = 2, 3, 4, 5, 6, 7$). This allocation pattern is called the basic allocation pattern. For example initial random allocation pattern in Figure 12.3 can be assigned to cell C_2 of RAN_1. Once this is obtained then for any other cell in the 1st tier and super-frame duration the chunk allocation pattern can be acquired as a cyclic frequency shift of the basic allocation pattern (for cells C_i with $i = 3, 4, 5, 6, 7$).

Within ST assignment cell negotiation between C_1 and C_{11} may result some chunks given to the greedy cell (C_{11}) can interfere the allocation of the same chunk in the neighbouring cells (neighbouring cells in the 1st tier of C_1 of RAN_1). Therefore, in ST assignment, it is important to define a maximum allowable interference threshold ($P_{threshold}$) to minimise the interference in the neighbouring cells of the generous cells caused by the deployment of negotiated chunks in greedy cells.

A binomial distribution describes the probability P_i of a simultaneous allocated chunk as:

$$P_i(x) = C_x^n k^x (1-k)^{n-x} \tag{1}$$

where n is the number of cells, x the number of simultaneous chunk allocations of the desired chunk by the interfering cells and k is the number of allocated chunks. For a successful spectrum assignment at cell level the following equation (2) has to be fulfilled where A is the number of negotiated chunks between RANs:

$$\sum_i^A P_i < P_{threshold} \tag{2}$$

where $P_{threshold}$ is the maximum allowable interference within ST negotiation that can be agreed between the cells of 1st tier in RAN_1.
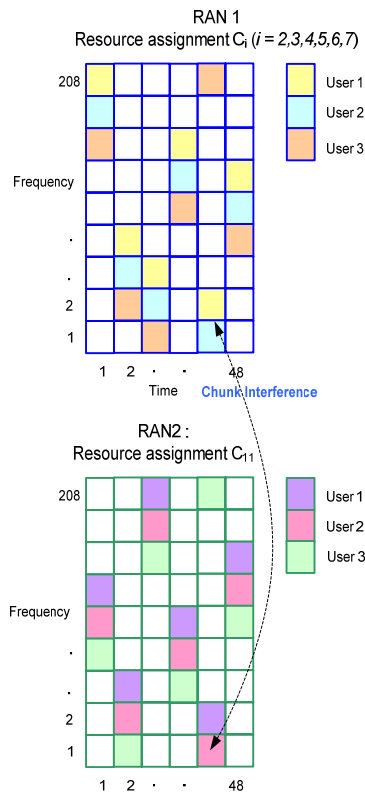

Figure 12.3: Inter-cell interference avoidance using Costas array

12.2.2 Performance Evaluation in ST Assignment

The following section presents the simulation study describing the issue of inter-cell interference in ST assignment in the above scenario. In this case, WINNER LA deployment with TDD mode of operation is considered. The ST assignment period is considered as a super-frame of 230 chunks in frequency direction and 16 chunks in time direction. Therefore truncated Costas array representation of 230*16 is considered for resource allocation patterns in each cell. At the same time, in order to avoid intra-cell interference in a single cell, only one user is assigned to a frequency chunk at one time. In the neighbouring cells, we assume that the same chunk is allocated to distant users.

RAN Topology and Traffic Demand

The cell topology of RAN_1 and RAN_2 is shown in Figure 12.4. The topology considered in this study consists of each RAN having 16 cells where only two cells are trying to negotiate spectrum resources on a fast basis. Cells in RAN_1 are numbered from C_1 to C_{16} whereas cells in RAN_2 are numbered from C_{17} to C_{32}.
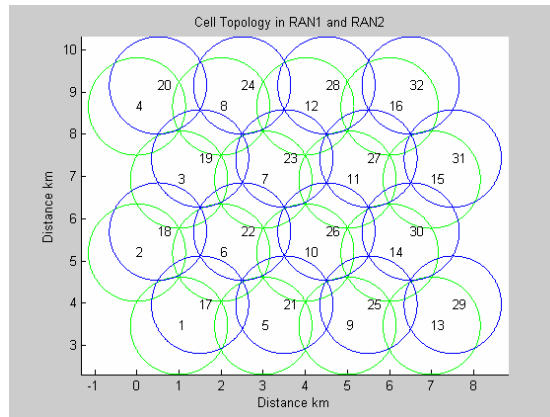

Figure 12.4: Cell Topology of two networks RAN_1 and RAN_2
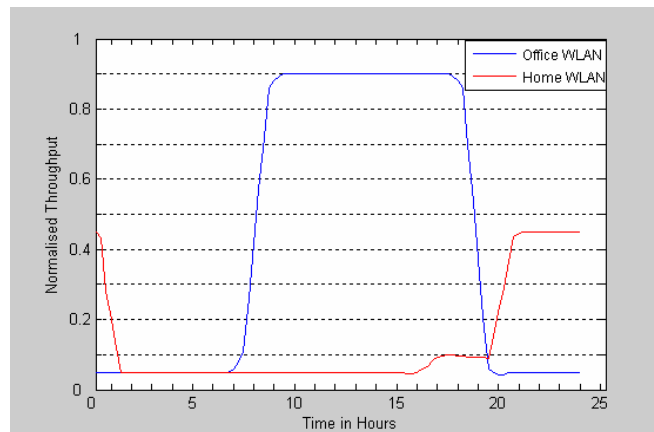

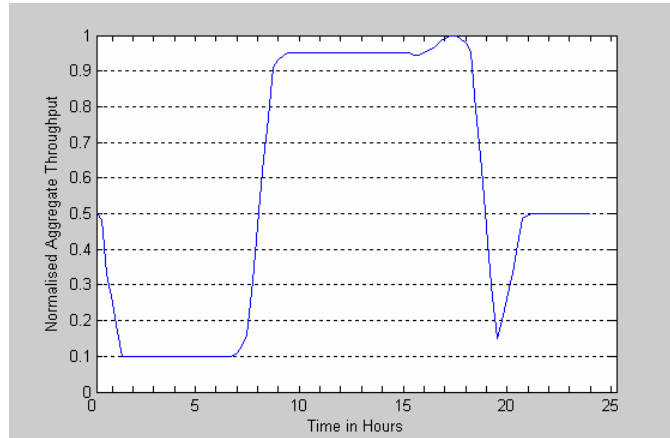**Figure 12.5: WLAN traffic pattern in different environment**

Figure 12.6: WLAN normalised aggregate traffic demand

Figure 12.5 and Figure 12.6 illustrate the traffic demand pattern for each cell. The major traffic contribution in LA scenario is considered as WLAN deployment in each RAN. The collective WLAN traffic consists of contributions from home WLAN and office WLAN systems. During the day time office, WLAN contributes more towards the aggregate traffic (or throughput), whereas during evenings and night, home WLAN contribution increases. These reasonable assumptions are taken into consideration for the construction of the aggregate WLAN traffic demand in LA scenario.
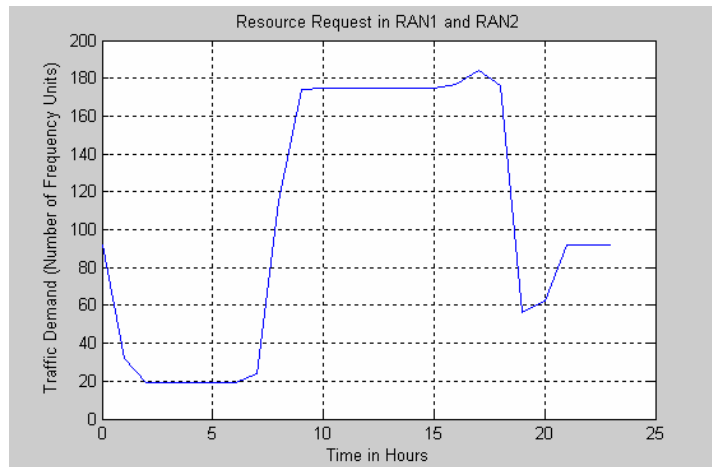

Figure 12.7: Pattern of traffic in a cell of RAN1 and RAN2 with the same average

Figure 12.7 represents the average usage of spectrum resources in LA deployment in each cell. The y axis presents the average number of spectrum resources, and the x axis the hours of the day (24 hour period). Due to operational limitations it is assumed that only 80% of the spectrum resources is utilized during the maximum demand. For example, during the busy hour period, only $(0.8 \times 230) = 184$ frequency chunks are used among the 230 available frequency chunks.

Although the average number of requested chunks can be drawn from the Figure 12.7, during each ST assignment there is an instantaneous variation in the actual requested number of chunks. During each ST assignment period the actual number of requested chunks is expressed as a random number drawn from a normal distribution (μ, σ), where μ is the average value from the traffic demand curves for each RAN and σ is the standard deviation where $\sigma = 0.1 * \mu$.

Cell Pair Identification for ST Assignment

Figure 12.8 presents the instantaneous resource request variations within the considered RAN topology. The x corresponds to the corresponding cell pairs selected from each RAN which may be the negotiation

pairs in ST assignment. Depending on the considered RAN topology, 16 cell pairs are selected. The LT spectrum assignment is given is at longer time scales than in the ST spectrum assignment. ST assignments take care of the tiny fluctuations of the traffic demand and negotiate resources accordingly. The following illustrates additional or insufficient frequency chunks in each cell pair due to traffic demand fluctuation at time 18hours, where the average number of frequency chunks is is 184 from the traffic demand curves. For example cell pair with C_1 (RAN_1) and C_{17} (RAN_2) may not be involved in any negotiation as they both need extra resources. On the other hand C_3 and C_{19} may choose to negotiate spectrum resources with each other since C_{19} has extra resources and C_3 needs more resources.
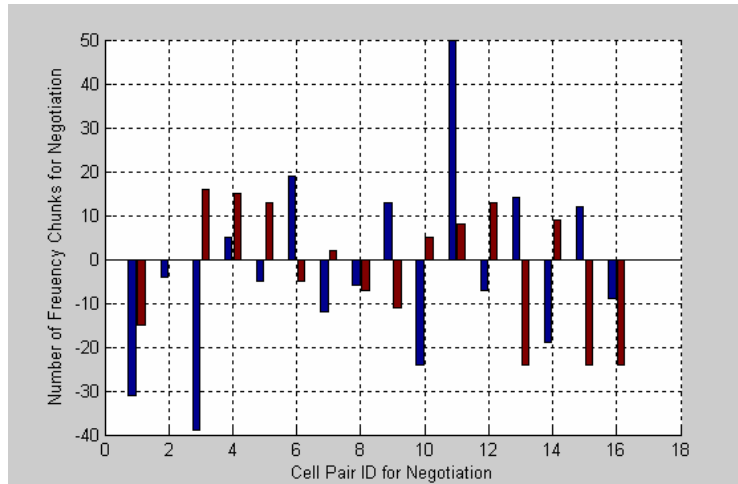

Figure 12.8: Resource request variation in RAN1 and RAN2 in ST period

For each RAN we define greedy cells and generous cells depending on the additional or insufficient resources. N_a is the number of resources allocated to each cell during LT assignment and N_d is the actual number of resources needed from the traffic demand curves. When ($N_a > N_d$) the cells are categorised as generous cells where extra resources are available for negotiation. If ($N_a < N_d$) the cells are greedy cells since they are starving for more resources. For example the C_1 and C_{17} are considered as greedy cells where as C_{19} can be considered as a generous cell. During ST assignment period only generous and greedy cells negotiate with each other. Also to avoid conflicts between more than one cell pairs entering into the ST negotiation, within this study we limit the number of cell pairs involved into negotiation to one.

Cell Pair Selection Algorithms for ST Assignment

To avoid conflicts between cell pairs, a single cell pair is selected within each ST assignment period. The selection of cell pair is based on the two following algorithms. The first algorithm is based on the selection of cell pair with least satisfaction. In this case the generous cell satisfies the minimum requirement of the greedy cell. The second algorithm is based on cell pair with the most flexibility in allocating chunks. In this case generous cell provides the maximum satisfaction to the greedy cells or much more than the required resources from the greedy cell. Having more resources than required allows flexibility in resource allocation for the greedy cell, thus avoiding interference to neighbouring cells of the generous cell.

Performance of ST Assignment – Results Discussion

Figure 12.9 presents the comparison between the above mentioned algorithms once applied to the ST assignment between two RANs. In the first case, selection of cell pair is performed according to the least satisfaction criteria. The amount of offered frequency chunks in the generous cell is similar to the number of extra frequency chunks required by the greedy cell. In the second case, the cell pair selection is based on maximum flexibility criteria. The generous cell offers much more than required by the greedy cell. For successful ST assignment, performance it is necessary to reduce extra interference caused by offered frequency chunks to the neighbouring cells of the generous cell. With plentiful resources greedy cell has

the flexibility of deploying chunks minimising interference to neighbouring cells in the 1st tier of the generous cell.
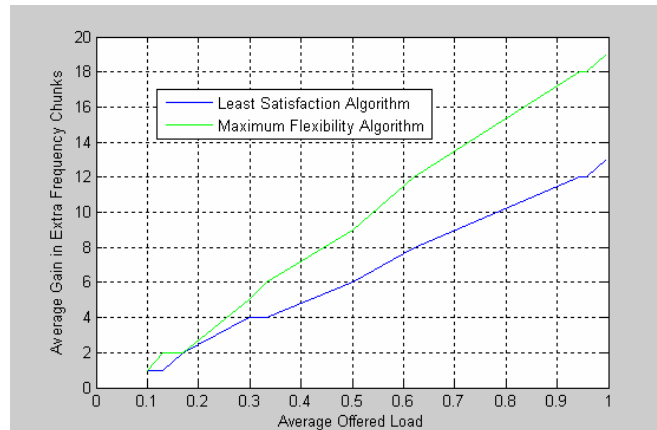

Figure 12.9: Algorithm comparison for average gain in ST assignment

In Figure 12.9 the *x* axis represents the average offered load in each RAN. This is given in terms of frequency units. The y axis represents the average extra frequency chunks that can be gained within ST assignment. As mentioned earlier, in each ST assignment period the negotiation is limited to a single cell pair. The selection of cell pair is based on the least satisfaction criterion or on the maximum flexibility criterion. In the case of least satisfaction the amount of extra frequency chunks is the minimum requirement to carry the offered load in the selected cell pair. But in the other case gain of extra frequency resources allows flexible deployment of frequency chunks reducing inter cell and inter RAN interference.

13. Conclusions

The WINNER system concept aims at providing ubiquitous wireless coverage in a wide range of deployment scenarios. From a unique concept, several proof of concepts can be derived to be suited to a specific deployment scenario. Three scenarios have been defined: Local Area (LA), Metropolitan Area (MA), Wide Area (WA), corresponding to different environments, traffic patterns, bandwidth, etc.

- This report presents the WINNER system concept suited to the LA environment and its performance assessment. The main result is that high spectral efficiencies, such as 30bps/Hz in the uplink and 40bps/Hz in the downlink, are provided by the use of distributed antennas at the base station.

- This report also addresses the enablers to provide self-organisation to the WINNER air interface by dynamically adapting to any change in the environment. The assessment of self-organised network synchronisation and of decentralized interference management proves that these mechanisms can efficiently contribute to build self-organising systems. The benefits of adaptation are also demonstrated for modulation and coding techniques and for spatio-temporal processing.

- The evaluation of handover algorithm and of spectral resource management shows that the WINNER system concept can efficiently deal with two different deployments.

This deliverable is complementary to the deliverables [WIN2D61310] and [WIN2D61311] which respectively focus on performance assessment of WINNER system concept in Wide Area and Metropolitan area cases.

References

[BCK03]   A. Bourdoux, B. Come, and N. Khaled, "Non-reciprocal transceivers in OFDM/SDMA systems: Impact and mitigation", in *Proc. RAWCON*, August 2003.

[BW06]   H. Boche, M. Wiczanoswski, "Stability-optimal transmission policy for the multiple antenna multiple access channel in the geometric view", Signal Processing, 86, pp. 1815-1833, Aug. 2006.

[E04]   N. C. Ericsson, Revenue Maximization in Resource Allocation: Applications in Wireless Communication Networks. PhD thesis, Uppsala University, Sept. 2004.

[EPG95]   U. Ernst, K. Pawelzik, , and T. Geisel, "Synchronization induced by temporal delays in pulse-coupled oscillators", Phys. Rev. Letters, 74(9):1570 – 1573, Feb. 1995.

[FOO+98]   P. Frenger, P. Orten, T. Ottosson, and A. Svensson, "Multi-rate Convolutional Codes", Communications Systems Group, Department of Signals and Systems, Chalmers University, Technical report no. 21, ISSN 02083-1260, Göteborg, April 1998.

[GDL+00]   X. Guardiola, A. Diaz-Guilera, M. Llas, and C.J. Perez, "Synchronization, diversity, and topology of networks of integrate and fire oscillators", Phys. Rev. E, 62(4):5565–5570, Apr. 2000.

[HNO06]   H. Haas, V. D. Nguyen, P. Omiyi, N. H. Nedev, and G. Auer, "Interference Aware Medium Access in Cellular OFDMA/TDD Network," in Proc. IEEE Int. Conference on Communications (ICC 2006),.Istanbul, Turkey, June 2006.

[HS03]   Y.-W. Hong and A. Scaglione, "Time synchronization and reach-back communications with pulse-coupled oscillators for UWB wireless ad hoc networks", in *Proc. IEEE Conference on Ultra Wideband Systems and Technologies 2003*, pp. 190–194, Nov. 2003.

[HSG05]   M. Haardt, V. Stankovic, and G. Del Galdo, ``Efficient multi-user MIMO downlink precoding schemes,'' in *Proc. IEEE Int. Workshop on Computational Advances in Multi-Sensor Adaptive Processing (CAMSAP 2005)*, (Puerto Vallarta, Mexico), Dec. 2005.

[HTL+06]   K.Hooli, S. Thilakawardana, J. Lara, J-P. Kermoal, and S. Pfletschinger, "Flexible Spectrum Use between WINNER Radio Access Networks", IST mobile and wireless summit, Mykonos, Greece, June 2006.

[Hug91]   D. Hughes-Hartogs, "Ensemble modem structure for imperfect transmission media", US Patent No. 5054034, October 1991.

[KC06a]   M. Kobayashi, G. Caire, "Iterative waterfilling for weighted rate sum maximization in MIMO-MAC", IEEE Workshop on Signal Processing Advances in Wireless Communications (SPAWC), Cannes, France, July 2006.

[KC06b]   M. Kobayashi, G. Caire, "An iterative water-filling algorithm for maximum weighted sum-rate of Gaussian MIMO-BC", IEEE J. Selected Areas Commun., vol 24, no. 8, Aug. 2006.

[LR07]   Y. Li and W. E. Ryan, "Mutual-Information-Based Adaptive Bit-Loading Algorithms for LDPC-Coded OFDM", IEEE Trans. On Wireless Comm., vol. 6, no. 5, May 2007.

[LZH+06]   T. Lestable, E. Zimmerman, M-H. Hamon, and S. Stiglmayr, "Block-LDPC Codes Vs Duo-Binary Turbo-Codes for European Next Generation Wireless Systems", VTC-Fall'06, Montreal, Canada.

[MS90]   R.E. Mirollo and S.H. Strogatz, "Synchronization of pulse-coupled biological oscillators", *SIAM J. APPL. MATH*, 50(6):1645–1662, Dec. 1990.

[OH04]   P. Omiyi and H. Haas, "Improving Time-Slot Allocation in 4th Generation OFDM/TDMA TDD Radio Access Networks With Innovative Channel-Sensing," in Proc. IEEE IEEE Int. Conference on Communications (ICC 2004), Paris, France, June 2004, pp. 3133–3137.

[OHA07]   P. Omiyi, H. Haas, and G. Auer, "Analysis of TDD Cellular Interference Mitigation using Busy-Bursts," in IEEE Transactions Wireless Communications, July 2007.

[PPS07]   S. Pfletschinger, A. Piątyszek and S. Stiglmayr, "Frequency-selective Link Adaptation using Duo-Binary Turbo Codes in OFDM Systems," IST Mobile and Wireless Communication Summit, Budapest, July 2007.

[SBC07]   S. Stiglmayr, M. Bossert, E. Costa, "Adaptive coding and modulation in OFDM systems using BICM and rate-compatible punctured codes", European Wireless, Paris, Apr. 2007.

[SH07]   V. Stankovic and M. Haardt, ``Generalized design of multi-user MIMO precoding matrices,'' *IEEE Trans. on Wireless Communications*, 2007, accepted for publication.

[TH98]   D. N. C. Tse, S. V. Hanly, "Multiaccess fading channels — Part I: Polymatroid structure, optimal resource allocation and throughput capacities", IEEE Trans. Inform. Theory, vol. 44, no. 7, Nov. 1998.

[WIND210]   IST-2003-507581 WINNER, "D2.10 Final report on identified RI key technologies, system concept, and their assessment", November 2005.

[WIN2D111]   IST-4-027756 WINNER II, "D1.1.1 WINNER II Interim channel models," November 2006.

[WIN2D112]   IST-4-027756 WINNER II, "D1.1.2 WINNER II channel models," September 2007.

[WIN2D223]   IST-4-027756 WINNER II "D2.2.3 Modulation and Coding Schemes for the WINNER II system", November 2007.

[WIN2D233]   IST-4-027756 WINNER II "D2.3.3 Link level procedures for the WINNER System", November 2007.

[WIN2D351]   IST-4-027756 WINNER II "D3.5.1 Relaying concepts and supporting actions in the context of CGs", October 2006

[WIN2D461]   IST-4-027756 WINNER II "D4.6.1 The WINNER II Air Interface: Refined multiple access concepts", November 2006

[WIN2D472]   IST-4-027756 WINNER II "D4.7.2 Interference avoidance concepts", June 2007

[WIN2D482]   IST-4-027756 WINNER II "D4.8.2 Cooperation schemes validation", June 2007

[WIN2D6111]   IST-4-027756 WINNER II "D6.11.1 Revised WINNER II System Requirements"

[WIN2D6112]   IST-4-027756 WINNER II "D6.11.2 Key Scenarios and Implications for WINNER II", June 2006

[WIN2D6114]   IST-4-027756 WINNER II "D6.11.4 Final WINNER II System Requirements", June 2007

[WIN2D6133]   IST-4-027756 WINNER II "D6.13.3 Intermediate concept proposal (wide area) and evaluation", November 2006

[WIN2D6134]   IST-4-027756 WINNER II "D6.13.4 "Intermediate concept proposal (metropolitan area) and evaluation", November 2006

[WIN2D6137]   IST-4-027756 WINNER II Deliverable "D6.13.7 Test Scenarios and Calibration Cases Issue 2", November 2006

[WIN2D61310]   IST-4-027756 WINNER II "D6.13.11 Final CG "wide area" description for integration into overall System Concept and assessment of key technologies", October 2007

[WIN2D61311]   IST-4-027756 WINNER II "D6.13.11 Final CG "metropolitan area" description for integration into overall System Concept and assessment of key technologies", October 2007

[WIN2D61314]   IST-4-027756 WINNER II "D6.13.14 WINNER II System Concept Definition." November 2007.

[WIND54]   IST-2003-507581 WINNER "D5.4 Final Report on Link Level and System Level Channel Models", September 2005

[WIND72]   IST-2003-507581 WINNER, "D7.2 – System Assessment Criteria Specification", July 2004

[Wod07]   M. Wódczak, "Extended REACT – Routing information Enhanced Algorithm for Cooperative Transmission", IST Mobile and Wireless Communications Summit 2007

[YC04]   E. M. Yeh, A. S. Cohen, "Information theory, queueing, and resource allocation in multi-user fading communications", Conference on Information Science and Systems (CISS), Princeton, USA, March 2004.